University of Massachusetts Medical School

eScholarship@UMMS

The Origin of Human White, Brown, and Brite/Beige Adipocytes

So Yun Min
University of Massachusetts Medical School

Let us know how access to this document benefits you.

Repository Citation

THE ORIGIN OF

HUMAN WHITE, BROWN AND BRITE/BEIGE ADIPOCYTES

A Dissertation Presented

By

SO YUN MIN

Submitted to the Faculty of the University of Massachusetts Graduate School of Biomedical Sciences, Worcester in partial fulfillment of the requirements for the degree of

DOCTOR OF PHILOSOPHY

NOVEMBER 4, 2016

INTERDISCIPLINARY GRADUATE PROGRAM

THE ORIGIN OF

HUMAN WHITE, BROWN AND BRITE/BEIGE ADIPOCYTES

A Dissertation Presented By

SO YUN MIN

This work was undertaken in the Graduate School of Biomedical Sciences
Interdisciplinary Graduate Program

Under the mentorship of

_____

Silvia Corvera, M.D., Thesis Advisor

The signatures of the Dissertation Defense Committee signify
completion and approval as to style and content of the Dissertation

_____

Michael A. Brehm, Ph.D., Member of Committee

_____

Manuel Garber, Ph.D., Member of Committee

_____

Gregory J. Pazour, Ph.D., Member of Committee

_____

Yu-Hua Tseng, Ph.D., External Member of Committee

The signature of the Chair of the Committee signifies that the written dissertation meets
the requirements of the Dissertation Committee

_____

Rene Maehr, Ph.D., Chair of Committee

The signature of the Dean of the Graduate School of Biomedical Sciences signifies
that the student has met all graduation requirements of the School.

_____

Anthony Carruthers, Ph.D.,
Dean of the Graduate School of Biomedical Sciences

NOVEMBER 4, 2016

Acknowledgement

Abstract

During embryonic development, adipocytes emerge from microvasculature [1, 2]. Lineage-tracing studies in mice have shown that adipocyte progenitors reside in the adipose tissue capillaries[3-6]. However, the direct evidence of an association between adipocyte progenitors and vasculature in humans is lacking. A specific class of adipocytes (brown and beige/brite) expresses the uncoupling protein 1 (UCP1), which consumes glucose and fatty acids to generate heat[7-9]. The abundance of UCP1-containing adipocytes correlates with a lean metabolically healthy phenotype in human[10, 11]. However, a causal relationship between the presence of these cells and metabolic benefits in human is not clear.

In this thesis, I report human adipocyte progenitors proliferate in response to pro-angiogenic factors in association with adipose capillary networks in-vitro. The capillary-derived adipocytes transform from being UCP1-negative to positive upon adenylate cyclase activation, a defining feature of the brite/beige phenotype. Activated cells have denser, round mitochondria with UCP1 protein, and display uncoupled respiration. When implanted into NOD-scid IL2rgnull (NSG) mice, the adipocytes can form a vascularized fat pad that induces vascularization and becomes integrated into mouse circulatory system. In normal or high fat diet-fed NSG mice, activated brite/beige adipocytes enhance systemic glucose tolerance and improved hepatic steatosis, thus providing evidence for their potential therapeutic use. The adipocytes also express neuroendocrine and secretory factors such as Interleukin-33, proprotein convertase PCSK1 and proenkephalin PENK, which are correlated with human obesity. Finally, analyses on

single-cell clones of capillary-sprout cells reveal the existence of diverse adipogenic

progenitor populations. Further characterization of the clones will define the identifying

features of the diverse adipocyte progenitor types that exist in human adipose tissue.

Table of Contents

List of Tables

List of Figures

List of copyrighted Materials Produced by the Author

So Yun Min, Jamie Kady, Minwoo Nam, Raziel Rojas-Rodriguez, Aaron Berkenwald, Jong Hun Kim, Hye-Lim Noh, Jason K. Kim, Marcus P. Cooper, Timothy Fitzgibbons, Michael A. Brehm and Silvia Corvera, Human 'brite / beige' adipocytes develop from capillary networks and their implantation improves metabolic homeostasis in mice. Nat Med, 2016. 22(3): p. 312-318.

List of Third Party Copyrighted Material

Chapter II, Figure 2.1.
Adapted from:
Gealekman et al., Depot-Specific Differences and Insufficient Subcutaneous Adipose Tissue Angiogenesis in Human Obesity. Circulation, 2011.123(2): p. 186-194.

Chapter II, Figure 2.1.
Adapted from:
Khanh-Van Tran et al., The Vascular Endothelium of the Adipose Tissue Gives Rise to Both White and Brown Fat Cells. 2012, Cell Metabolism. 15(2), 8: p. 222-229.

Chapter V, Figure 5.1.
Adapted from:
Pellegrinelli, V. and A. Vidal-Puig, Deriving functional beige fat from capillaries. Nat Med, 2016. 22(3): p. 234-236.

CHAPTER I: Introduction

The role of adipose tissues in whole-body energy balance and metabolic health

Glucose homeostasis is crucial for the survival of multicellular organisms

including humans. Despite intermittent food intake, blood glucose levels in human

remain relatively steady through the day (approximately 5mM). This requires the

orchestrated play of several organs[12]. Pancreatic β-cells secrete insulin in response to

the increase of glucose after eating. Insulin then promotes glucose uptake in

adipose tissue and muscle while inhibiting liver glucose production. In the fasting state,

circulating glucose levels decrease, by which pancreatic α-cells release glucagon.

Glucagon stimulates the breakdown of glycogen in the liver to produce glucose and

increases synthesis of glucose from pyruvate and other substrates, thus stabilizing glucose

levels[13]. Adipocytes release fatty acids into the circulation for fuel when glucose is

limited. Fatty acids are generated from triacylglycerols, which hold more energy per unit

mass than carbohydrates do[14].

Energy storage and utilization, which is directly associated with the function of

adipose tissue, plays an essential role in the development of metabolic diseases such as

type 2 diabetes, cardiovascular disease, osteoarthritis and fatty liver disease[15]. Failure

of adipose expansion can lead to the disturbed balance of glucose homeostasis and insulin

resistance. A-ZIP/F-1 fat-less mice develop severe insulin resistance, which can be

attributed to the impaired insulin action in liver and muscle[16]. On the other hand, there

are severely obese individuals who are protected from the development of insulin

1

resistance or metabolic diseases[17], which implies that proper storage of surplus nutrients is important to achieve insulin-glucose homeostasis.

It is also noteworthy that the location of fat storage is important. Pear-shaped obesity with expanded subcutaneous adipose tissues is typically protective from metabolic complications and associated with metabolic health[18, 19]. In contrast, apple-shaped obesity accumulates visceral adipose tissues, resulting in deleterious consequences[19-21]. Storing lipids in proper adipose depots (subcutaneous) while sequestering them from other non-adipose tissues, such as the liver, muscle, heart, and pancreatic-islets prevents lipotoxicity and consequent insulin resistance[22] Lipotoxicity refers to the deleterious effects of lipid accumulation in peripheral tissues when the supply of nutrient exceeds the capacity of adipose tissue. Unger reviewed in 2002 that lipotoxicity of pancreatic β-cells, myocardium and skeletal muscle results, respectively, in type 2 diabetes, cardiomyopathy and insulin resistance. Spilling-over fatty acids can enter harmful pathways such as ceramide production, which causes apoptosis of lipid-laden cells including β-cells and cardiomyocytes[23]. Chronic exposure to fatty acids recapitulates the key features of type 2 diabetes associated with β-cell failure such as β-cell apoptosis, elevated basal insulin secretion, diminished glucose stimulated insulin secretion, reduced insulin content and gene expression, and defective pro-insulin processing[24].

Adipose tissue grow by both an increase of cell number, hyperplasia, by preadipocytes (or adipocyte progenitor) proliferation, and an increase of cell size, hypertrophy by accumulating lipids in the cell body[25-27] under required circumstances

such as significant calorie intake[28, 29]. Correlation studies between adipocyte size, adipocyte number, and plasma insulin levels have revealed that hyperplastic growth, which requires proliferation of preadipocytes, is metabolically healthier. Hyperplastic expansion is observed more frequently in subcutaneous than in visceral, which might explain the metabolic health of obese humans who gained their weight subcutaneously[30-33]. Rojas-Rodriguez *et al*. in our laboratory also showed that gestational diabetic patients possessed larger visceral adipocytes and fewer blood capillaries in subcutaneous and visceral adipose tissues compared to pregnant women with normal glucose tolerance. These results are consistent with those of previous studies in non-pregnant humans where large adipocytes are linked to dyslipidemia and glucose-insulin abnormalities[34, 35].

Unlike fat-storing white adipose tissues described so far, brown and brite/beige adipose tissues can contribute to metabolic homeostasis by actively consuming circulating glucose and fatty acids. These adipocytes contain the mitochondrial uncoupling protein (UCP1), and release heat to regulate body temperature[36]. Detailed explanation regarding white, brown, and brite/beige adipocytes will be discussed later.

Adipose tissues play multiple essential roles in regulating metabolism and energy homeostasis. Thus, insights on mechanisms that harness the expansion and function of adipocytes will not only contribute to the basic knowledge of adipocyte biology, but will also be useful for potential therapeutic strategies.

Angiogenesis and adipocyte progenitors

A principal mechanism of blood vessel formation is termed angiogenesis. Angiogenesis is essential for the development and growth of all tissues to meet the demand of gas and nutrient exchange[28]. It is also essential in many biological processes in development, adipose tissue expansion, reproduction and wound repair. Due to its crucial roles in every tissue, angiogenesis is a highly coordinated process. The main cellular components of vessel walls are endothelia cells, forming tight junctions through membrane protein vascular endothelial-cadherins. This the tubular structure is coated with vascular basement membrane and pericytes, which support the vasomotion and regulate of vascular basement membrane and endothelial barrier function[37]. Major inducers of angiogenesis include the vascular endothelial growth factor family, angiopoietins, transforming growth factors, platelet-derived growth factor, tumor necrosis factor-α, interleukins and the fibroblast growth factor family. Vascular endothelial growth factor-A is the most potent pro-angiogenic factor identified among the numerous angiogenic factors. It stimulates endothelial cells to proliferate, sprout, and form the vessel tubes[38-40].

During embryonic development, angiogenesis occurs before the emergence of adipocytes, and then adipocytes arise along the expending vessels[3, 41, 42]. Han *et al*. investigated the postnatal epididymal adipose tissue in mice and showed the co-localization of blood vessels and newly forming adipocytes. From postnatal day 1 to 4, epididymal adipose tissue was composed of various types of progenitor cells lacking

adipogenic differentiation capacity when tested *in vitro*. However, after day 4 the progenitor cells of epididymal adipose tissue obtained their adipogenic differentiation capacity and the impairment of the vascular endothelial growth factor/ vascular endothelial growth factor receptor 2 signaling pathway blocked adipogenesis[3]. Supporting the notion of interdependency between angiogenesis and adipogenesis, onset of obesity in mice correlates with an increase in micro-vessel formation[43]. In contrast, inhibition of angiogenesis in adipose tissue by inhibitors of endothelial cell proliferation (TNP-470, angiostatin, endostatin) or calorie restriction reduced body weight gain and fat mass in animals, suggesting neovascularization is mandatory for adipose tissue expansion in adults as well[44]. The associated growth of adipocytes with blood vessels has been partially explained by the observations that adipocyte precursors reside in the adipose tissue vasculature[5, 45, 46]. This result is further supported by the findings that a peptide inducing apoptosis of adipose tissue endothelial cells blunted weight gain in mice and primates with high fat diet feeding[47, 48].

Multiple studies including Tran *et al*. from our laboratory illustrated the juxtaposition between preadipocytes and vasculature by utilizing lineage-tracing experiments. Results suggest that preadipocytes might emerge from the vasculature or from the endothelial cell or pericyte themselves [5, 45, 49, 50]. Using genetically marked mice, Tang *et al*. indicated that the stromal vascular compartment of mouse adipose tissues contains peroxisome proliferator-activated receptor gamma (PPARγ)-expressing cells that divide, travel along, and notably repopulate the stromal vascular fraction, amplifying the population that contributes to adipocyte generation[5]. Gupta *et al.* labeled

committed murine adipose progenitors by marking Zfp423, a gene controlling

preadipocyte determination, with green fluorescent protein (GFP). The GFP-expressing

population from subcutaneous or visceral adipose tissue was stably committed to

preadipocytes that undergo robust adipogenesis. Immunohistochemistry for Zfp423-GFP

expression verified a perivascular origin of adipocyte progenitors in both white and

brown adipose depots. Unexpectedly, a subset of endothelial cells also expressed GFP,

suggesting a contribution of endothelial cells to the adipose lineage[6]. These results are

consistent with the findings from our laboratory by Tran *et al*. where lineage tracing

experiments showed the vascular endothelial cadherin promoter-driven reporter was

expressed not only in endothelial cells but also in progenitors and white and brown

adipocytes. Moreover, in response to PPARγ activation by rosiglitazone, endothelial

characteristics of human adipose sprouting cells were progressively lost while sprout

cells started to form structurally and biochemically defined adipocytes[49]. Suggested

markers for the adipocyte progenitors in rodents include pericyte markers and stem cell

markers [5, 51]. As Tang *et al*. reported the peri-vascular origin of preadipocytes, the

authors also confirm the expression of pericyte markers (NG2, SMA, PDFGR β) and Sca-

1 on PPARγ-expressing preadipocytes[5]. In the same month, Rodeheffer *et al*. also

identified a series of adipocyte progenitor markers in mice, which include CD24, CD29,

CD34, and Sca-1. The authors utilized fluorescence-activated cell sorting on mouse

adipose tissue stromal vascular fraction in combination with an *in vivo* transplantation to

show early adipocyte precursor cells reside in the adipose vascular stroma[51].

Despite the extensive studies on the characteristics of adipocyte progenitors in

mice, our knowledge of human adipocyte progenitors is limited due to the technical restrictions of humans (e.g. lineage-tracing). Moreover, insufficient understanding of the biology regarding the growth and differentiation of human adipocyte progenitors made it almost impossible for researchers to isolate them as experimental materials. Previous reports have also shown that cells derived from the stromal vascular fraction, also called adipose-derived stem cells from mice and humans can differentiate into adipocytes[52, 53]. However, the capacity of adipose-derived stem cells to differentiate remained low in several protocols[54-56]. Thus, the identity of the human adipocyte progenitor cells remains unknown. In this thesis, I describe the efforts we have made in our laboratory to overcome these limitations by exploiting our knowledge of the interdependency between angiogenesis and adipogenesis.

Thermogenic Fat cells: Brown and Brite/Beige Adipocytes

Brown adipose cells have the capacity to consume glucose and fat to produce heat, dissipating energy rather than making ATP. The uncoupling protein 1 (UCP1) localizes at the inner mitochondrial membrane of brown adipocytes and mediates this thermogenic function. UCP1 dissipates the proton gradient generated by the electron transport chain. This leak of protons reduces mitochondrial inner membrane potential, which in turn boosts substrate oxidation and results in the generation of heat[57, 58]. Brown fat cells express high amounts of constitutive UCP1 even under non-stimulated conditions.

In mice, the major brown adipose tissue depots include the interscapular, axillary,

and cervical brown adipose tissue that developed to generate heat to protect newborns from cold exposure. The sympathetic nervous system intimately regulates both the growth and thermogenic function of brown adipose tissue. Brown adipocytes get innervated by sympathetic fibers upon cold exposure, releasing norepinephrine to directly activate thermogenesis[57]. Cold exposure recruits brown adipose tissue through stimulating the proliferation and differentiation of brown adipose progenitor cells[59, 60].

Recruitable brown-like adipocytes that have a multi-locular, mitochondria-dense and UCP1-postivie morphology can also be found in white adipose tissue depots[61-63]. These ''brite (brown-in-white)''[64] or ''beige''[65] adipocytes induce UCP1 expression only upon cold exposure or other stimuli, which is a distinctive feature of brite/beige fat. Notably, fully stimulated beige adipocytes can gain a comparable level of UCP1 expression and UCP1-mediated uncoupled respiration as brown adipocytes do [66]. The inducibility of beige adipocytes is highly adipose depot specific. In mice, the subcutaneous inguinal WAT is most prone to the induction of beige adipocytes, whereas the epididymal WAT is fairly resistant to ''browning''[63].

Studies have suggested multiple genes that seem to be preferentially expressed either in brown (ZIC1, LHX8 and EVA1) or beige (CD137, TBX1, CITED1) adipocytes in rodents and humans[7, 66-68]. The detailed signature of human brown and beige adipocyte markers will be discussed in depth in Chapter III.

The profound interest in brown and brite/beige fat is driven by the potential benefits of these cells to counteract obesity and metabolic diseases. Findings from rodent studies evidently demonstrate that brown adipose tissue plays a significant role in whole-

body energy homeostasis. Ucp1 knockout mice under thermo-neutral conditions exhibit impaired diet-induced thermogenesis and develop obesity[69], whereas brown adipose tissue transplantation improves glucose homeostasis and insulin sensitivity[70]. Brown adipose tissue clears 75% and 50% of the serum circulatory glucose and triglycerides, respectively[71]. In humans, retrospective 18 F-fluoro-2-deoxy-d-glucose positron emission tomography/computed tomography (18F-FDG-PET/CT) studies revealed brown adipose tissue activity was correlated with decreased incidence of insulin resistance and diabetes mellitus, leanness, and improved lipid profile[10, 72-74] The role of brown adipose tissue on energy expenditure in adult humans has been extensively investigated. By cold exposure, brown adipose tissue activation increases energy expenditure 10% to 27% in brown adipose tissue-positive individuals[75-78]. Blood HbA1c, total cholesterol, and low density lipoprotein cholesterol levels can also be significantly lowered in brown adipose tissue-positive humans[79]. On the other hand, there are findings suggesting that clinical significance of human brown adipose tissue is still debatable. Orava *et al*. demonstrated no differences in whole body insulin-stimulated glucose disposal in the individuals with detectable brown adipose tissue [80]. Ouellet *et al*. also showed that plasma glucose and free fatty acid oxidation by brown adipose tissue was marginal under acute cold exposure though the authors verified oxidization of fatty acids by brown adipose tissue[81]. Nevertheless, the idea of activating brown adipose tissue as a therapeutic strategy still holds valid points, supported by the studies done in clinically applicable settings. Prolonged (5 hours) but mild cold exposure (~20 °C) enhanced whole-body glucose disposal, plasma glucose oxidation, and insulin sensitivity in brown

adipose tissue -positive (>50 ml) men[75]. Taken together, adult humans have active

brown adipose tissue (though the amount varies in each individual), which can function

as a promising new target for treating metabolic diseases. Future studies will refine the

methodologies for clinical applications and pharmacological agents that stimulate brown

adipose tissue activity, resulting in an improved metabolic profile in humans.

Project Goals

While intensive research in mice has developed useful insights into the regulatory

mechanisms of thermogenic adipose tissues, the development of models to study the

expansion and function of human adipose tissues is critically demanded in the field,

especially due to the possible substantial differences between rodents and humans.

Hence, this thesis aims: 1) to establish a method that enables the expansion and isolation

of human adipose progenitor cells, 2) to test the ability of isolated adipogenic progenitors

to form an integrated fat pad *in vivo*, 3) to characterize the cellular properties of adipocyte

progenitors that in part give rise to brite/beige adipocytes, 4) to analyze the functions and

effects of human brite/beige adipocytes on whole body metabolism in animals, and 5) to

compare the transcriptome signatures of the progenitors and adipocytes, derived from

classical brown (carotid perivascular), beige (outer neck subcutaneous), or white

(abdominal subcutaneous) adipose tissue.

CHAPTER II: Generation of human adipocyte progenitors and formation of human adipose tissue in mice

Author Contributions

Jorge Lujan-Hernandez, Raziel Rojas-Rodríguez, Tiffany DeSouza, Cara Berg, Patrick Teebagy

Summary

This chapter is dedicated to demonstrating that human adipocyte progenitor cells can be generated and expanded upon pro-angiogenic stimuli in conjunction with adipose tissue capillary sprouting. Adipose tissue capillary-derived adipocyte progenitors can be differentiated into adipocytes with a conventional adipogenic cocktail including insulin, dexamethasone and 3-isobutyl-1-methylxanthine. Differentiated adipocytes respond to insulin, increase leptin secretion with insulin, and express classic adipogenic genes, presenting the characteristics of human primary adipocyte *in vivo*. *In vitro* differentiated adipocytes formed a vascularized fat pad, which successfully retained human adipocytes *in vivo*, when put into Nude mice. Progenitors that had never been differentiated *in vitro* could also form a fat pad in Nude mice though the level of human adipocyte-specific message detected from implants was lower than that with *in vitro* differentiated capillary cells. These results support the interdependent growth of vessels and adipocyte progenitors, and further describe the methods by which we can produce human adipocyte progenitor cells *in vitro* and generate human fat pads *in vivo*.

Introduction

Proliferation of human adipogenic precursors requires angiogenesis. During human embryonic development adipocytes first appear from emergent vascular networks [82], and lineage-tracing studies have demonstrated that adipocyte progenitors reside within the walls of adult mouse adipose tissue capillaries [83-86]. These findings suggest that proliferation of adipocyte and vascular progenitors may be interdependent.

Result published over the past few years from our laboratory[49, 87-89] also indicate that adipogenesis occurs concomitantly with angiogenesis, and adipocyte progenitors can be generated using very small amounts of human adipose tissue *ex vivo*. Olga *et al*. reported that the sprouts formed from human adipose tissue explants consist of well-known blood vessel forming cells such as endothelial cells and mural cells (pericytes and smooth muscle cells)[89]. Furthermore, Tran *et al.* demonstrated classical endothelial capillary-forming ultra-structural features, including tight junctions, irregular nuclei, and pinocytic vesicles in cells comprising sprouts. In the same study, capillary lumens could be also observed, indicating that angiogenesis was recapitulated *ex vivo* in this system[49]. I adopted the same strategy as in Tran *et al.* to grow the capillary networks from human adipose tissue explants in order to characterize adipocyte progenitor cells and test their ability to form a fat pad in animals.

The identification and development of a robust adipose stem cell population is attracting great attention due to the strong need for tissue replacement and regeneration in human patients. "Adipose-Derived Stem Cells," or ADSC, is a heterogeneous population

12

of cells harvested from adipose tissue stromal vascular fraction (SVF), excluding

adipocytes. ADSC or SVF has been extensively investigated as a most promising stem

cell population and proved to contain adult stem cells that can differentiate into

adipocytes, osteoblasts, chondrocytes and myocytes etc. Before SVF became available,

autologous fat grafting had been frequently performed to augment soft tissues in clinical

settings. Fat grafts, however, are restricted by varying rates of re-sorption[90] and

complications of palpable indurations, pain, infection, abnormal breast discharge,

lymphadenopathy and abnormalities on breast cancer screening, resulting in unreliable

long-term outcomes after transplantation[91]. To overcome the limitations of fat grafts,

SVF-enriched lipo-transfer is contrived where aspirated fat is combined with

concentrated SVF of lipo-aspirate to create SVF-rich fat grafts. This approach has

markedly improved the survival of transplanted fat as well as decreased adverse effects in

human patients[92, 93]. The beneficial effects of these stem cells on wound healing have

also been extensively reviewed with multiple possible mechanisms suggested, including

secretion of pro-angiogenic factors, anti-inflammatory, anti-oxidant, and anti-apoptotic

factors and replenishing endothelial cells, keratinocytes, fibroblasts, and smooth muscle

cells[94, 95]. Nevertheless, the limited expandability and the significant variability in cell

quality in terms of differentiation potential under conventional protocols necessitate the

development of more proliferative and enriched adipogenic adult adipose stem cell

population. In this chapter, the ability of fat pad formation *in vivo* was compared between

capillary-derived adipocyte progenitors and SVF.
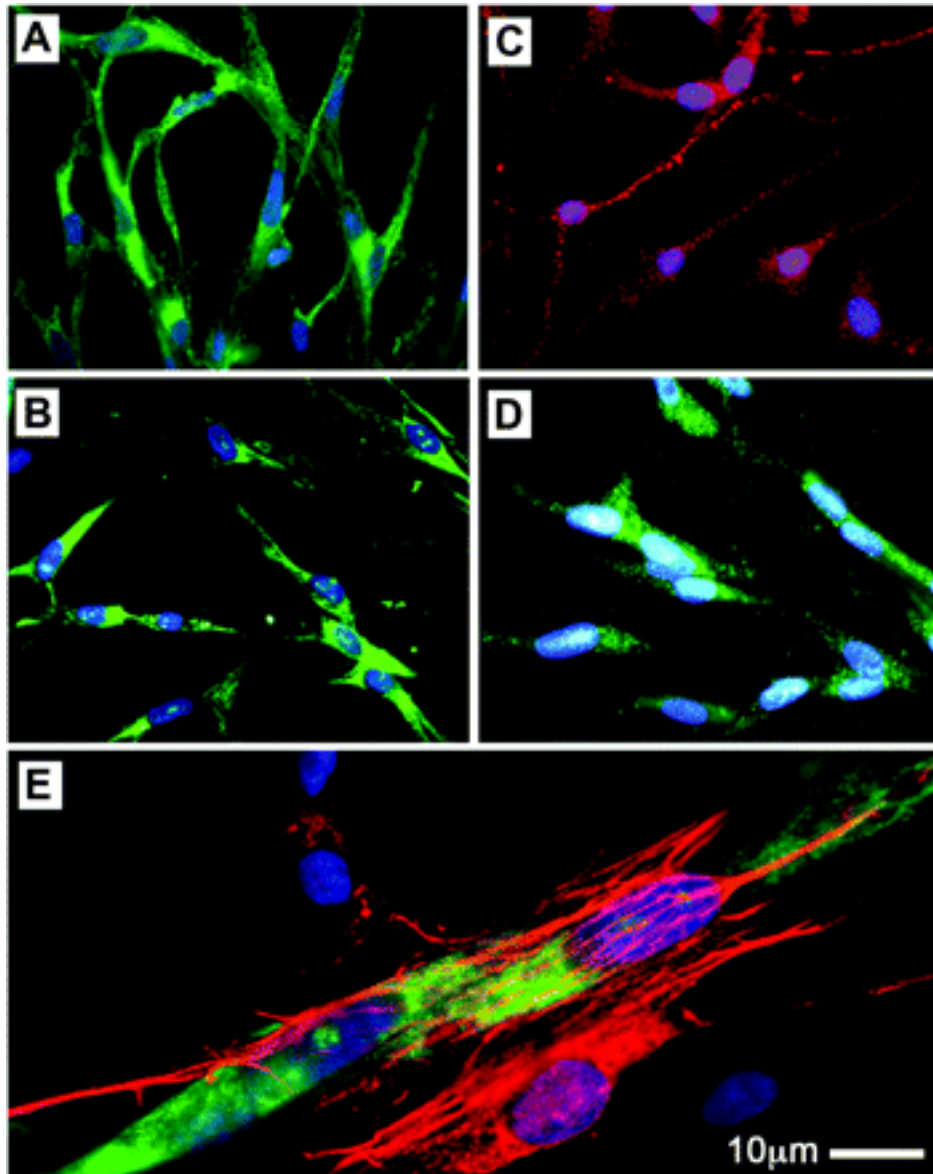
Figure 2.1. Immuno-phenotype of cells comprising the sprouts formed from human adipose tissue explants.
Representative photomicrographs of newly formed cells stained for endothelial cell markers CD31 (A), CD34 (B), endothelial nitric oxide synthase (C), and vWF (D) are shown. (E) displys cells expressing α-smooth muscle actin (red) with presumably pericytes forming a vWF-positive capillary branch (green). *Gealekman et al., Depot-Specific Differences and Insufficient Subcutaneous Adipose Tissue Angiogenesis in Human Obesity. Circulation, 2011.123(2): p. 186-194.*
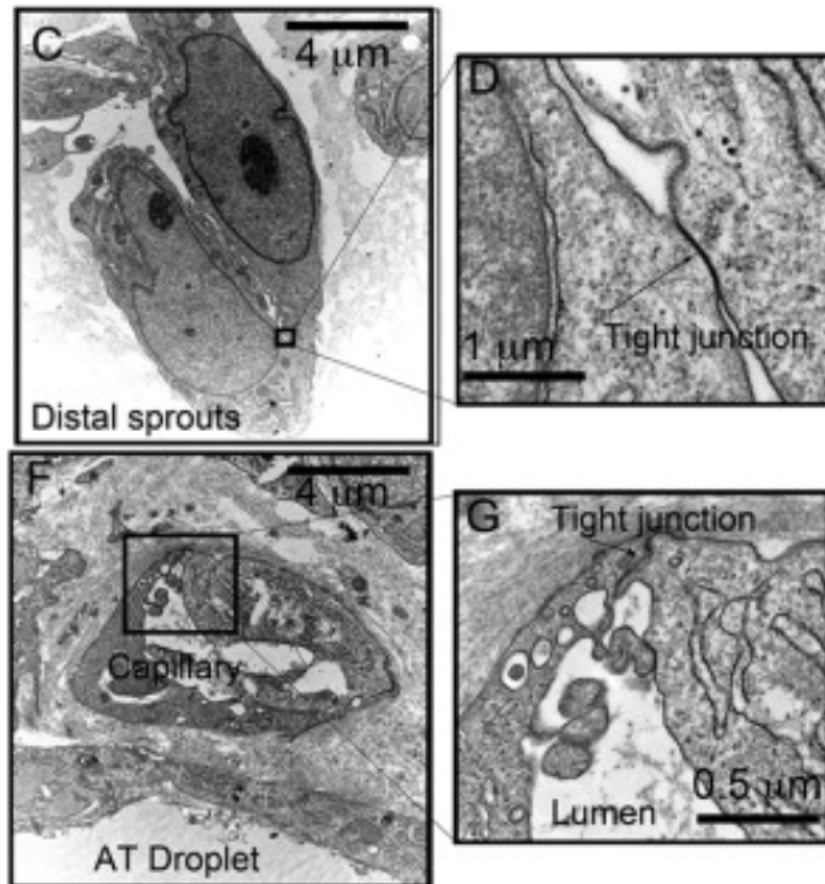
Figure 2.2. Angiogenic Sprouts Originating from Human Adipose Tissue.
(C) Electron microscopy of area similar to that shown in (B), where tight junctions can be seen to connect cells.
(D) Enlargement of tight junction found between two ECs.
(F) Electron microscopy of area similar to that shown in (E), revealing lumenized capillaries formed by ECs joined by tight junctions.
(G) Enlargement of area shown in (F).
(K) Electron microscopy of lipid-laden cells revealing features of classical white adipocytes and of ECs, such as the tight junction in the squared area.
(L) Enlargement of area outlined in (K).
Khanh-Van Tran *et al*., The Vascular Endothelium of the Adipose Tissue Gives Rise to Both White and Brown Fat Cells. 2012, Cell Metabolism. 15(2), 8: p. 222-229.

Materials and methods

General Methodology. No samples, mice or data points were excluded from the reported analyses. Samples were not randomized to experimental groups except where indicated. Analyses were not performed in a blinded fashion except where noted below.

Adipose Tissue. Subcutaneous adipose tissue was obtained from panniculectomies, with no a-priori selection of individual donors. All specimens were collected after informed consent in accordance with procedures approved by the University of Massachusetts Institutional Review Board.

Explants. Detailed methods for harvesting adipose tissue, culture of adipose tissue explants in Matrigel are published[96]. In brief, explants from human subcutaneous adipose tissue were cultured in EBM-2 media supplemented with endothelial growth factors (EGM-2 MV) (Lonza). In indicated experiments, Dulbecco's Modified Eagles Medium (Gibco) supplemented with 10% fetal bovine serum ((DMEM-FBS) was used, without or with supplementation with human fibroblast growth factor-B, human epidermal growth factor, long R3 insulin-like growth factor 1 and vascular endothelial growth factor at the concentrations used in EGM2-MV, as indicated. To induce adipogenesis we used a minimal adipogenic cocktail of DMEM +10% FBS, 0.5 mM 3-isobutyl-1-methylxanthine, 1 μM dexamethasone, and 1 μg/ml insulin (MDI) for 72 hours. The medium was then replaced with DMEM plus 10% FBS. Subsequently, 50% of

the medium was replaced with fresh medium every other day. Adipocyte markers were measured by RT-PCR in RNA extracted from 3 explants per condition. Results shown in Figures were reproduced in explants from all panniculectomy samples studied, albeit the magnitude of the induction of individual markers varied.

Cells. Detailed methods for harvesting adipose tissue, culture of adipose tissue explants in Matrigel, and harvesting of single cells from explant growth are published[96]. In brief, explants from human subcutaneous adipose tissue were cultured in EBM-2 media supplemented with endothelial growth factors (EGM-2 MV) (Lonza) for 14 days. Single cells suspensions from capillary growth (capillary network cells) were obtained using dispase[96], and plated on standard tissue culture plates. Growth and passaging of these cells was done using EGM-2 MV. Where indicated, adipogenic differentiation was induced by replacement of EGM-2 MV by DMEM +10% FBS, 0.5 mM 3-isobutyl-1-methylxanthine, 1 μM dexamethasone, and 1 μg/ml insulin (MDI). 72 hours later, the differentiation medium was replaced by DMEM-FBS, which was replaced every 48 hours until analysis. Adipocyte markers were measured by RT-PCR in RNA extracted from one well of a confluent 6 well multi-well dishes of cells. Stromal vascular fraction from human subcutaneous adipose tissue was isolated as described in Fitzgibbons *et al* [97]. In brief, the tissue was mechanically dissociated and treated with 2 mg/ml collagenase, respectively, in 20 mg/ml bovine serum albumin in phosphate-buffered saline at pH 7.4, 37°C for 1 hour. Samples were filtered through 200, 100 and 40 μM spectra mesh sequentially and red blood cells were lysed. The isolated cells by centrifuging the cell

suspension at 400 g were grown and expanded in 10% FBS DMEM.

Mice. Cells from capillary networks were grown to confluence on 150 mm dishes and differentiated using MDI for 10 days. Cells were detached from culture dishes by trypsin (0.5%)-collagenase (0.05%) digestion, suspended in Matrigel and injected (approximately 10^7 cells per mouse) into the dorsal region of 8 week-old male Nude mice. 7 mice were injected with 0.6 ml of differentiated capillary cells re-suspended in the same volume of Matrigel or 0.6 ml of DMEM with Matrigel as a control in each flank. Mice with differentiated capillary cells were sacrificed 24 weeks after the injection. Mice with non-differentiated capillary cells or stromal vascular cells were sacrificed 28 weeks after the injection. Human implants and endogenous mouse inguinal and epididymal adipose tissues were collected for RNA extraction.

Immunofluorescence. Capillary cells were incubated in culture media with 500 nM MitoTracker Red CMXRos (Invitrogen M7512) and 1:2000 Hoechst (Molecular Probes H21486) at 37°C for 30 minutes. After 30 minutes, media were changed before visualization under the microscope. Images were taken with a Zeiss Axiovert 100 inverted microscope and AxioCam HRm camera. Image processing and quantification was performed using ImageJ (FIJI) software, on a file containing all raw images to be analyzed thereby applying all corrections equally for all comparison groups. After background subtraction, the grey-scale image of adipocytes, images were converted into a binary image, and the size of particles

(individual adipocytes) was calculated by FIJI.

ELISA. Leptin concentration in the culture medium was measured using a human leptin ELISA from Invitrogen (KAC2281). 100 μl of media without dilution were loaded onto each well of ELISA plate. 9 well per group were measured. ELISA was run according to the manual.

RT-PCR. Adipocyte markers were measured by RT-PCR in RNA extracted from one well of a confluent 6 well multi-well dish of cells. Adipocyte markers were measured in RNA extracted from 3 explants per condition, or from one well of a confluent 6 well multi-well plates of cells. Probe sets used are shown in **Table 1**.

Statistical analyses. RT-PCR results are presented as means of technical replicates with error range indicated. Experiments shown are representative, and have been repeated a minimal of 5 times with cells derived from different individuals undergoing panniculectomy surgery, with no a priori selection. Software employed was GraphPad Prism v.6. To compare groups with normally distributed values, 2-tailed unpaired Student t-tests were used. When normality could not be determined, the Mann-Whitney test was used. Data are presented as mean values ± s.e.m., or range between technical replicates when experiments were representative, as indicated in each figure legend. P-values are indicated in each case. All representative experiments have been repeated a minimum of 5 times with tissue from different individuals, with similar results.

Results

To determine whether human adipocyte progenitors proliferate in conjunction with adipose tissue capillaries we used an *in vitro* system in which microvessels develop from adipose tissue fragments *in vitro*. Explants from human subcutaneous adipose tissue from individuals undergoing panniculectomy surgery were embedded in Matrigel and cultured in DMEM (Dulbecco's Modified Eagle's Medium) + 10% FBS (Fetal Bovine Serum), or in EGM2-MV (Endothelial Cell Growth Medium-Microvascular) in the absence or presence of pro-angiogenic growth factors VEGF (vascular endothelial growth factor), hFGF-B (human fibroblast growth factor B), hEGF (human epidermal growth factor), R³-IGF-1 (long R3 insulin-like growth factor 1) (**Fig 1a**), and imaged after 10 days in culture.

Capillary growth was negligible in explants cultured in either DMEM of EGM-2 MV in the absence of growth factors, but clearly measurable in DMEM or EGM-2 MV in their presence (Figure 2.3). Maximal growth was seen in EGM2-MV, consistent with the optimized pro-angiogenic properties of this medium. Over time cells at the tips of the sprouts projected thin filopodia into the gel, divided, and aligned to form thicker branches (Figure 2.4), which previously have been seen to include endothelial and non-endothelial cells[98, 99]. To determine whether any of these cells correspond to adipocyte progenitors, we exposed cultures to adipogenic conditions. Because activation of peroxisome-proliferator activated receptor gamma (PPARγ) by ligands such as thiazolidenediones can induce lipid accumulation in cells independently of adipogenic

conversion[100], we used a minimal adipogenic cocktail of 3-isobutyl-1-methylxanthine, dexamethasone and insulin (MDI). After approximately 6 days, we observed a loss of continuity between cells forming the capillary structure, and lipid droplets in cells within the capillaries (Figure 2.4). These morphological changes were accompanied by induction of classical adipocyte markers (Figure 2.5). These results were reproduced in explants from all panniculectomy samples studied (Table 2), albeit the magnitude of the induction of individual markers varied. Thus, proliferation of human adipocyte progenitors occurred in conjunction with capillary growth, and is critically dependent on pro-angiogenic growth factors.

Expanded and differentiated capillary cells, as embedded in Matrigel, were subjected to the human recombinant insulin (1 μM in culture) to address the question whether these capillary-derived human adipocytes behave *in vitro* as they do *in vivo*. After embedding of human adipose tissue explants, I grew the cells in EGM-2 MV for 18 days and induce adipocyte differentiation with MDI cocktail in 10% FBS DMEM for 14 days. Fresh insulin was added to the medium every the other day for 14 weeks. Picture of adipocytes were taken and smaller volume of fresh medium with insulin was introduced to detect human adiponectin secreted into the media. The fresh media was incubated for 3 days without media change and collected for human leptin ELISA. Compared to capillary-derived adipocytes appeared in Figure 2.3., adipocytes stimulated by insulin accumulated more lipid droplets and significantly enlarged their cell body. Also, as they grow larger adipocytes changed their distribution of lipid droplets from small multi-locular into large uni-locular. Adipocytes survived for at least 14 weeks *in vitro* culture

with insulin and still retained healthy mitochondria, confirmed by mitochondrial staining with 500 nM MitoTracker Red CMXRos and 1:2000 Hoechst. Human leptin ELISA detected human leptin from cultured media from these adipocytes. With insulin, leptin secretion was approximately 3-folds increased when 9 wells were tested in each group.
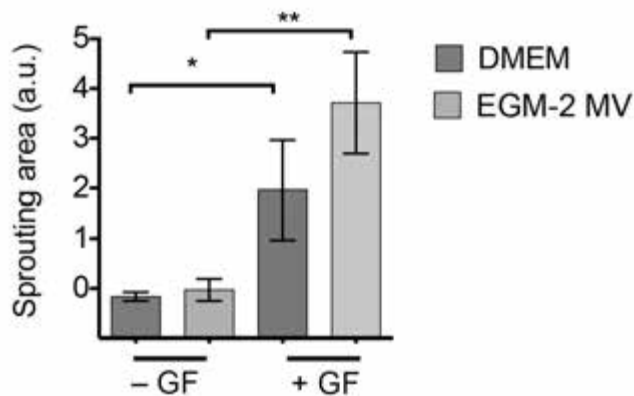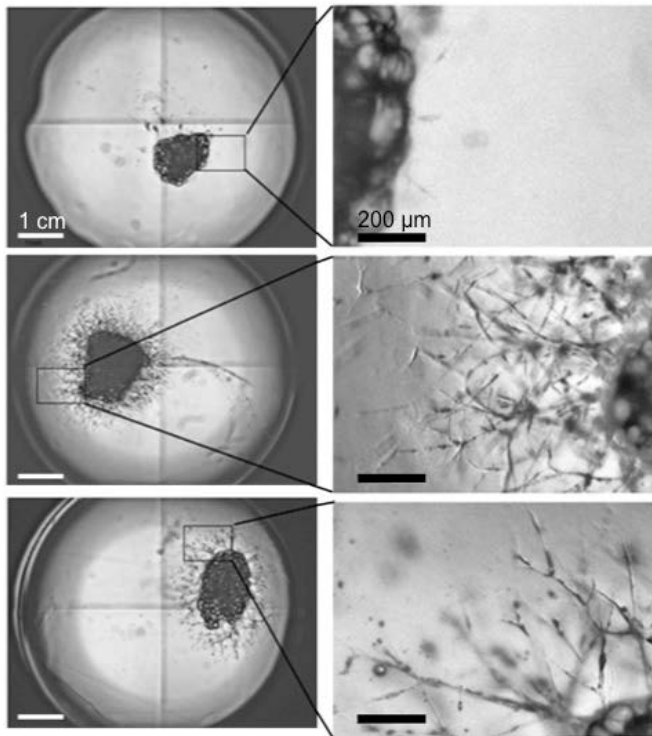
Figure 2.3. Quantification of capillary growth.
Top: Explant growth in DMEM (top), DMEM + angiogenic growth factors (middle) or
EGM-2 MV + angiogenic growth factors (bottom). Scale bars are 1 cm (left panels) and
200 μm (right panels).
Bottom Graph: Growth area (arbitrary units) from explants grown for 11 days in the
absence (– GF) or presence (+ GF) of angiogenic growth factors. Plotted are means and
s.e.m., from 6 explants per condition from 2 different individuals (*n* = 12). Statistical
significance was calculated using the Mann Whitney test * *P* < 0.05 ** *P* < 0.05.
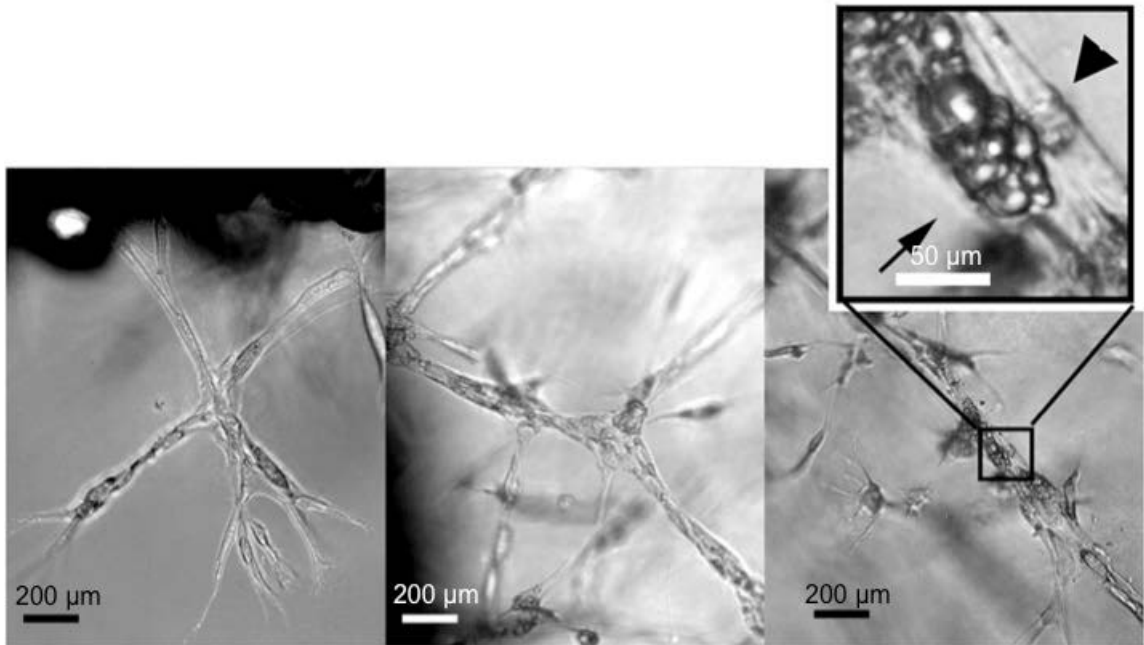
Figure 2.4. High-resolution representative images of explants grown for 5 (left), 12 (middle) or 18 (right) days, exposed to MDI at day 12. Arrowheads indicate elongated cells forming the sprouts, and arrows indicate lipid droplets. Scale bars are 200 μm and 50 μm (insert).
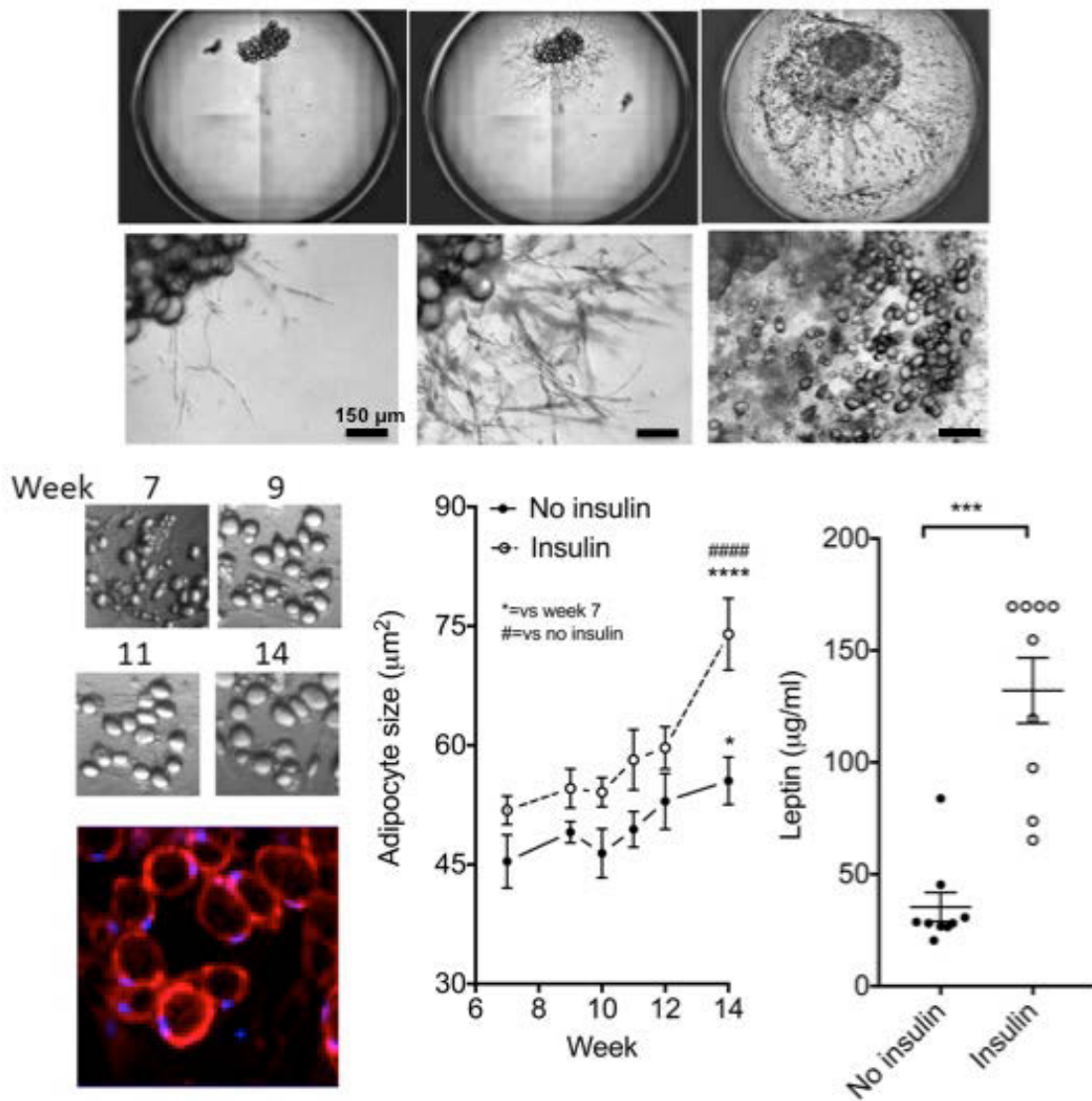
Figure 2.5. Biochemical characteristics of capillary-derived adipocytes.
Top: Left figure shows embedded human adipose explant in Matrigel with few sprouting capillary cells. Middle panel displays more capillary growth with EGM-2 MV. Adipocytes stimulated with human insulin in the left panel appear to be larger than those without insulin presented in Figure 2.4.
Bottom Left: Enlargement of adipocytes over time up to 14 weeks with insulin in culture. Cells stained with MitoTracker Red CMXRos (500 nM) and Hoechst (1:2000).
Bottom middle: Quantified adipocyte size by analyzing the pictures of adipocytes.
Bottom Right: Human leptin ELSA with 9 replicate wells.

To determine whether proliferation and/or differentiation of adipocyte progenitors required intercellular interactions within the capillary, or on interactions with Matrigel components, we generated single cell suspensions from the micro-vessels, passaged them once on standard tissue culture dishes and subjected them to differentiation. Numerous cells differentiated into adipocytes, identifiable by lipid droplets that increased in size and coalesced over time (Figure 2.6), and by the induction of adipocyte genes (Figure 2.7). Results shown were similar in capillary network cells from all explants studied, albeit the magnitude of the induction of individual genes varied.
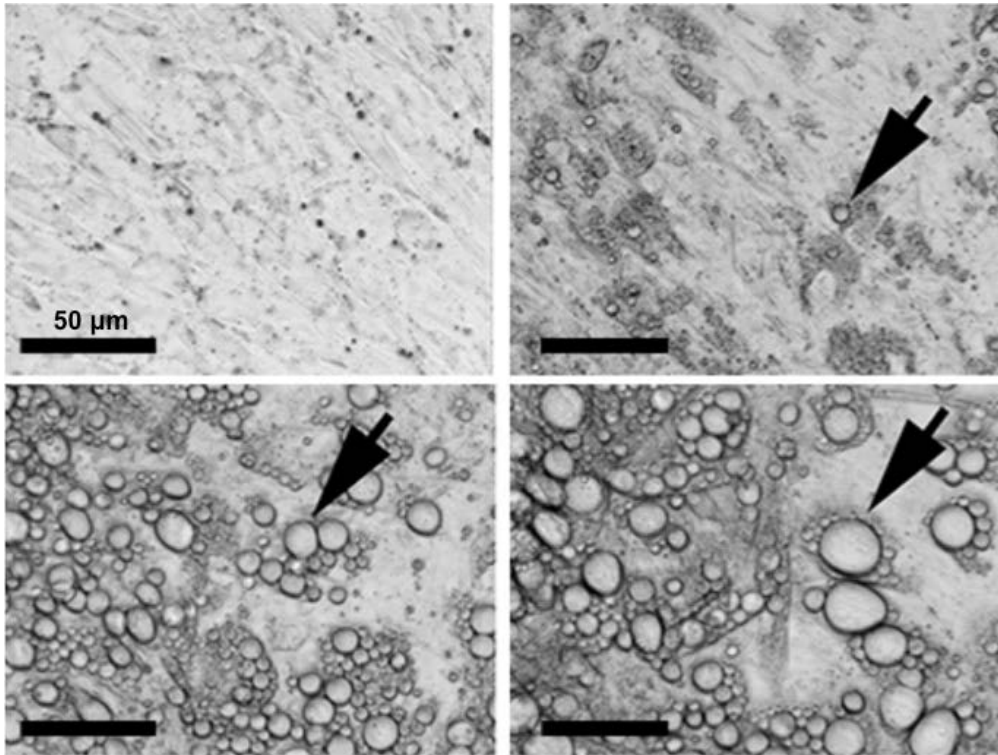
Figure 2.6. Morphology of capillary-derived adipocytes.
A representative field of capillary network cells at days 0 (top left), 6 (top right), 12 (bottom left) and 18 (bottom right) after induction of differentiation; arrows indicate growth of lipid droplets within a single adipocyte. Scale bars are 50 μm.
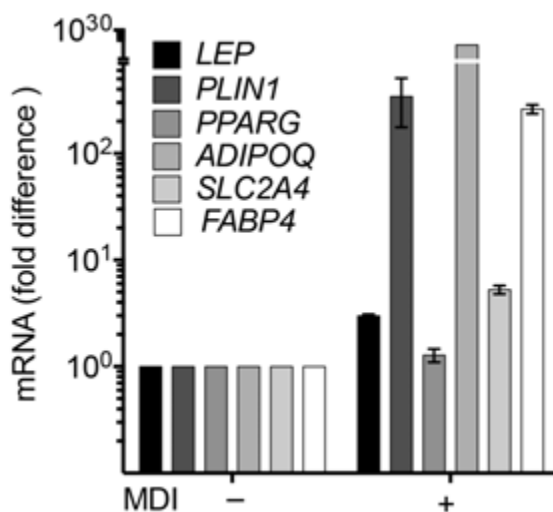
Figure 2.7. RT-PCR for adipogenic genes in non-differentiated (− MDI) or differentiated (+ MDI) cells seven days after induction of differentiation. RT-PCR results are expressed as the fold over the minimum detectable value in the series, and represent the means and range of 2 technical replicates, of representative experiments that have been replicated a minimum of three times with cells from separate individuals.

Next we tested whether these adipocytes from capillary networks can form a fat pad *in vivo*. The ability of forming a fat pad was compared among three cell types: capillary cells after differentiation (ASC-diff; adipose subcutaneous capillary cells-differentiated), capillary cells without differentiation (ASC) and stromal vascular fraction without differentiation (SVF). SVF or adipose-derived stromal cells is an entire cell population except for adipocytes harvested from adipose tissue. It is heterogeneous, yet has been studied in numerous studies as adipocyte progenitors[101]. Thus, the comparison between ASC and SVF could be useful to better understand the characteristics of adipocytes progenitors. All three populations were expanded in EGM-2 MV and maintained in 10% FBS DMEM with or without MDI. Then each was prepared for injection in a suspension with Matrigel as described in the Materials and Methods section. 28 weeks after the injection, mice injected with non-differentiated ASC or SVF were sacrificed. Mice with diff-ASC were sacrificed 28 weeks post injection. When put into Nude mice, all three cell-types formed a vascularized fat pad *in vivo* (Figure 2.8). However, RT-PCR results (Figure 2.9) showed the level of adiposity and vascularization of the fat pad varied in each condition. ASC-diff contained the highest amount of human adipocytes, followed by ASC and SVF. On the other hand, formation of human vascular endothelial tight junctions, assessed by CDH5, was highest in SVF and lowest in ASC-diff. We could also detect the infiltration of mouse adipocytes and vascular endothelial cells into the structure. To conclude, ASC retain their entity as adipocytes *in vivo* once they differentiation *in vitro* and can also can differentiate into adipocytes *in vivo* even when they are put into mice as preadipocytes. SVF preadipocytes are able to differentiate

into adipocyte *in vivo* as well but at a much lower level of differentiation compared to ASC.

Figure 2.8. Morphology of the implants.

Formed fat pad in a mouse injected with ASC-diff. The implant was harvested 24 weeks after the injection.

Formed fat pad in a mouse injected with ASC without *in vitro* differentiation. The implant was harvested 28 weeks after the injection.
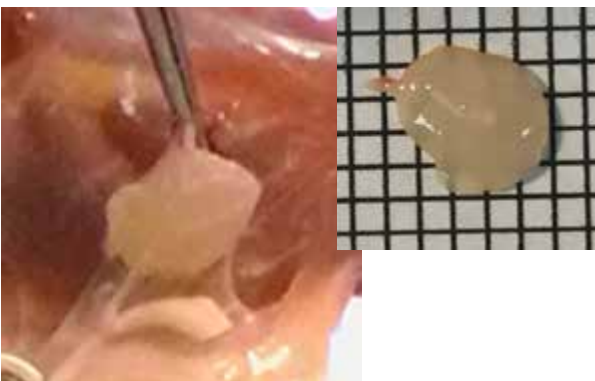
Formed fat pad in a mouse injected with SVF without *in vitro* differentiation. The implant was harvested 28 weeks after the injection.
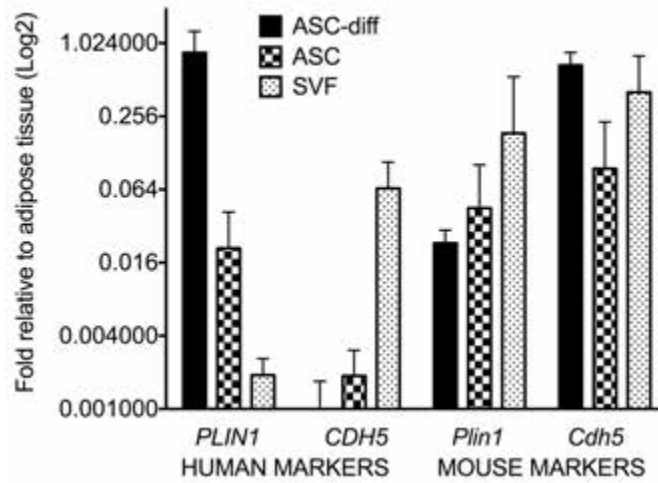
Figure 2.9. RT-PCR on formed fat pads. ASC-diff (n=4), ASC (n=7) and SVF (n=4). Technical triplicates. Human or mouse primers were designed to specifically detect human or mouse exclusively. PLIN1: perilipin1, CDH5: V-Cadherin. Values were plotted relative to the ASC-diff PLIN1.

Table 1. Human or mouse-specific probes used for RT-PCR

Gene name	Forward (Fw) or Reverse (Rv) probe Sequences
Human-specific CDH5 Fw	CTGCTGCAGGGTCTTTTTCT
Human-specific CDH5 Rv	AGGGCATGATGGTCAGTCTC
Mouse-specific CDH5 Fw	TACTCAGCCCTGCTCTGGTT
Mouse-specific CDH5 Rv	TGGCTCTGTGGTGCAGTTAC
Human-specific Perilipin1 Fw	ACCAGCAAGCCCAGAAGTC
Human-specific Perilipin1 Rv	CATGGTCTGCACGGTGTATC
Mouse-specific Perilipin1 Fw	CTGTGTGCAATGCCTATGAGA
Mouse-specific Perilipin1 Rv	CTGGAGGGTATTGAAGAGCCG
Human RPL4 Fw	TGTTTGCACCAACCAAAACCT
Human RPL4 Rv	GCAGAACAGATGGCGTATCGT
Mouse RPL4 Fw	CCCCTCATATCGGTGTACTCC
Mouse RPL4 Rv	ACGGCATAGGGCTGTCTGT

Discussion

In this chapter, the results showed that human adipocyte progenitor cells could be generated and expanded upon pro-angiogenic stimuli in adipose tissue capillary networks. Differentiated adipocyte progenitors responded to insulin, increased leptin secretion with insulin treatment, and expressed canonical adipogenic genes. These cells recapitulated the characteristics of human primary adipocyte *in vitro* and also *in vivo*. *In vitro* differentiated adipocyte progenitors formed a vascularized fat pad when put into Nude mice, which successfully maintained live human adipocytes with adipogenic gene expression signatures *in vivo*.

Comparison between adipose subcutaneous capillary cells (ASC) and adipose stromal vascular fraction (SVF) suggested that ASC better enriched adipocyte progenitors or the quality (viability, differentiation potential) of cells was superior in ASC. When injected with the same number of cells into Nude mice, ASC showed a higher level of human-specific adipocyte gene expression in the formed fat pad than SVF did. Considering the significant interests and frequent usage of SVF in the clinical fields, the discoveries from this thesis regarding improved harvesting and expanding methods for adult adipose stem cells could have a great impact on clinical applications. Given the fact that adipocyte progenitors were highly enriched in capillary associated cells, understanding the characteristics (markers, responsiveness to certain growth factors, differentiation potential into multiple cell types) of the ASC population will bolster the advancement of basic research on mechanism of adult stem cell expansion and

differentiation. Further investigation into cellular attributes of ASC at the clonal level is

described in the following CHAPTER V: Concluding remarks and future directions.

CHAPTER III: Human 'brite/ beige' adipocytes develop from capillary networks and their implantation improves metabolic homeostasis in mice

Author Contributions

Jamie Kady, Minwoo Nam, Raziel Rojas-Rodriguez, Aaron Berkenwald, Jong Hun Kim, Hye-Lim Noh, Jason K. Kim, Marcus P. Cooper, Timothy Fitzgibbons, Michael A. Brehm

Summary

The results in this chapter reveal that human adipocyte progenitor cells proliferate in response to pro-angiogenic stimuli in conjunction with adipose tissue angiogenesis, and display the cardinal feature of 'brite/beige' adipocytes. Brite/ beige adipocytes have the near absence of thermogenic gene expression under basal conditions, but their transcriptome profile changes remarkably in response to adrenergic stimulation, inducing a wide range of thermogenic genes. To our knowledge, these findings are the first to show the growth and differentiation of human 'brite/beige' cells, and the assessment of their effects of systemic glucose homeostasis. These cells differ from human brown adipocyte cell lines established through immortalization of human precursors [102, 103] or differentiation of human pluripotent stem cells[104] in their highly inducible expression of a thermogenic phenotype, in the development of uncoupled respiration, and in their capacity to affect metabolism upon transplantation *in vivo*. Unexpectedly, global gene expression analyses reveal that activation of human brite/beige adipocytes induces a

neuroendocrine phenotype including expression of interleukin-33, known to regulate glucose homeostasis in mice, and the proprotein convertase PCSK1, which is genetically associated with human obesity. The findings demonstrated in this chapter suggest a direct effect of human beige/brite adipocytes to improve glucose homeostasis, and reveal neuroendocrine properties that might contribute to these beneficial metabolic actions.

Introduction

Due to the energy wasting property of brown fat, researchers have been trying to answer these questions: 1) Do humans have thermogenic brown or inducible beige adipose tissue? 2) If so, do these thermogenic fat depots affect systemic metabolism? 3) If they are beneficial, how can we activate these depots?

For the first question, the use of 18F-fluoro-2-deoxy-d-glucose positron emission tomography computed tomography (18F-FDG-PET) imaging has made it evident that humans also have substantial amount of adipose depots with UCP1-positive adipocytes, and these tissues can take up glucose by cold or b-adrenergic agonist stimulation[77, 105-109].

Various selective markers for brown and beige adipocytes have been identified in mice and humans, although in human there are discrepancies among the literature primarily due to the high heterogeneity within human thermogenic fat depots. Unlike human infants with interscapular brown adipose tissue that resembles rodent brown fat[77], adult humans have the most enriched with uncoupling protein1 (UCP1)-positive adipocytes in the supraclavicular region with both *bona fid* brown (UCP1, ZIC1 and LHX8)[110] and beige (Tbx1, Cd137, Tmem26, Cited1) adipocytes, depending on the depth in the neck [110-112].

Hence, to clarify these complex findings, Xue *et al*.[113] and Shinoda *et al*.[114] have recently isolated and immortalized clonal UCP1-positive adipocytes from adult human neck brown adipose tissue. Genome-wide analyses based on microarray indicated

that the cloned human brown adipocytes possess molecular signatures that resemble murine beige adipocytes, rather than classical brown adipocytes[114]. This evidence suggests that adult human neck brown fat is mainly, if not all, composed of recruit-able beige adipocytes. This view is supported by other works on chronic cold acclimation–recruited brown fat in the supraclavicular region of adult humans, which did not present detectable brown fat activity before activation[76, 115, 116].

Excitingly, the presence of inducible brown adipose tissue is associated with an increase in cold-induced energy expenditure[76, 78, 81, 109, 115] and an improvement in postprandial insulin sensitivity[116].

The last question whether we can activate these thermogenic depots can be in part answered by the complete summary by Shingo *et al*. of recently discovered molecular mechanisms of environmental cues that induce beige adipocyte biogenesis[117]. The list includes cold exposure, exercise, bariatric surgery, cachexia, BDNF, innate immunity (IL-33, IL4, BMP4, BMP7, BMP8b), endocrine hormones (FGF21, GDF5, natriuretic peptides, VEGF, PPARγ agonists, FXR agonist) and compounds (notch inhibitor, GLP1 agonist, TBK1 and IKK-e inhibitor, guanylyl cyclase, TGFβ antagonists).

A profound number of studies have contributed to our understating of human brown and beige adipocytes, by which we can answer those three key questions. However, we still have limited knowledge on cellular identities of UCP1-positive adipocytes in other adipose depots such as in the subcutaneous white adipose depots. In this chapter, our study validated the presence of beige adipocyte progenitors in human subcutaneous adipose tissue, adipocytes from which induced UCP1 expression upon

adrenergic stimuli, displayed uncoupled respiration, and finally exhibited metabolic

benefits in mice.

Materials and methods

General Methodology. No samples, mice or data points were excluded from the reported analyses. Samples were not randomized to experimental groups except where indicated. Analyses were not performed in a blinded fashion except where noted below.

Materials. Matrigel from BD biosciences (56231); EGM-2 MV from Lonza; Anti-human UCP1 antibody from Abcam (ab10983); anti Heat Shock Protein 70 from ThermoFisher Scientific (MA3-028); anti human IL-33 from ThermoFisher Scientific (PA5-20397); Adiponectin human-specific ELISA kits from Invitrogen (KHP0041); Forskolin and Isoproterenol hydrochloride from Sigma (F3917 and I6504, respectively). iButtons were purchased from Embedded Data Systems (DS1922L-F5#).

Adipose Tissue. Subcutaneous adipose tissue was obtained from panniculectomies, and peri-carotid adipose tissue from elective vascular surgeries with no a-priori selection of individual donors. All specimens were collected after informed consent in accordance with procedures approved by the University of Massachusetts Institutional Review Board. The characteristics of patients from which tissues were used for indicated experiments are described (Table 2).

Explants. Detailed methods for harvesting adipose tissue, culture of adipose tissue explants in Matrigel are published[96]. In brief, explants from human subcutaneous

adipose tissue were cultured in EBM-2 media supplemented with endothelial growth

factors (EGM-2 MV) (Lonza). In indicated experiments, Dulbecco's Modified Eagles

Medium (Gibco) supplemented with 10% fetal bovine serum (DMEM-FBS) was used,

without or with supplementation with VEGF (vascular endothelial growth factor), hFGF-

B (human fibroblast growth factor B), hEGF (human epidermal growth factor), R^3-IGF-1

(long R3 insulin-like growth factor 1) at the concentrations used in EGM2-MV, as

indicated. To induce adipogenesis we used a minimal adipogenic cocktail of DMEM

+10% FBS, 0.5 mM 3-isobutyl-1-methylxanthine, 1 μM dexamethasone, and 1 μg/ml

insulin (MDI) for 72 hours. The medium was then replaced with DMEM plus 10% FBS.

Subsequently, 50% of the medium was replaced with fresh medium every other day.

Adipocyte markers were measured by RT-PCR in RNA extracted from 3 explants per

condition. Results shown in Figures were reproduced in explants from all panniculectomy

samples studied (Table 2), albeit the magnitude of the induction of individual markers

varied.

Cells. Detailed methods for harvesting adipose tissue, culture of adipose tissue explants

in Matrigel, and harvesting of single cells from explant growth are published[96]. In

brief, explants from human subcutaneous adipose tissue were cultured in EBM-2 media

supplemented with endothelial growth factors (EGM-2 MV) (Lonza) for 14 days. Single

cells suspensions from capillary growth (capillary network cells) were obtained using

dispase[96], and plated on standard tissue culture plates. Growth and passaging of these

cells was done using EGM-2 MV. Where indicated, adipogenic differentiation was

induced by replacement of EGM-2 MV by DMEM +10% FBS, 0.5 mM 3-isobutyl-1-methylxanthine, 1 μM dexamethasone, and 1 μg/ml insulin (MDI). 72 hours later, the differentiation medium was replaced by DMEM-FBS, which was replaced every 48 hours until analysis. In experiments to investigate the effects of 'brite/beige' adipocytes *in vivo*, cells from capillary networks were grown to confluence into 150 mm dishes, differentiated using MDI for 10 days, and browning induced for 7 days with forskolin. Cells were then were recovered from culture dishes by trypsin-collagenase digestion, suspended in Matrigel and injected (approximately 10^7 cells per mouse) into the dorsal region of male NOD-*scid IL2rg^{null}* (NSG) mice[118].

ELISA. Adiponectin concentration in the culture medium was measured using a human-specific adiponectin ELISA from Invitrogen (KHP0041). For analysis of thermogenic gene expression, isoproterenol and forskolin were used at final concentrations of 10 and 50 μM, unless otherwise indicated in the figures.

RT-PCR. Adipocyte markers were measured by RT-PCR in RNA extracted from one well of a confluent 6 well multi-well dish of cells. Adipocyte markers were measured in RNA extracted from 3 explants per condition, or from one well of a confluent 6 well multiwell dish of cells. Probe sets used are shown in **Table 3**.

Immunofluorescence. Cells were fixed in 4% formaldehyde, stained, mounted and imaged with a Zeiss Axiovert 100 inverted microscope and AxioCam HRm camera. Image processing and quantification was performed using ImageJ (FIJI) software, on a

file containing all raw images to be analyzed thereby applying all corrections equally for all comparison groups. After background subtraction the greyscale image is converted into a binary image, and the sum of white pixels in each individual image is recorded.

Oxygen consumption. Oxygen consumption and mitochondrial parameters in intact cells were obtained using the XF24 Extracellular Flux Analyzer equipped with a FluxPak mini kit (#100867-100) from Seahorse Biosciences. In this system, oxygen consumption rates are calculated from 4 independent measurements obtained at 5 min intervals at baseline and after addition of specific drugs. For each experiment, the means from 3 replicate wells were recorded. For assessment of mitochondrial parameters, the values for the 4 independent measurements recorded for each condition were averaged, and parameters calculated as follows: ATP-linked respiration = basal OCR - oligomycin OCR; Proton leak = oligomycin OCR - rotenone+antimycin OCR; maximal capacity= FCCP OCR; reserve capacity = FCCP OCR – basal OCR; non-mitochondrial respiration = rotenone + antimycin OCR. Values presented are the means and s.e.m. of 4 independent experiments. For assessment of GDP sensitivity, cells were detached using trypsin/collagenase and suspended in respiration buffer[119], permeabilized with 20 μg/ml digitonin in respiration buffer for 5 minutes, washed again and oxygen consumption measured at 1 sec intervals using a Clark-type Oxygraph Plus recorder (Hansatech Instruments). Oxygen consumption rates were expressed as the slopes of the linear regression fits for each trace, derived from a minimum of 300 points, after each addition. GDP was used at a final concentration of 1 mM.

Affymetrix arrays. Total RNA was isolated using TRIzol. Affymetrix protocols were followed for the preparation of cRNA, which was hybridized to HTA-2.0 arrays. Raw expression data collected from an Affymetrix HP GeneArrayScanner was normalized across all data sets using the RMA algorithm as implemented by the Affymetrix Expression Console. Expression analysis was performed using the Affymetrix Transcriptome Analysis Console v.3.0. The data discussed in this publication have been deposited in NCBI's Gene Expression Omnibus and are accessible through GEO Series accession number GSE73385.

Mice. All animal use was in accordance with the guidelines of the Animal Care and Use Committee of the University of Massachusetts Medical School. For all experiments reported male NOD.Cg-PrkdcscidIl2rgtm1Wjl/SzJ (NOD-scid IL2rγnull, NSG) mice[118] were used, at 12-14 weeks of age. Mice were obtained from the Jackson Laboratory.

In experiments to investigate the effects of 'brite/beige' adipocytes *in vivo*, cells from capillary networks were grown to confluence into 150 mm dishes, differentiated using MDI for 10 days, and browning induced for 7 days with forskolin. Cells were then were recovered from culture dishes by trypsin-collagenase digestion, suspended in Matrigel and injected (approximately 10^7 cells per mouse) into the dorsal region of male NOD-*scid IL2rg^{null}* (NSG) mice[118].

Mice were injected subcutaneously with Matrigel or cells suspended in Matrigel After the times indicated, animals were sacrificed and tissues were removed for further study. Where indicated, mice were fed with a 60% high fat diet (Research Diets, Inc. D12492). Glucose tolerance curves were performed with 2g/Kg glucose after 8 or16h fasting, as indicated. The sample size chosen for glucose tolerance tests, temperature recordings and hyperinsulinemic-euglucemic clamp studies were based on preliminary data in control mice to determine variance for each parameter. Male animals of similar age bred under the same conditions were randomly assigned to Matrigel or cells, or to non-stimulated or forskolin-stimulated cells, and the investigator conducting the glucose tolerance tests, hyperinsulinemic-euglycemic clamps, and serum adiponectin measurements was blinded to the group (matrigel or cells, normal diet or high fat diet) allocation.

Hyperinsulinemic-euglycemic clamp. Survival surgery was performed at 5~6 days before clamp experiments to establish an indwelling catheter in the jugular vein. On the day of the clamp experiment, mice were fasted overnight (~15 hours), and a 2-hour hyperinsulinemic-euglycemic clamp was conducted in conscious mice with a primed and continuous infusion of human insulin (150 mU/kg body weight priming followed by 2.5 mU/kg/min; Humulin, Eli Lilly & Company, Indianapolis, IN, USA). To maintain euglycemia, 20% glucose was infused at variable rates during clamps. Whole body glucose turnover was assessed with a continuous infusion of [3-^{3}H] glucose (PerkinElmer, Waltham, MA, USA), and 2-7deoxy-D-[1-^{14}C]glucose (2-[^{14}C]DG) was

administered as a bolus (10 µCi) at 75 minutes after the start of clamps to measure insulin-stimulated glucose uptake in individual organs.

Statistical analyses. RT-PCR results are presented as means of technical replicates with error range indicated. Experiments shown are representative, and have been repeated a minimal of 5 times with cells derived from different individuals undergoing panniculectomy surgery, with no a priori selection. The number of animal chosen for glucose tolerance tests, temperature recordings and hyperisnulinemic-euglucemic clamp studies were based on preliminary data in normal control mice to determine variance for each parameter. Software employed was GraphPad Prism v.6. To compare groups with normally distributed values, 2-tailed unpaired Student t-tests were used. When normality could not be determined, the Mann-Whitney test was used. Data are presented as mean values ± s.e.m. or range between technical replicates when experiments were representative, as indicated in each figure legend. P-values are indicated in each case. All representative experiments have been repeated a minimum of 5 times with tissue from different individuals, with similar results.

Results

To determine whether cells generated from capillary networks include 'brite/beige' adipocytes, we stimulated cultures acutely and chronically with the adenylate cyclase activator forskolin, and analyzed thermogenic gene expression by RT-PCR (Figure 3.1). UCP1 mRNA was almost undetectable before and after adipogenic differentiation, but was induced rapidly in response to forskolin, and remained elevated in response to chronic exposure to the drug, as were canonical brown fat cell genes CIDEA (cell death inducing DFFA-like effector a) and DIO2 (deiodinase 2) (Figure 3.1). We also detected genes previously identified in mouse adipocyte progenitors, including CD29 (integrin beta 1), CD24 (cluster of differentiation 24), PDGFRA (platelet-derived growth factor receptor alpha) and ZNF423 (zinc finger protein 423), or enriched in 'brite/beige' adipocytes and human and mouse adipose tissue[120] (Fig. 3.2). To determine whether cells responded to physiological stimuli that cause "browning" *in vivo,* we compared the responses of non-differentiated and differentiated cells to forskolin and isoproterenol (Fig. 3.3). No induction was seen in non-differentiated cells, but differentiated adipocytes responded to both stimuli (Fig. 3.3). Notably, the human-selective β3 adrenergic agonist Mirabegron, which activates human supraclavicular fat[121], was more potent than the murine-selective β3 agonist CL316,243 in inducing UCP1 expression in differentiated cells (Fig. 3.3), consistent with the presence of functional β3 adrenergic receptors in these human adipocytes.
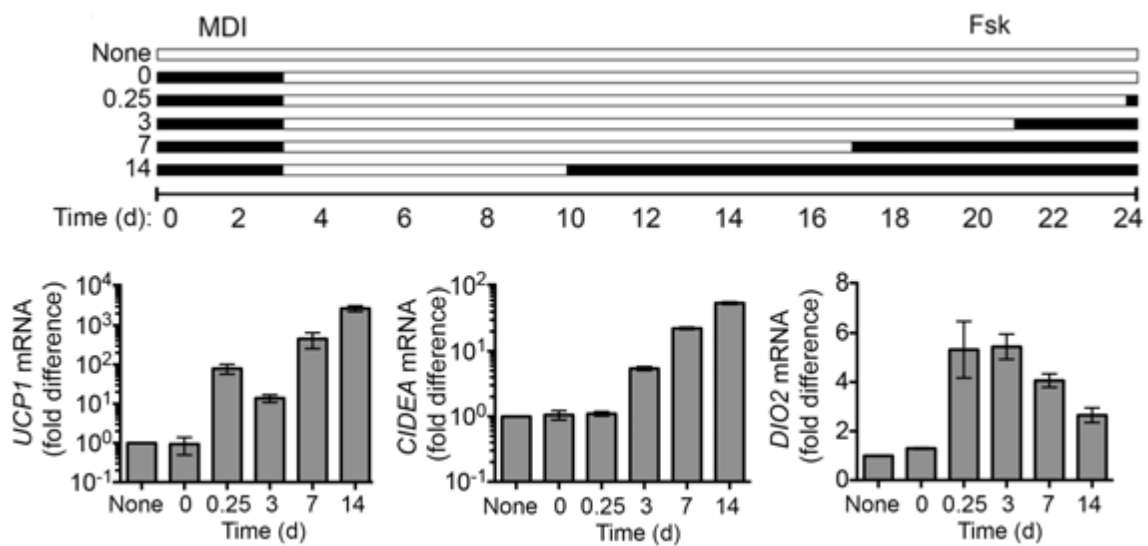
Figure 3.1. RT-PCR of thermogenic genes. Experimental scheme (top) and RT-PCR of indicated genes (bottom), expressed as the fold over the minimum detectable value in the series. Shown are means and range of 2 technical replicates. These results have been replicated with cells from 3 separate individuals.
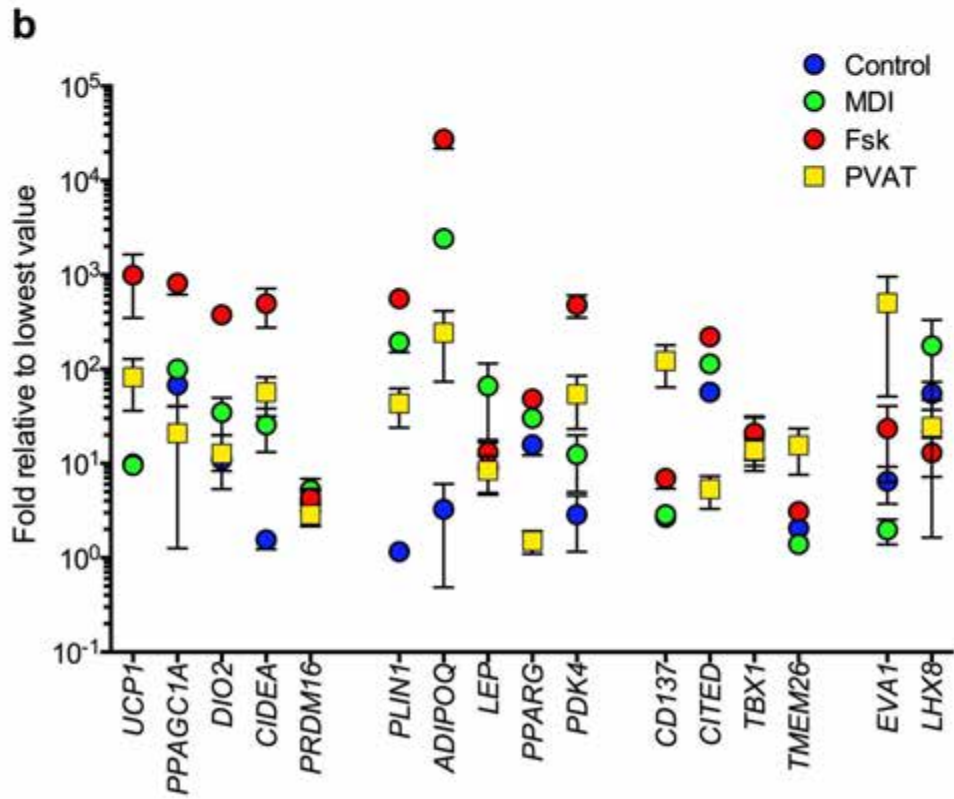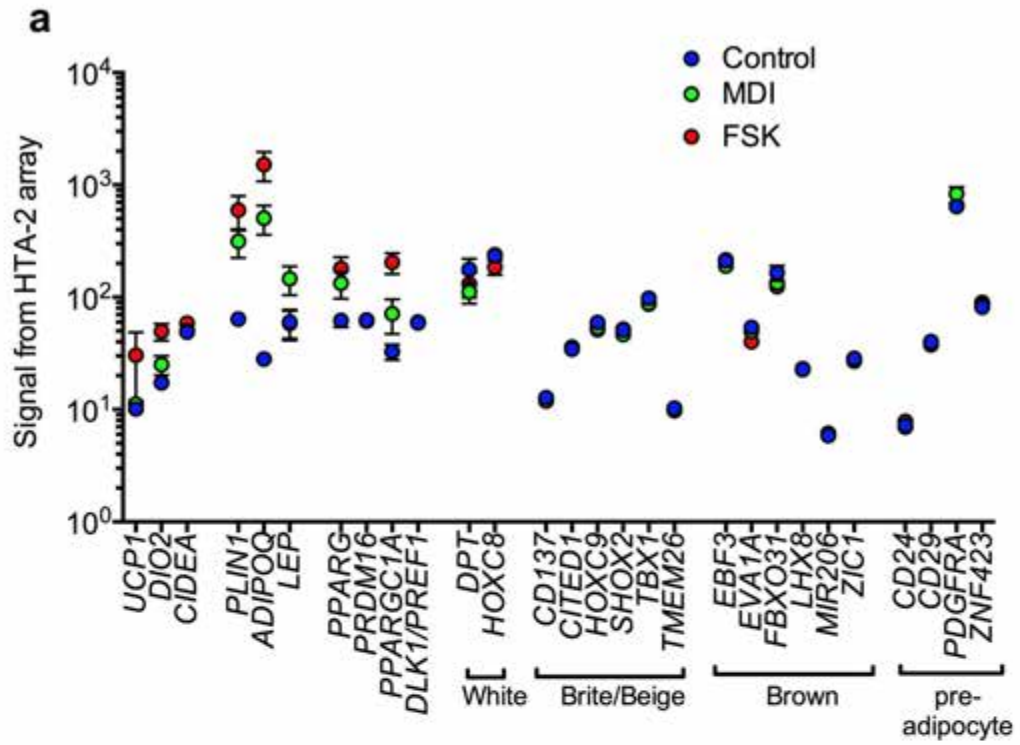
Figure 3.2. Expression of pre-adipocyte and beige/brown adipocyte markers in cells from human capillary networks. a) Mean probe intensity values obtained in HTA-2.0 Affymetrix arrays for the genes indicated on the x-axis, for cells without exposure to differentiation cocktail (Control), exposed to MDI for 3 days and cultured for an additional 11 days (MDI), or treated as in MDI but exposed to forskolin for 7 days prior to RNA extraction (FSK). b) RT-PCR analysis for genes indicated in the x-axis, for cells prepared as described in (a), compared to samples from peri-carotid fat obtained from 4 individuals. Values are expressed as the fold over the lowest detected value in the set for each gene. Values for C, MDI and FSK represent the mean and SEM from cells derived from three individuals.
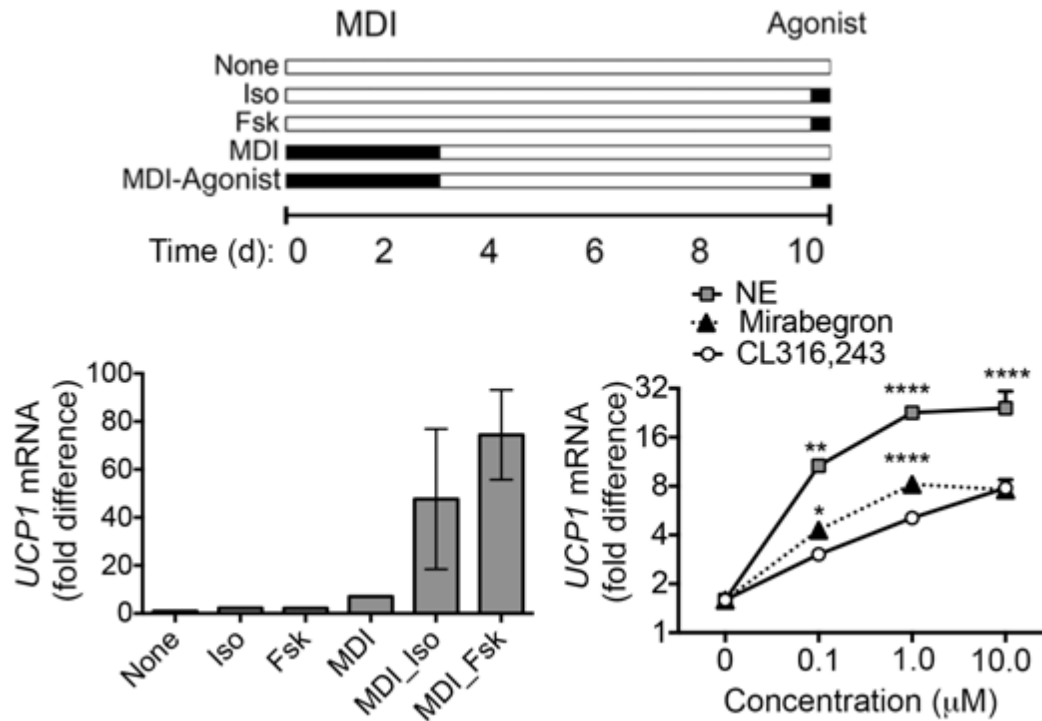
Figure 3.3. UCP1 mRNA expression. Experimental scheme (top) and UCP1 mRNA expression (bottom left) in cells exposed to isoproterenol or forskolin as indicated in the scheme, or in response to different concentrations of adrenergic agonists (bottom right). Plotted are means and s.e.m. of 3 biological replicates ($n = 3$); statistical difference relative to CL316,243 was determined at each concentration using Student t-tests corrected for multiple comparisons using the Holm-Sidak method * $P < 0.05$, ** $P < 0.01$, **** $P < 0.0001$.

The increase in UCP1 mRNA levels translated into an increase in protein as UCP1 was detected by immunofluorescence in most adipocytes, and progressively increased in abundance upon chronic exposure to forskolin (Figure 3.4). Mitochondria containing UCP1 were rounded, dense and abundant (Figure 3.5), a feature reminiscent of brown adipose tissue mitochondria[122]. In contrast, interspersed cells containing no detectable UCP1 contained the linear, sparse mitochondria (Figure 3.5).
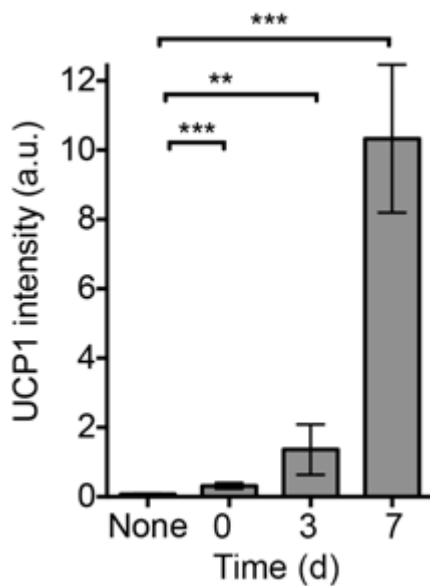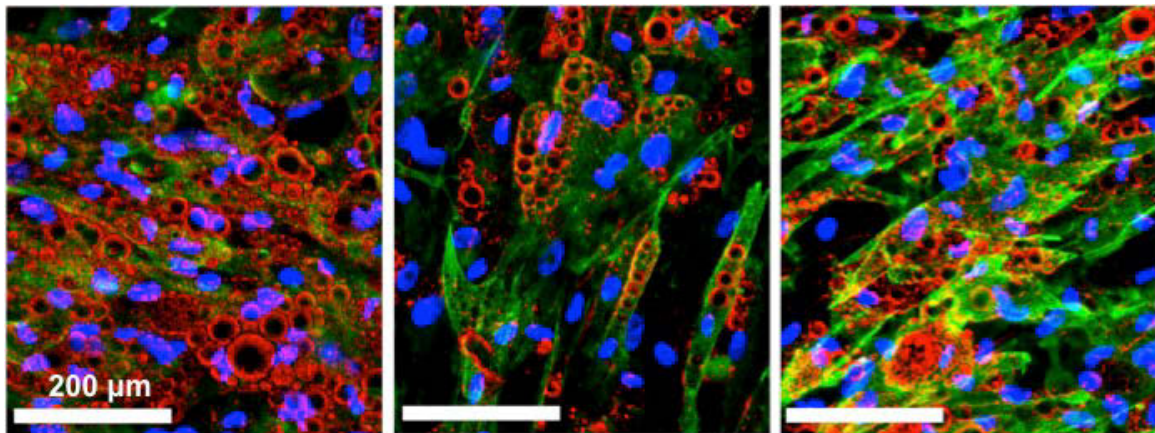
Figure 3.4. UCP1-protein expression. Differentiated cells exposed to forskolin for 0 (left panel), 3 (middle panel) and 7 (right panel) days showing UCP1 (green), lipid droplets (red), and nuclei (blue). Scale bars are 200 μm. Plotted are means and s.e.m. of UCP1 staining intensity from 2 fields per coverslip, of cells from 3 different individuals ($n = 6$). Statistical significance was assessed using the Mann-Whitney test versus non-differentiated cells, ** $P < 0.01$ *** $P < 0.001$.
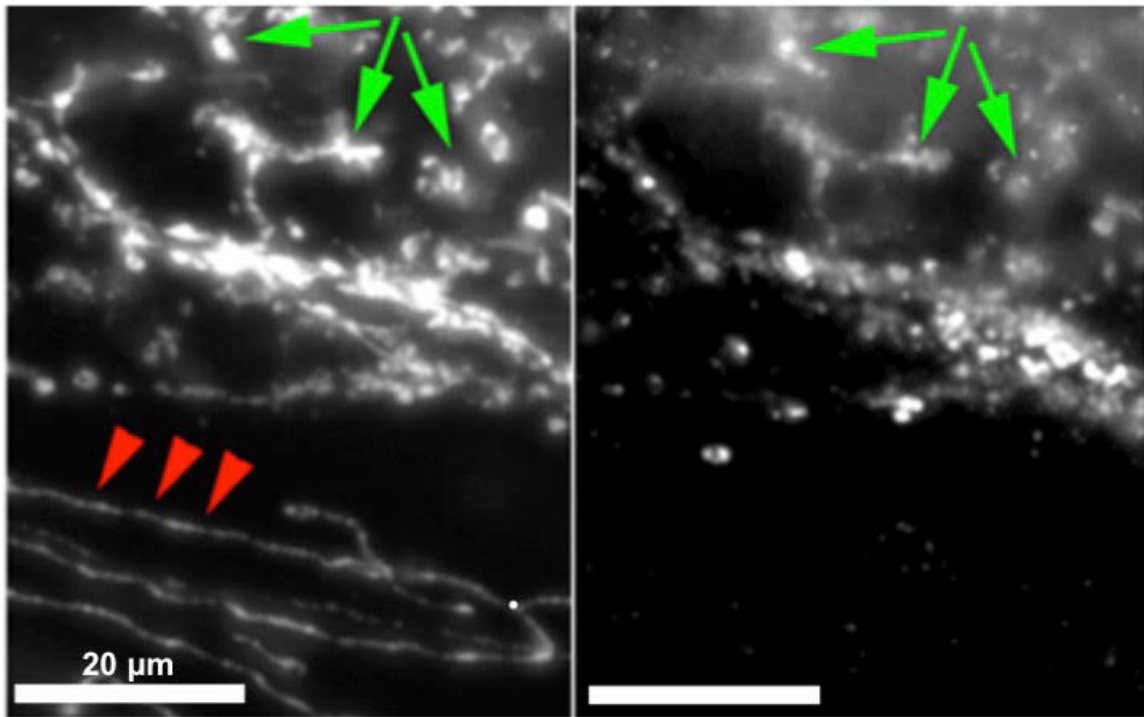
Figure 3.5. Immunofluorescence-staining for mitochondria. Mitochondrial Hsp70 (left panel) and UCP1 (right panel) in adipocytes exposed to forskolin for 1 week. Arrowheads indicate linear mitochondrial structures in cell devoid of UCP1. Arrows indicate rounded mitochondrial structures containing both UCP1 and Hsp70. Scale bars are 20 μm.

UCP1 was functionally significant, as cells treated chronically with forskolin displayed enhanced basal and uncoupled oxygen consumption (Figure 3.6), and mitochondrial parameters following addition of specific inhibitors (Figure 3.6) revealed decreased ATP-linked oxygen consumption and enhanced proton leak. The enhanced proton leak was at least in part attributable to the presence of UCP1, as respiratory rate was inhibited in response to 1 mM GDP in digitonin-permeabilized cells (Figure 3.7).
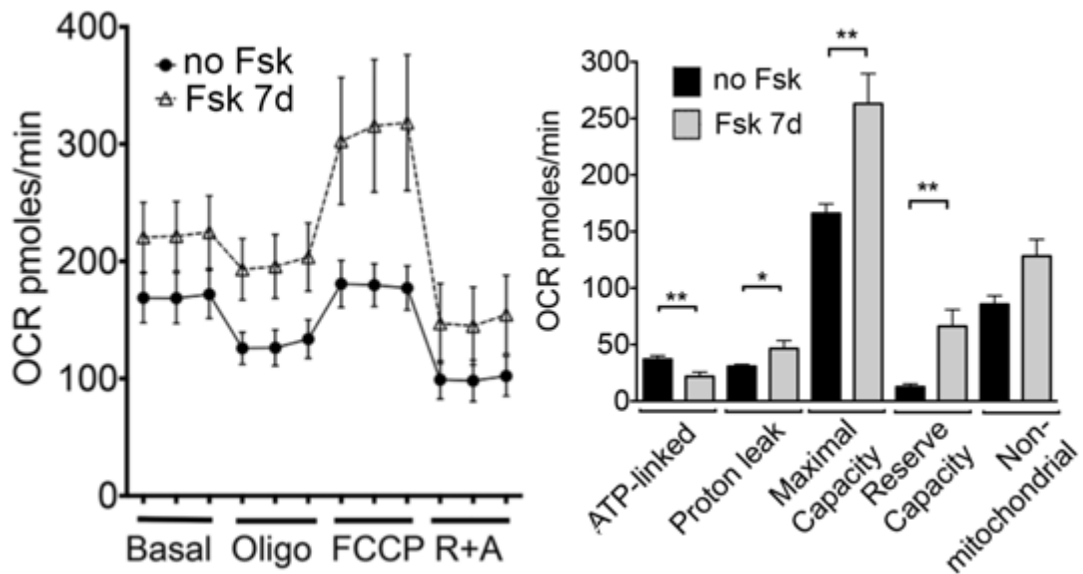
Figure 3.6. Oxygen consumption rate by Seahorse.
Left: Oxygen consumption by adipocytes exposed to vehicle or forskolin for 7 days. Plotted are the means and s.e.m. of 4 experiments assayed in triplicate ($n = 4$).
Right: Summary data for oxygen consumption parameters, calculated as described in online methods, derived from the means and s.e.m. of cells from 4 separate individuals assayed in triplicate ($n = 4$). Statistical significance was assessed using 2-tailed unpaired Student t-tests, $* P < 0.05$, $** P < 0.005$.
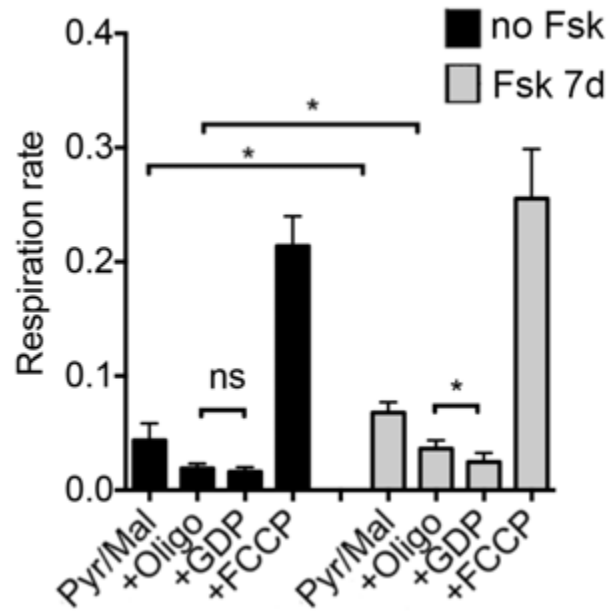
Figure 3.7. Oxygen consumption rate with digitonin.
Oxygen consumption rate in digitonin-permeabilized adipocytes exposed to vehicle or forskolin for 7 days. Plotted are the means and s.e.m. of four experiments (n=4). Statistical significance assessed using 2-tailed unpaired Student t-tests, *$P < 0.05$.

Other changes consistent with known properties of thermogenic adipocytes were also seen, including the remodeling of large lipid droplets into numerous small lipid droplets (Figure 3.8)[123, 124], accompanied by a large increase in expression of PLIN1 (perilipin-1) (Figure 3.9), consistent with an increase in droplet surface. Increased expression of FABP4 (fatty acid binding protein 4) and SLC2A4 (Glut 4), involved in uptake of lipids and glucose, and changes in expression of LEP (leptin) (decreased) and ADIPOQ (adiponectin) (increased) were observed (Figure 3.9), a pattern consistent with circulating concentrations of these adipokines in mice treated with 'pro-browning' β3 adrenergic agonists[125]. Thus, adipocytes derived from human capillary networks possess the cardinal biochemical and physiological characteristics of 'brite/beige' cells.
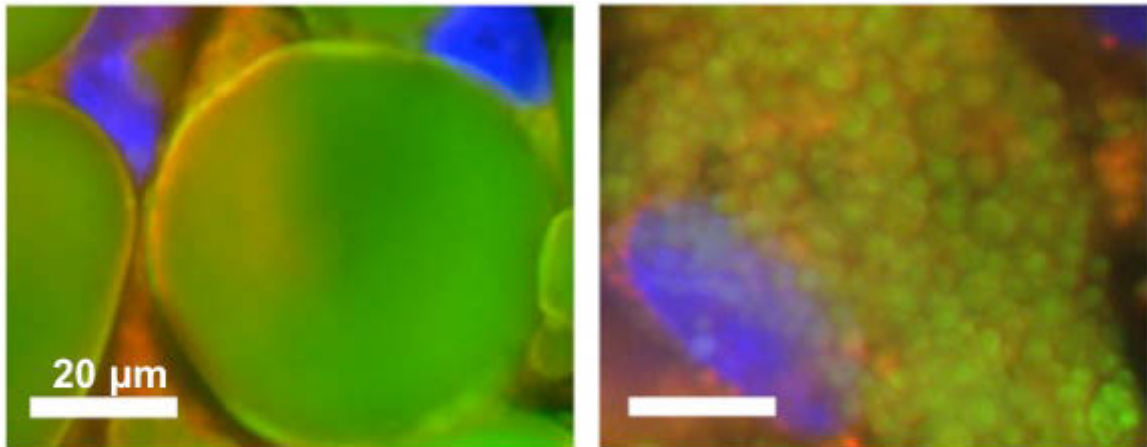
Figure 3.8. **Lipid droplets (green), mitochondria (red) and nuclei (blue) in adipocytes** without (left) or with (right) exposure to forskolin for 14 days. Scale bars are 20 μm**.**
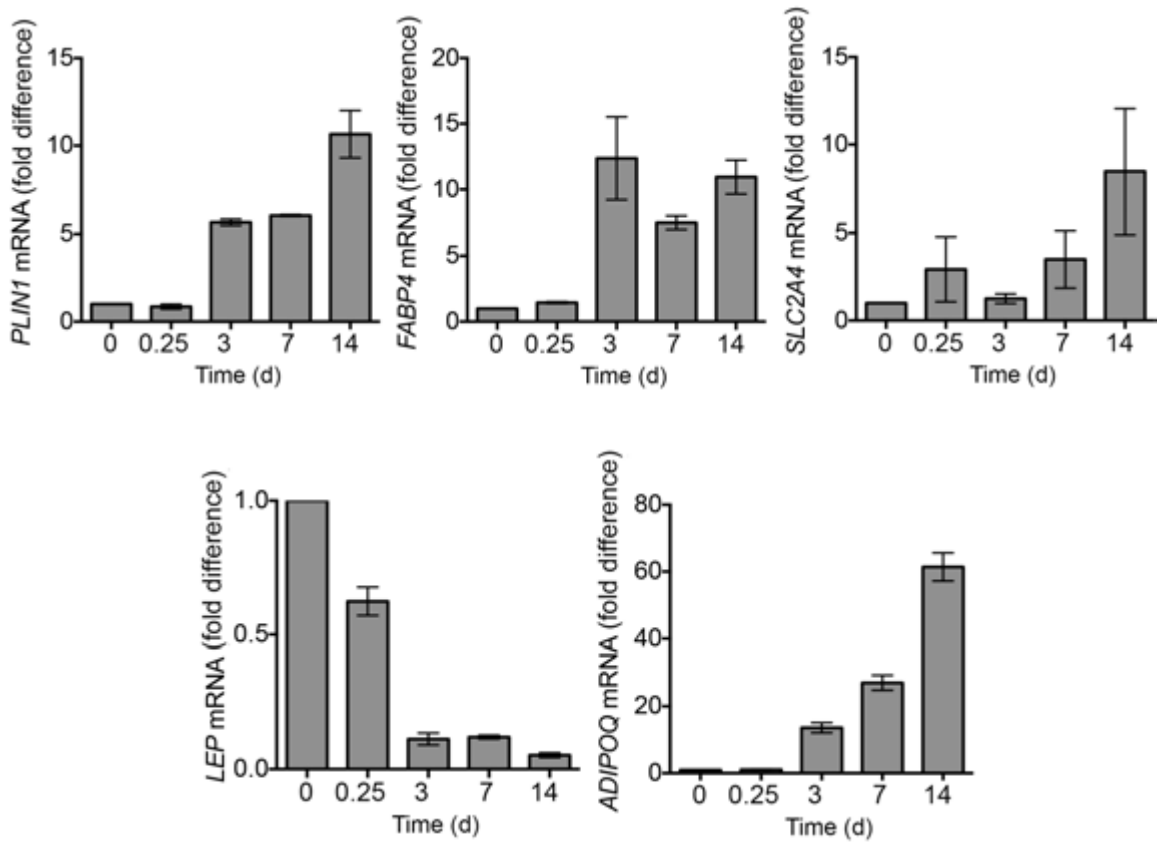
Figure 3.9. RT-PCR of PLIN1, FABP4, SLC2A4, LEP and ADIPOQ, expressed as
the fold relative to t = 0. Shown are means and range of 2 technical replicates. These
results have been replicated a minimum of 3 times with cells from separate individuals.

To determine the similarity of 'brite/beige' adipocytes generated from capillary networks to human thermogenic fat we obtained peri-carotid adipose tissue from four individuals undergoing elective carotid endarterectomy (Table 2). Relative to the expression of ADIPOQ, significant variability in UCP1 and DIO2 levels amongst samples of peri-carotid fat was observed (Figure 3.10), but higher values were comparable to those seen in 'brite/beige' adipocytes from capillary networks. Thus, these adipocytes resemble thermogenic adipose tissue in humans.

Table 2. Patient Characteristics (Panniculectomy)

Experiment	Patient	Age	Gender	Type of Surgery	BMI	DM	Insulin	Oral hypoglycemic	HMG CoA Reductase Inhibitor
Neck adipose tissue	1	64	M	CEA	29	No	No	No	Yes
	2	57	M	CEA	28	No	No	No	Yes
	3	59	F	CEA	25	No	No	No	Yes
	4	77	F	CEA	29	Yes	No	No	Yes
	mean:	64.25			27.75				
HTA-2 arrays, RT-PCR	7	39	F	PAN	26	No	No	No	No
	8	47	F	PAN	24	No	No	No	No
	9	43	F	PAN	37	No	No	No	No
	11	35	F	PAN	30	Yes	Yes	No	No
	mean:	41			29.25				
NSG-HFD at thermoneutrality	12	35	F	PAN	30	No	No	No	No
	15	50	F	PAN	41	Yes	No	Yes	Yes
	mean:	42.5			35.5				
NSG-Room Temperature; Metabolic Phenotyping	18	63	F	PAN	36	No	No	No	No
	19	58	M	PAN	32	No	No	No	Yes
	mean:	60.5			34				

CEA:carotid endartarectomy; PAN: panniculectomy; BMI: body mass index, at time of surgery; DM: Diabetes Mellitus
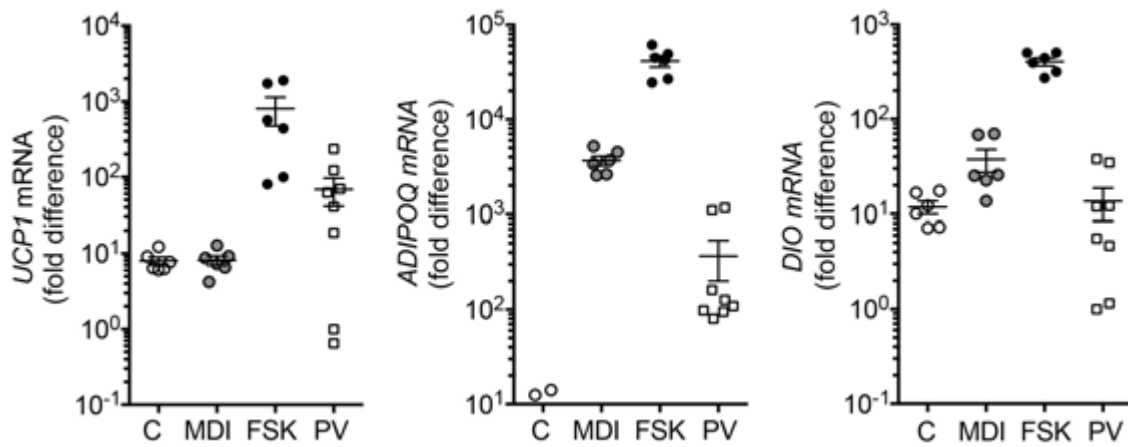
Figure 3.10. RT-PCR for UCP1, ADIPOQ and DIO2 in non-differentiated (C), differentiated (MDI), and forskolin-treated adipocytes (FSK), and perivascular adipose tissue (PV). Values represent fold difference over the lowest detectable value in the series for the respective probe set. Plotted are means and s.e.m. from 2 technical replicates of samples from 3 (cells) or 4 (PV) individuals.

We next asked whether human 'brite/beige' cells could be functional *in vivo*. Cells were grown, differentiated, and stimulated with forskolin as described in Online Methods. We routinely obtained cultures with unilocular and multilocular adipocytes, collected them by trypsinization, resuspended them in Matrigel and implanted them into the dorsal region of NOD-*scid IL2rg^{null}* (NSG) mice (Figure 3.11). After up to 11 weeks following implantation we observed only solidified remains of the gel in the dorsal region under the skin of mice receiving only Matrigel (Figure 3.11). In contrast, we observed well-delineated vascularized adipose tissue structures in mice implanted with cell suspensions (Figure 3.11). These structures were clearly demarcated from surrounding tissue and contained large patches of adipocytes and vasculature (Figure 3.12). Human adipocytes were viable and integrated into the mouse circulation, as we detected human adiponectin in serum from mice harboring implanted cells, but not in mice receiving Matrigel only (Figure 3.13).
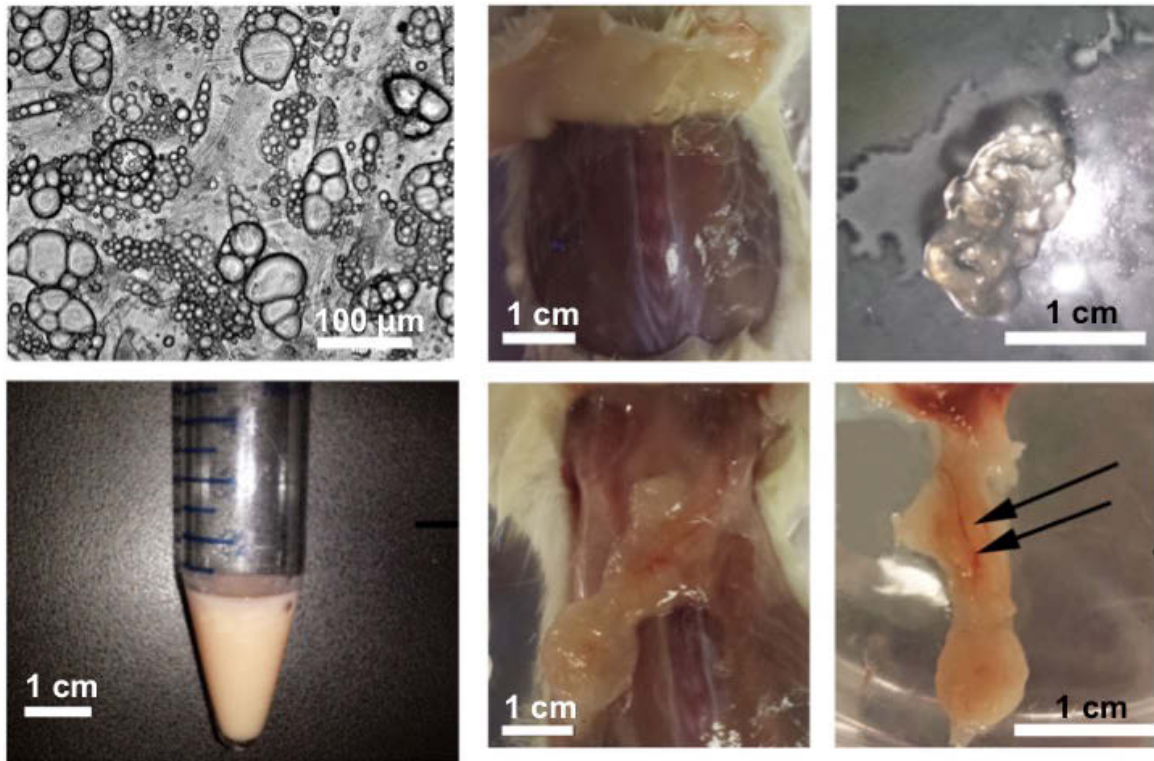
Figure 3.11. Phase image of cells for implantation (top left, scale bar is 100 μm); suspension of cells (bottom left); dorsal area of mouse injected with Matrigel alone (top middle, scale bar is 1 cm); collected remnants of the hydrogel (top right, scale bar is 1 cm); dorsal area of mouse injected with cells (bottom middle, scale bar is 1 cm); excised adipose structure (bottom right, scale bar is 1 cm) displaying vascularization (arrows).
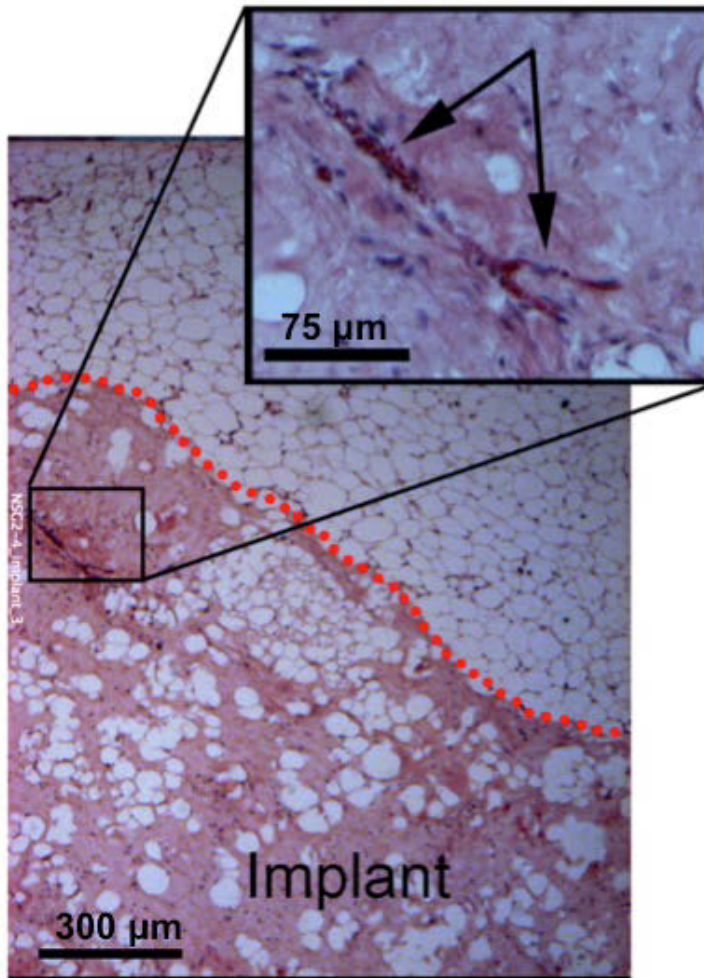
Figure 3.12. Representative H&E staining of implant; dotted red line separating implant from surrounding mouse adipose tissue, blood vessels within the implant (arrow). Scale bars are 300 μm and 75 μm (enlargement). Similar results were seen in 8 additional implants.
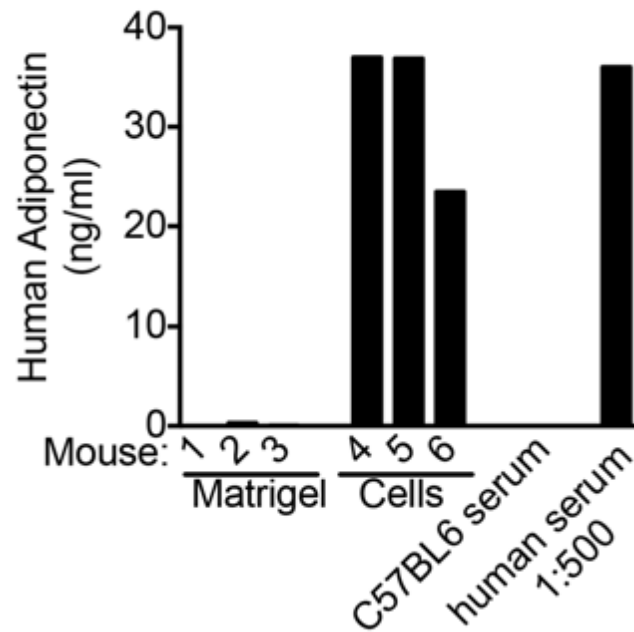
Figure 3.13. Human adiponectin in mice sera from 6 mice implanted with either Matrigel alone or with cells, in serum from a control C57BL6 mouse, and in a 1:500 dilution of normal human serum.

Remarkably, implanted adipocytes maintained the 'brite/beige' phenotype, as we detected human-specific UCP1 and PLIN1 expression in the adipose tissue structure at levels comparable to those found in cells prior to implantation (Figure 3.14), and we observed multi-locular adipocytes in the excised structure (Figure 3.15).
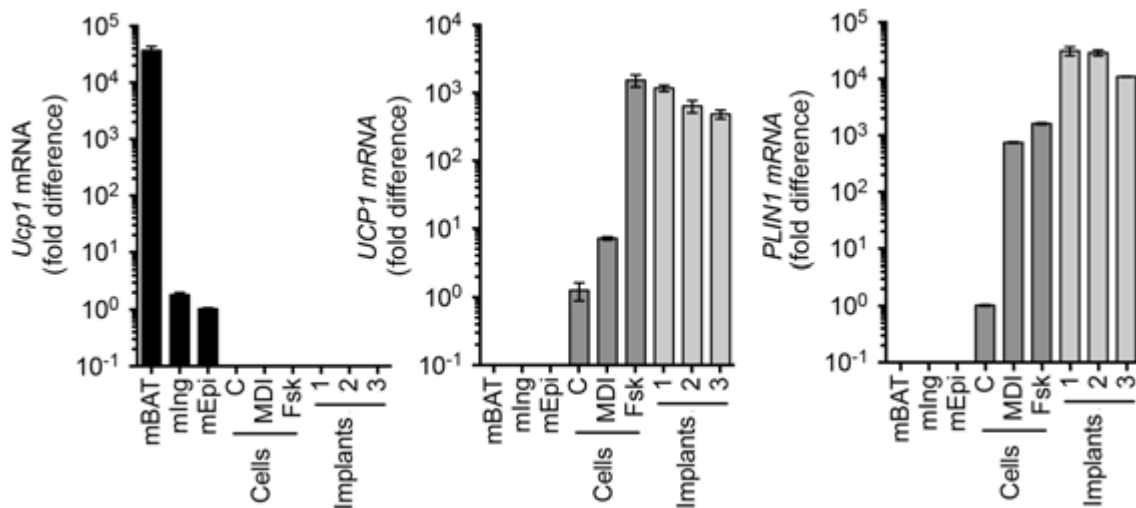
Figure 3.14. RT-PCR for mouse Ucp1, human UCP1 and human PLIN1 in mouse adipose depots (mBAT, mIng and mEpi), human capillary-derived cells (C, MDI and Fsk), and adipose structures from three mice, excised 7 weeks following implantation. Values represent the fold difference relative to the lowest detectable value in the series for each respective probe set a value of 0 was given to non-detectable values. Error bars represent range of 2 technical replicates.
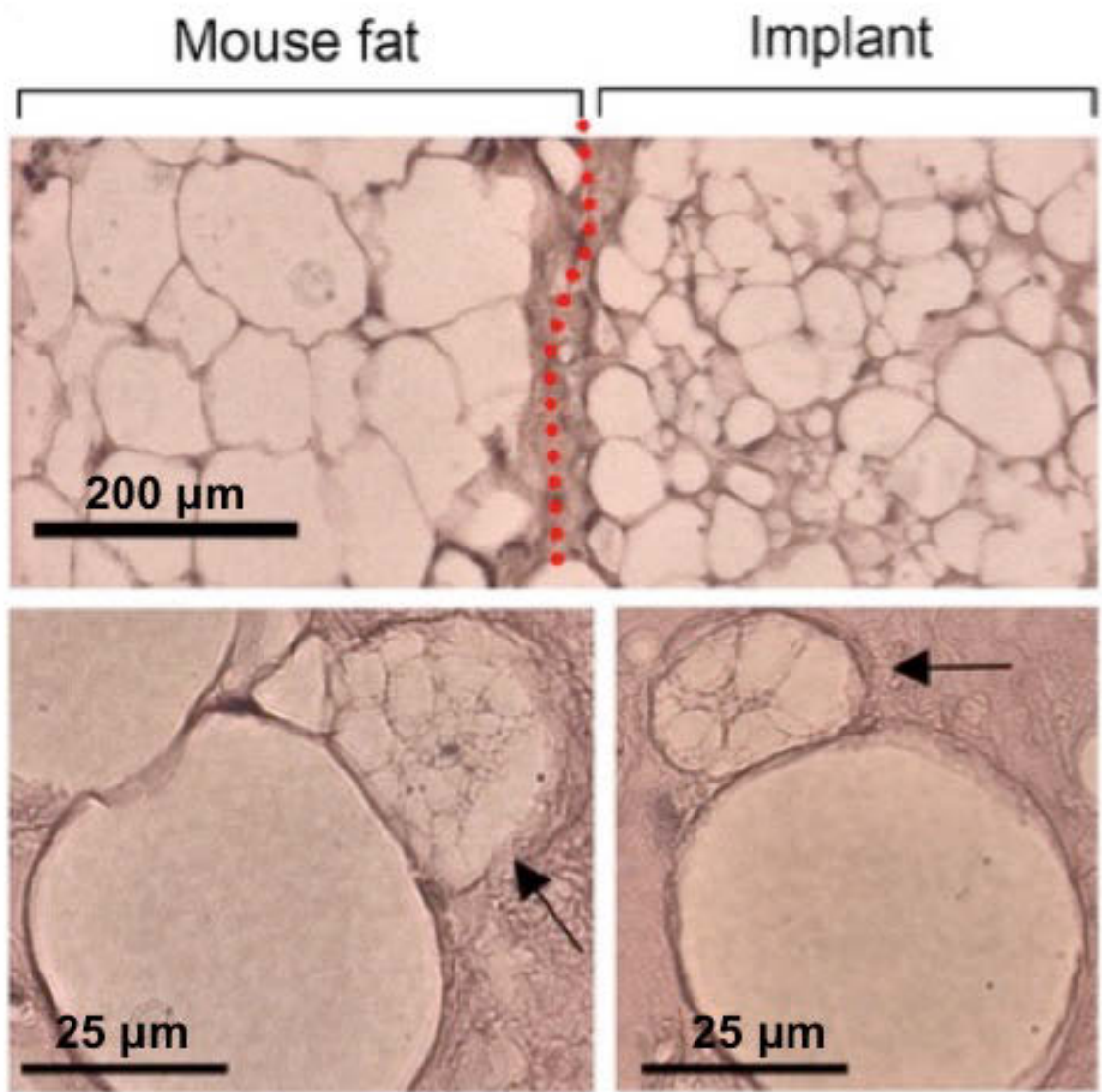
Figure 3.15. Multi-locular adipocytes in implants of human 'brite/beige' cells.
H&E staining of adipose structure formed from implanted human cells. The adjacent regions of host adipose issue and implanted cells are indicated by the red dotted line (top), and arrows (bottom) point to examples of multi-locular cells in the sections. Scale bars are 200 μm (top), and 25 μm (bottom).

We next asked whether human 'brite/beige' cells could affect glucose metabolism. Mice implanted with cells displayed lower fasting glucose (Figure 3.16) and a more rapid glucose disposal rate (Figure 3.17) compared to those receiving Matrigel only. NSG mice have been reported to be highly resistant to high fat diet-induced obesity[126]. Because susceptibility to high fat diet induced obesity and glucose intolerance are enhanced by thermo-neutrality[127], we subjected a cohort of NSG mice to high fat diet at 30°C. Within 2 weeks mice displayed significant glucose intolerance (Figure 3.18, Left). At 2 weeks of high fat diet, mice were randomized to receive Matrigel or 'brite/beige' adipocytes as above. Seven weeks following implantation, glucose tolerance was higher (Figure 3.18, Right) and liver steatosis was lower (Figure 3.19) in mice receiving cells compared to those receiving only Matrigel. Thus, 'brite/beige' adipocytes derived from human capillary networks can enhance glucose metabolism in mice under normal conditions and in the context of impaired glucose tolerance.
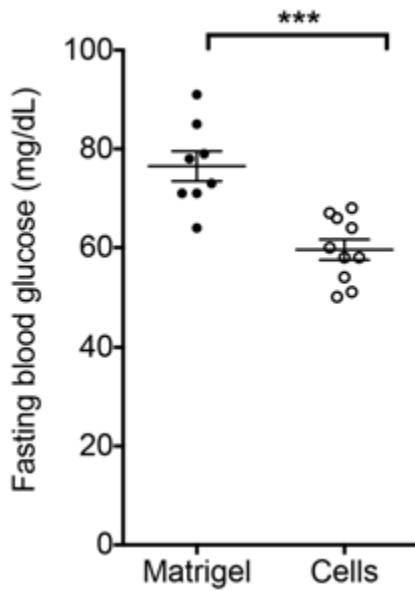
Figure 3.16. Fasting glucose levels after 16 hour-fast in male mice implanted with Matrigel ($n = 8$) or cells ($n = 10$).
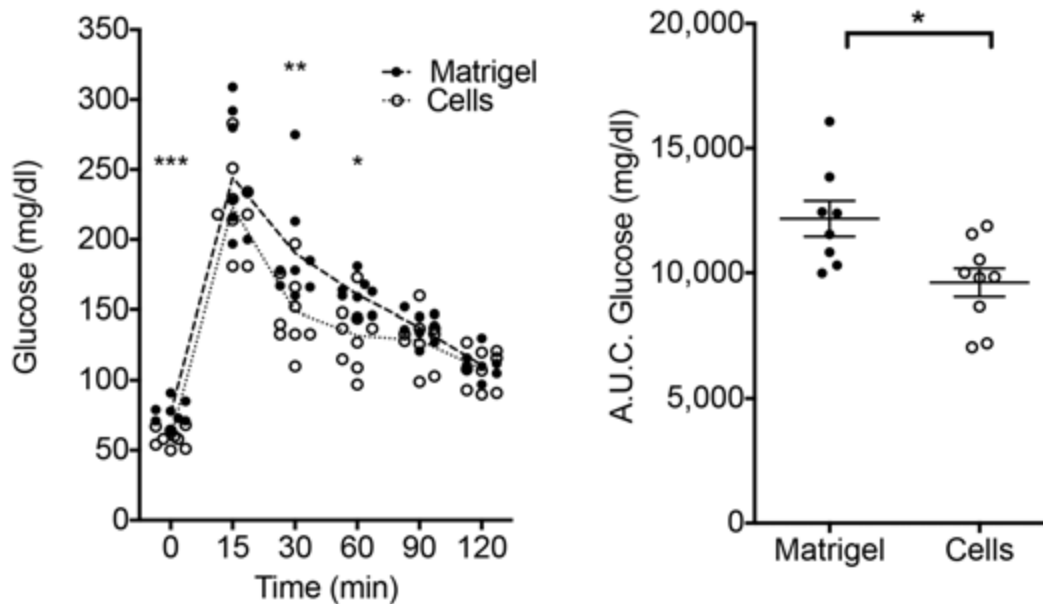
Figure 3.17. Glucose tolerance test.
Left: Glucose tolerance curves.
Right: Areas under the curve (A.U.C) of the glucose excursion after 16 hour-fast in male mice implanted with Matrigel ($n = 8$) or cells ($n = 10$).
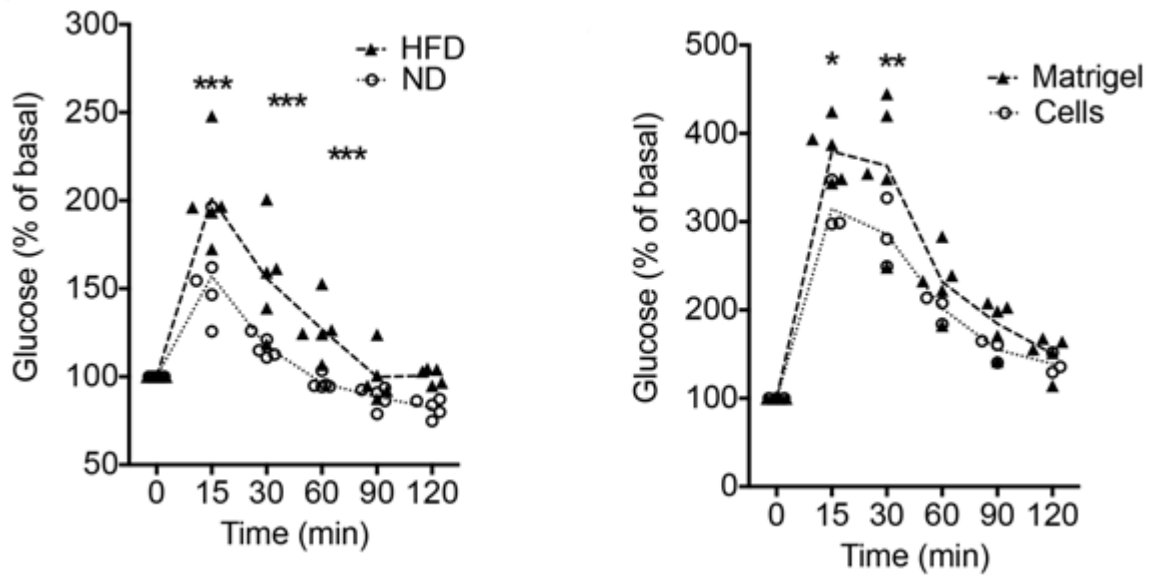
Figure 3.18. **Glucose tolerance test with high fat diet.**
Left: Glucose tolerance curves after an 8 h fast in mice housed at 30 °C for 2 weeks, fed a normal ($n = 5$) or 60% high fat diet ($n = 5$).
Right: Glucose tolerance curves after 11 weeks of 60% high fat diet and an 8 hour-fast in mice housed at 30 °C, implanted with either Matrigel ($n = 5$) or cells ($n = 3$) after 2 weeks of high fat diet. Statistical analysis was performed using 2-tailed unpaired Student-t tests at each time point of glucose tolerance curves, and Mann-Whitney test between groups for fasting blood glucose and area under the curves, * $P < 0.05$, ** $P < 0.01$, *** $P < 0.0001$.
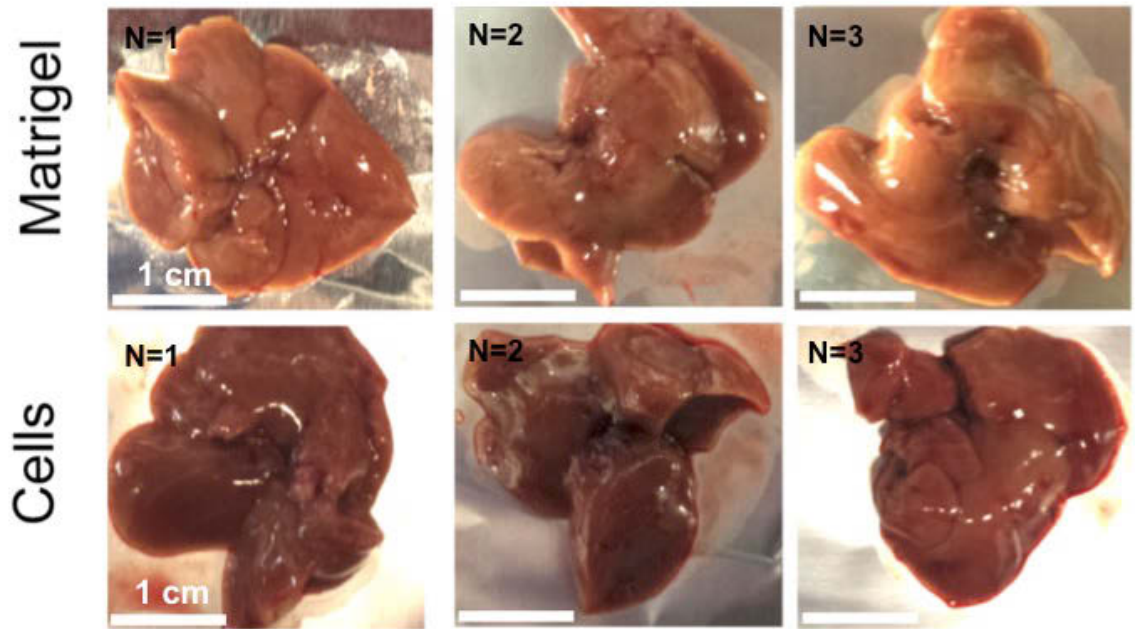
Figure 3.19. Livers from mice used in 2.18, immediately following sacrifice at 11 weeks. Three representative livers from each group. Scale bars are 1 cm.

While to our knowledge this is the first description of transplanted human adipocytes improving systemic glucose homeostasis, it has been reported that mouse subcutaneous adipose tissue can improve glucose homeostasis in high fat diet-treated mice[128]. To determine whether the improvement in glucose tolerance seen in mice implanted with capillary-derived human adipocytes was indeed attributable to their 'brite/beige' characteristics, we compared the effects of non-activated versus forskolin-activated adipocytes. We used *in vivo* hyperinsulinemic-euglycemic clamps to measure whole body glucose turnover, which was normalized to circulating human adiponectin to adequately control for the quantity and functional integration of implanted human cells. Mice implanted with forskolin-activated cells displayed higher glucose turnover compared to those implanted with non-stimulated cells (Figure 3.20), demonstrating that the 'brite/beige' phenotype directly contributed to improved glucose metabolism. Indeed this value is likely to be underestimated, as adiponectin expression is higher in activated 'brite/beige' adipocytes (Figure 3.9). We noted a strong correlation between serum human adiponectin and whole body glucose turnover when the entire cohort of mice with non-activated and activated cells were analyzed (Figure 3.22), suggesting that non-activated cells were also capable of affecting glucose turnover, or that the cells became activated following transplantation. RT-PCR analysis of the implanted structures revealed detectable UCP1 expression in tissue formed from non-activated cells, albeit at lower levels than that seen in tissue formed from forskolin-activated cells (Figure 3.22). These results support the conclusion that cells derived from human capillary networks give rise

to 'brite/beige' adipocytes, which can be activated *in vitro* and *in vivo,* and can affect glucose homeostasis.
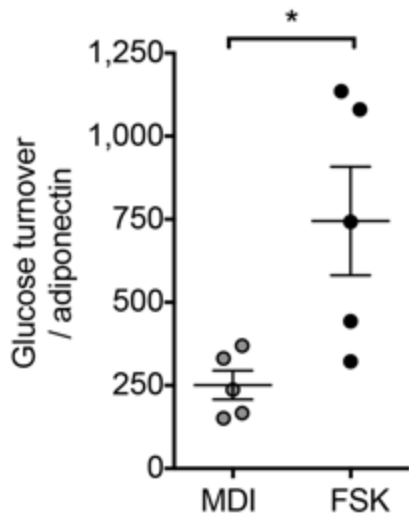
Figure 3.20. Glucose turnover (μmol/Kg/min)
normalized to serum human adiponectin (ng/ml) in
male mice implanted with non-stimulated (MDI, $n = 5$) or
forskolin-stimulated (FSK, $n = 5$) adipocytes, seven
weeks prior to hyperinsulinemic-euglycemic glucose
clamps. Statistical analysis was performed using the
Mann-Whitney test, $*P < 0.05$.
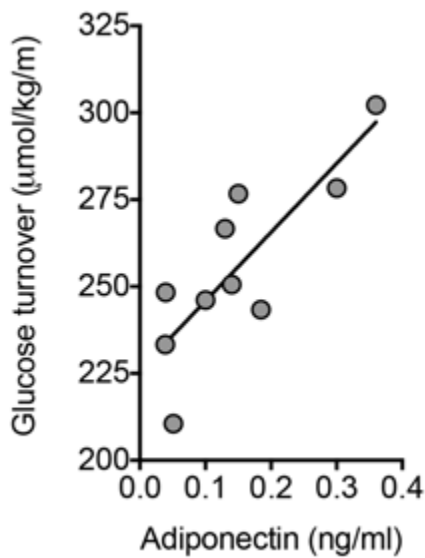
Figure 3.21. Adiponectin v.s. glucose turnover.
Relationship between serum human adiponectin levels
and glucose turnover in implanted mice ($n = 10$).
Linear regression P value = 0.0027, $R^2 = 0.601$.
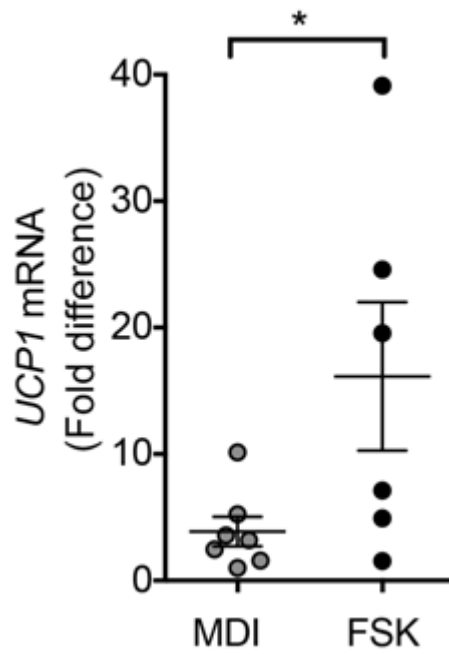
Figure 3.22. RT-PCR for human UCP1 in implanted cell structures from mice studied in Figure 3.20. Statistical analysis was done using unpaired 2-tailed Student t-test, * $P < 0.05$.

To determine whether the enhanced glucose tolerance seen in mice implanted with 'brite/beige' adipocytes was related to the thermogenic properties of these cells, body temperature was measured using subcutaneously implanted Thermochron iButton temperature loggers, which have a resolution of $0.025^{o}C$, set to record at 30 min intervals. Mice housed at room temperature harboring 'brite/beige' adipocytes did not differ significantly from Matrigel controls in their basal body temperature, or in their response to cold exposure (Figure 3.23). It remains possible that local thermogenic effects, undetectable by whole body temperature measurements, contribute to improved glucose metabolism. Alternatively, implanted cells might contribute to glucose tolerance independently of thermogenesis. To determine whether glucose uptake into implanted cells contribute to glucose turnover, we measured 2-[^{14}C] deoxyglucose uptake into tissues during hyperinsulinemic-euglycemic clamps. On a per gram of tissue basis, the rate of glucose uptake by implanted cell structures was significantly higher compared to epididymal white fat, but lower than interscapular brown fat in the same animal (Figure 3.24, Left). Because the density of cells in the implant is lower than in tissue due to dilution with Matrigel, these values may represent an underestimate of glucose consumption by human cells. Thus, improved glucose tolerance may be in part attributable to glucose consumption by implanted cells. However, whole body glucose turnover was not directly correlated with the amount of glucose uptake by the implanted cells (Figure 3.24, Right), suggesting that additional effects on peripheral tissues underlie enhanced glucose turnover. Indeed, improved metabolism attributable to brown adipose tissue effects on liver has been reported[129].
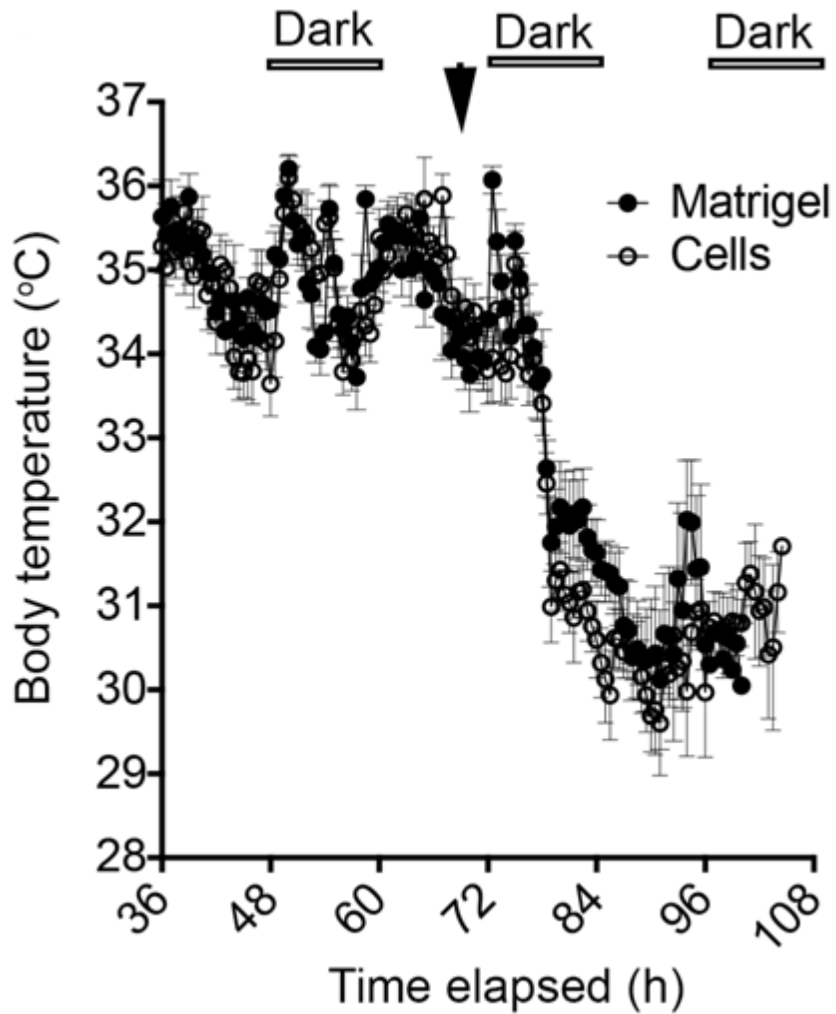
Figure 3.23. Temperature recordings from subcutaneous iButtons in mice implanted with Matrigel or cells 7 weeks following implantation. Arrow represents time at which mice were placed at 5°C.
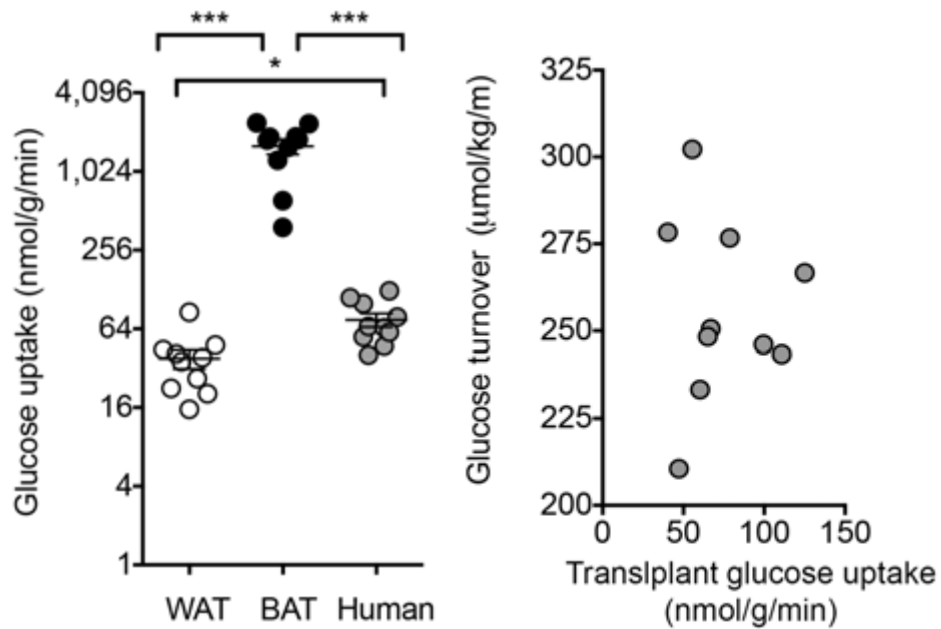
Figure 3.24. Glucose uptake and turnover.
Left: Glucose uptake into epididymal fat (WAT), interscapular brown fat (BAT) and implanted cell structures from mice studied in (b), $n = 10$. Statistical analysis was performed using unpaired 2-tailed Student-t tests * p< 0.05, ** $P < 0.01$, *** $P < 0.0001$.
Right: Relationship between glucose uptake into implanted cell structures and glucose turnover ($n = 10$).

To explore the possibility that the metabolic benefits of human 'brite/beige' adipocytes could be due to secreted factors, we conducted global gene expression analysis of adipocytes before and after 7 days of forskolin stimulation (Figure 3.25). Unexpectedly, amongst the most significantly induced genes were the proprotein-convertase subtilisin/kexin type-1 (PCSK1), its substrate proenkephalin (PENK), and interleukin 33 (IL-33). Mutations and polymorphisms in PCSK1 are strongly associated with human obesity[130, 131], although the underlying mechanisms are unclear. Cleavage of PENK by PCSK1 produces enkephalins, which are made in peripheral tissues in addition to the brain[132]. IL-33 has been shown to decrease adiposity, mitigate atherosclerosis and be necessary for normal glucose homeostasis in mouse models[133, 134]. Interestingly, enkephalins and IL-33 have been shown to induce adipose tissue browning[134]; thus, production of these factors by implanted 'brite/beige' cells could explain the sustained expression of UCP1 seen weeks following implantation (Figure 3.26). While we were not able to detect IL-33 in the circulation of transplanted mice, immunostaining revealed punctate structures containing IL-33 within activated adipocytes (Figure 3.27). Further studies will be required to determine possible autocrine effects of IL-33 on the induction or maintenance of the 'brite/beige' adipocyte phenotype *in vivo*.
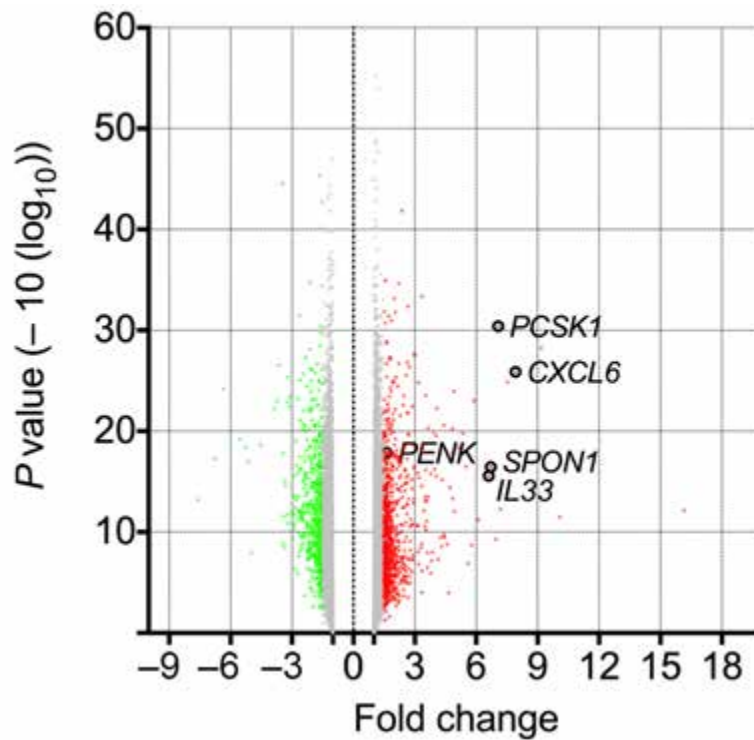
Figure 3.25. Volcano plot of differential gene expression in adipocytes without or with forskolin-treatment for 7 days, indicating genes of interest such as PCSK1, IL-33, PENK, SPON1 and CXCL6. Fold change in forskolin-treated cells relative to non-treated cells.
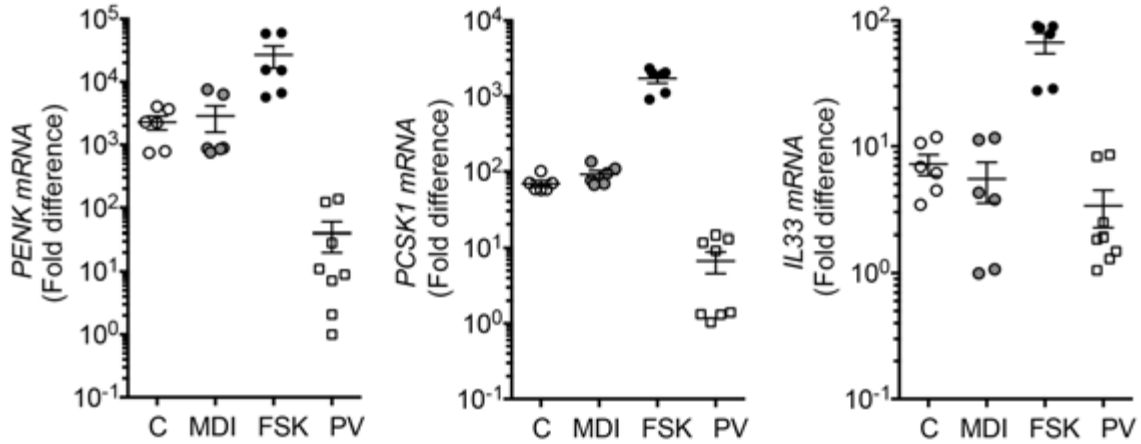
Figure 3.26. RT-PCR of PCSK1, PENK and IL-33 expression in non-differentiated (C), differentiated (MDI), and forskolin-treated adipocytes (FSK), and perivascular adipose tissue (PV). Values represent fold difference over the lowest detectable value in the series for the respective probe set. Plotted are means and s.e.m. from 2 technical replicates of samples from 3 (C, MDI, FSK) or 4 (PV) individuals.
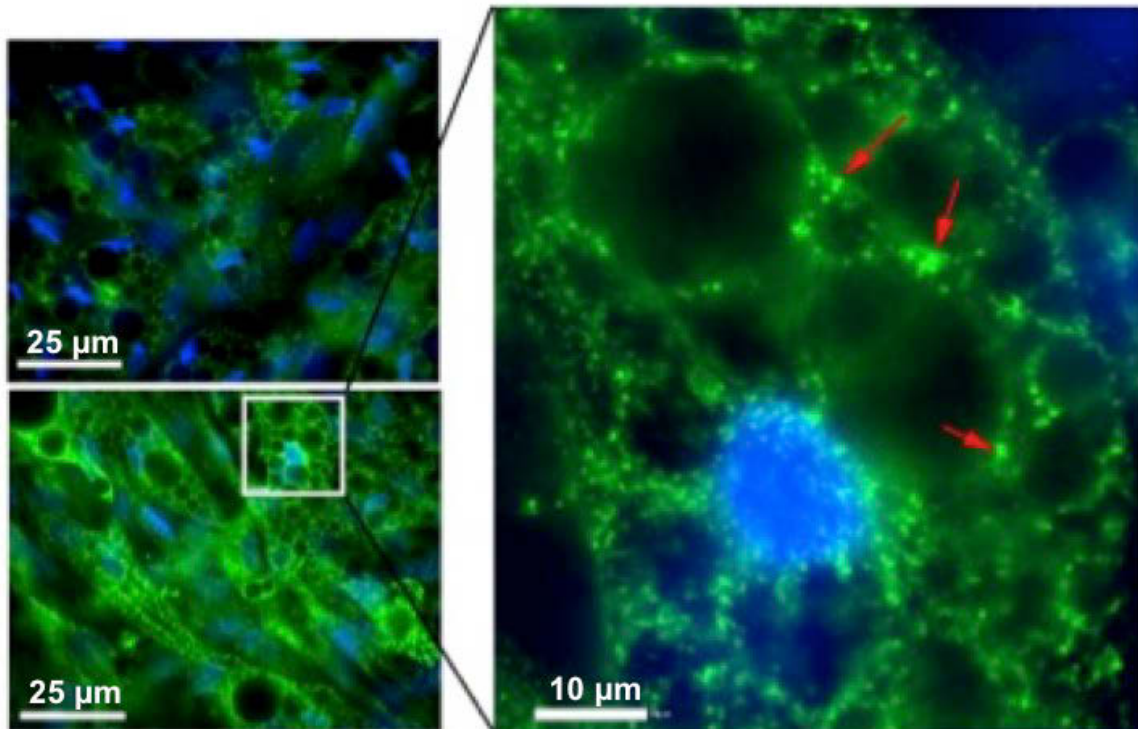
Figure 3.27. Expression of IL-33 in 'brite/beige' adipocytes. Cells isolated from capillary networks were sub-cultured on coverslips, grown to confluence and subjected to adipogenic differentiation. Differentiated cells (top left) or differentiated cells treated with forskolin for 7 days (bottom left), were fixed, permeabilized and stained with antibody to human IL-33 (green) and Hoechst (blue). Scale bars are 25 µm and 10 µm (enlargement, right). Arrows point to numerous vesicular structures containing IL-33.

Table 3. Probes used for RT-PCR

Gene name	Forward (Fw) or Reverse (Rv) probe Sequences
Mouse UCP1 Fw	GTGAACCCGACAACTTCCGAA
Mouse UCP1 Rv	TGCCAGGCAAGCTGAAACTC
Human UCP1 Fw	AGAAGGGCGGATGAAACTCT
Human UCP1 Rv	ATCCTGGACCGTGTCGTAG
PPARGC1A Fw	TCTGAGTCTGTATGGAGTGACAT
PPARGC1A Rv	CCAAGTCGTTCACATCTAGTTCA
DIO2 Fw	GGATGCCCCCAATTCCAGTG
DIO2 Rv	GGCTCGTGAAAGGAGGTCAAG
CIDEA Fw	TTATGGGATCACAGACTAAGCGA
CIDEA Rv	TGCTCCTGTCATGGTTGGAGA
PRDM16 Fw	CTTCGGATGGGAGCAAATACTG
PRDM16 Rv	TCCACGCAGAACTTCTCACTG
Human PLIN1 Fw	ACCAGCAAGCCCAGAAGTC
Human PLIN1 Rv	CATGGTCTGCACGGTGTATC
ADIPOQ Fw	TGCTGGGAGCTGTTCTACTG
ADIPOQ Rv	TACTCCGGTTTCACCGATGTC
LEPTIN Fw	TGCCTTCCAGAAACGTGATCC
LEPTIN Rv	CTCTGTGGAGTAGCCTGAAGC
PDK4 Fw	GGAGCATTTCTCGCGCTACA
PDK4 Rv	ACAGGCAATTCTTGTCGCAAA
CD137 Fw	AGCTGTTACAACATAGTAGCCAC
CD137 Rv	GGACAGGGACTGCAAATCTGAT
CITED1 Fw	CCTCACCTGCGAAGGAGGA
CITED1 Rv	GGAGAGCCTATTGGAGATCCC
TBX1 Fw	ACGACAACGGCCACATTATTC
TBX1 Rv	CCTCGGCATATTTCTCGCTATCT
TMEM26 Fw	ATGGAGGGACTGGTCTTCCTT
TMEM26 Rv	CTTCACCTCGGTCACTCGC
EVA1 Fw	TTAATGGGACAGATGCTCGGT
EVA1 Rv	AAGACACCCGGTCCTTAAACC
LHX8 Fw	GAATGACCTATGCTGGCATGT
LHX8 Rv	ACCCAGTCAGTAGAATGGATGTG
PENK Fw	CTGGATGGCATTGTGACGGAT

Gene name	Forward (Fw) or Reverse (Rv) probe Sequences
PENK Rv	GCCCCAGCTTGCACTGTAAA
PCSK1 Fw	CGGTTCCTGACACTTTGCACT
PCSK1 Rv	CACATTCCATTACGCAAGCCA
IL33 Fw	GTGACGGTGTTGATGGTAAGAT
IL33 Rv	AGCTCCACAGAGTGTTCCTTG
SLC2A4 Fw	TGGGCGGCATGATTTCCTC
SLC2A4 Rv	GCCAGGACATTGTTGACCAG
FABP4 Fw	ACTGGGCCAGGAATTTGACG
FABP4 Rv	CTCGTGGAAGTGACGCCTT
RPL4 Fw	GCCTGCTGTATTCAAGGCTC
RPL4 Rv	GGTTGGTGCAAACATTCGGC

Discussion

In summary, our data reveal that human adipocyte progenitor cells proliferate in response to pro-angiogenic stimuli in conjunction with adipose tissue angiogenesis. These cells display the cardinal feature of 'brite/beige' adipocytes, which is the near absence of thermogenic genes under basal condition, but their strong induction in response to adrenergic stimulation. To our knowledge, these findings are first to enable the growth and differentiation of human 'brite/beige' cells, and the assessment of their effects of systemic glucose homeostasis. These cells differ from human brown adipocyte cell lines established through immortalization of human precursors[102, 113] or differentiation of human pluripotent stem cells[104] in their highly inducible expression of a thermogenic phenotype, in the development of uncoupled respiration, and in their capacity to affect metabolism upon transplantation *in vivo*.

Our finding of a functional relationship between angiogenesis and 'brite/beige' adipocyte development converges with existing studies where overexpression of the pro-angiogenic factor VEGF in mouse adipose tissue results in extensive browning[135, 136]. In addition, perivascular adipose tissue surrounding major blood vessels displays thermogenic characteristics[137, 138], and its loss results in cold intolerance, endothelial dysfunction and susceptibility to atherosclerosis[137]. The finding that human 'brite/beige' adipocytes enhance glucose homeostasis provides a clear rationale for their potential therapeutic use.

85

Moreover, the expression of neuroendocrine and secreted factors by activated cells suggests that secreted products identified in these studies could also contribute to metabolic effects. Future studies to systematically assess the mechanisms by which human 'brite/beige' cells develop and affect glucose homeostasis will be greatly facilitated by the ability to generate these cells from human adipose tissue by the methods described herein.

CHAPTER IV: Exploring the distinct gene expression signatures of human brown, beige, white adipose-derived progenitors and adipocytes

Author Contributions

Khanh-Van Tran, Timothy Fitzgibbons, Raziel Rojas-Rodríguez, Tiffany DeSouza and Anand Desai

Summary

Adipose tissue plays numerous functions, some of which are restricted to regional depots. Differences amongst adipocytes within these depots can arise from distinct lineage origins, differing regional stimuli, or a combination of both. Thermogenic adipose tissue, defined as containing the uncoupling protein UCP1, is found in distinct depots. In humans, UCP1 containing adipocytes have been identified in the neck and supraclavicular region. To define the mechanisms involved in this specific distribution of thermogenic fat, we determined whether progenitors for beige adipocytes differ in abundance between three human depots: peri-carotid, subcutaneous from the neck, and subcutaneous from the abdominal region. All three depots contain adipocyte progenitors that proliferate in association with emerging capillary networks, and all depots contain beige adipocyte progenitors. This supports the notion that differences between depots are resulted less from clearly distinct progenitor lineages than from the local environment in which those progenitors differentiate. However, cells derived from these three depots retain a distinct identity, discerned through hierarchical clustering analyses of their

expressed genome. We also identify regional differences in expression level of LINC00473, recently shown to determine responsiveness to cAMP signaling; Levels of LINC00473 directly correlate with the extent of UCP1 expression in beige cells from different depots. These results suggest that, through genes such as LINC00473, small regional differences in gene expression can greatly amplify local stimuli to develop the substantially different functional properties associated with each adipose depot in humans.

Introduction

The sheath of adipose tissue surrounding blood vessels, called perivascular adipose tissue (PVAT), was long considered as mechanical protection to the vessels[139] until the recent findings on other roles of PVAT, which include the secretion of leptin, adiponectin, resistin, free fatty acids, and vasoactive substances, have been explored[140]. Furthermore, early studies of PVAT from human coronary arteries unexpectedly detected expression of BAT-specific genes such as PRDM16 and UCP1 at an intermediate level of WAT and BAT[141]. Notably, mouse PVAT surrounding the abdominal aorta displays characteristics of WAT, whereas PVAT surrounding the thoracic aorta appears to be morphologically closer to BAT with multi-locular lipid droplets and abundant mitochondria[142, 143]. Our collaborator Fitzgibbon *et al.[97]* showed by microarray analysis that global gene expression profiles of mouse PVAT are nearly identical to BAT, with high expression of thermogenic genes (UCP1, Cidea, etc.) and morphological traits (multi-locular lipid droplets and abundant mitochondria). Moreover, in C57BL6/J mice fed with high-fat diet, PVAT and BAT showed markedly lower expression of inflammation-related genes, compared to that of WAT, which suggests these depots are resistance to obesity-induced inflammation. In accordance, macrophage markers (F4/80 and CD68) in BAT and PVAT of obese mice showed no macrophage infiltration. Chang *et al*. also found a similar proteomic profile between thoracic PVAT and BAT[144]. In their proteomics analysis of the PVAT from mice stimulated with a cold exposure, the authors identified virtually identical protein

expression profiles, which were highly related to cellular metabolic processes.

The functional role of PVAT was discovered in a mouse model deficient of PPARγ in smooth muscle cells, which unexpectedly had low PVAT. These results uncovered that an absence of PVAT results in loss of its thermogenic capability, impaired vascular homeostasis that caused body temperature decrease and endothelial dysfunction[144]. Another recent study also suggested that at least some beige adipocytes may derive from smooth muscle-like precursors[66]. Using translating ribosome affinity purification (TRAP) technology, the authors demonstrated a smooth muscle-like signature expressed by beige, but not classical brown, adipocytes. In the data TRAP set, they further investigated Myh11, the most selective marker known for bona fide mature smooth muscle and other smooth muscle-like cells. Lineage tracing using either a constitutive or an inducible Myh11-driven Cre suggested that at least a subset of beige cells arise from a smooth muscle-like origin. Finally, ectopic expression of PRDM16 converts bona fide vascular smooth muscle cells into UCP1-positive adipocytes *in vitro*.

To investigate whether we can translate the PVAT characterization studies performed in rodent models into humans, our laboratory decided to leverage our expertise in generating adipocyte progenitors and adipocytes to study the differences in the precursor population in human brown (carotid), beige (neck subcutaneous), and white fat (abdominal subcutaneous) depots[110, 145].

The proper organization of the vertebrate body requires local information in the embryo that can coordinate an orchestrated global pattern. The generation of targeted loss-of-function mutations in mice and transplantation experiments have been useful to

examine detailed genetic functions of Homeobox (HOX) paralogues in mammalian development[146]. Nowicki et al. performed heterotopic transplantation of segmental plate from quail to chick and clearly presented that the donor tissue retained its own HOX paralogue expression after transplantation, except for the abaxial domain, and the specific Hox gene expression correlates with axial specification[147]. Numerous studies investigated the correlation between the mutation of Hox genes and the consequential phenotypes[148], thereby concluding the patterning of Hox paralogues as following[146]: HOX5 (cervical, thoracic); HOX6 (cervical, thoracic, upper ribs); HOX9 (lower ribs); HOX10 (lumber, sacral); HOX11 (sacral, caudal).

Interestingly, several hormones and their receptors have been shown to regulate Hox gene expression. Estradiol, progesterone, testosterone, retinoic acid, and vitamin D have been shown to regulate Hox gene expression[149]. *Vice versa*, HOX genes build a network of transcription factors (homeoproteins) to control essential functions of adult cells embryonic development [150], which also include the regulation of metabolic processes[151]. Cantile *et al*. analyzed the expression of the HOX genes in different depots of human white adipose tissue, and found that HOX genes displayed a depot-specific expression. Moreover, expression of the paralogues group 4 genes (HOX A4, HOX B4, HOX C4, and HOX D4), appeared to distinguish white and brown adipose tissues[150]. Regarding the Fat distribution in humans, HOXA2, HOXA3, HOXA4, HOXA5, HOXA9, HOXB7, HOXB8, HOXC8 are found to be down-regulated in the gluteal depot, while HOXA10 and HOXC13 are highly expressed[152]. Conversely, visceral adipocytes express higher levels of HOXA5, HOXA4, HOXC8, whereas

subcutaneous fat showed higher levels of HOXA10, HOXC9, TBX15 and SHOX2[153]. The expression of HOXC8 is highly enriched in brown adipose tissue[154]. Remarkably, HOX genes are shown to play roles in metabolic diseases. For example, the contribution of multiple variants at POU class 2 homeobox 1 (POU2F1), also known as octamer-binding transcription factor-1 (OCT1), to the risk of Type 2 diabetes has been established[155]. Hyper-expression of HOXA5 induces an increase in insulin-like growth factor binding protein1 (IGFBP1), which has a crucial role in adipocyte biology and metabolism[156]. The interplay between Hox and hormones orchestrates the function of adult organs in specific locations as well as the developmental program, thus implying the potential roles of Hox genes in human brown and brite/beige adipose tissues maintenance in various anatomical locations.

Long-noncoding RNAs (lncRNAs) have recently gained widespread attention as a crucial player of biological regulation. LncRNAs function as modular molecules with individual domains[157]. The embedded motifs in the lncRNA sequences enable the RNA to specifically bind with DNA, RNA or protein. Both mis-expression and mutations of lncRNAs is linked to numerous diseases[158]. Taking just few examples, Finnish subjects with type 2 diabetes possessed a large number of single nucleotide polymorphisms in the INK4/ARF loci, which is associated with increased risk of type 2 diabetes[159]. Also, a chromosomal translocation (1;11)(q42.1; q14.3) was identified to be strongly associated with schizophrenia and other neuropsychiatric disorders, directly affecting DISC1 and DISC2 (disrupted in schizophrenia 1 and 2)[160]. DISC2 encodes the lncRNA that is antisense to DISC1 and it is postulated that DISC2 is involved in

regulating expression of DISC1. The suggested mechanisms of how lncRNAs may function in their biological roles include disrupting translation, working as a transcriptional co-activator, forming functional nuclear bodies, looping chromatin, masking splice sites, competing with microRNAs, increasing mRNA stability, localizing transcriptional factors and decreasing mRNA stability[161].

Materials and methods

General Methodology. No samples, mice or data points were excluded from the reported analyses. Samples were not randomized to experimental groups except where indicated. Analyses were not performed in a blinded fashion except where noted below.

Materials. Matrigel from BD biosciences (56231); EGM-2 MV from Lonza; Forskolin from Sigma (F3917).

Adipose Tissue. Among the human thermogenic depots, we collected carotid peri-vascular (human brown) and neck subcutaneous (human beige), adipose tissues from carotid endarterectomies with no a-priori selection of individual donors. All specimens were collected after informed consent in accordance with procedures approved by the University of Massachusetts Institutional Review Board. The characteristics of patients from which tissues were used for indicated experiments are described in Table 3.

Explants. Detailed methods for harvesting adipose tissue, culture of adipose tissue explants in Matrigel are published[96]. In brief, explants from human subcutaneous adipose tissue were cultured in EBM-2 media supplemented with endothelial growth factors (EGM-2 MV) (Lonza). In indicated experiments, Dulbecco's Modified Eagles Medium (Gibco) supplemented with 10% fetal bovine serum (DMEM-FBS) was used, without or with supplementation with VEGF (vascular endothelial growth factor), hFGF-

B (human fibroblast growth factor B), hEGF (human epidermal growth factor), R^3-IGF-1 (long R3 insulin-like growth factor 1) at the concentrations used in EGM2-MV, as indicated. To induce adipogenesis we used a minimal adipogenic cocktail of DMEM +10% FBS, 0.5 mM 3-isobutyl-1-methylxanthine, 1 μM dexamethasone, and 1 μg/ml insulin (MDI) for 72 hours. The medium was then replaced with DMEM plus 10% FBS. Subsequently, 50% of the medium was replaced with fresh medium every other day. Adipocyte markers were measured by RT-PCR in RNA extracted from 3 explants per condition.

Cells. Detailed methods for harvesting adipose tissue, culture of adipose tissue explants in Matrigel, and harvesting of single cells from explant growth are published[96]. In brief, explants from human subcutaneous adipose tissue were cultured in EBM-2 media supplemented with endothelial growth factors (EGM-2 MV) (Lonza) for 14 days. Single cells suspensions from capillary growth (capillary network cells) were obtained using dispase[96], and plated on standard tissue culture plates. Growth and passaging of these cells was done using EGM-2 MV. Where indicated, adipogenic differentiation was induced by replacement of EGM-2 MV by DMEM +10% FBS, 0.5 mM 3-isobutyl-1-methylxanthine, 1 μM dexamethasone, and 1 μg/ml insulin (MDI). 72 hours later, the differentiation medium was replaced by DMEM-FBS, which was replaced every 48 hours until analysis. In experiments to investigate the effects of 'brite/beige' adipocytes *in vivo*, cells from capillary networks were grown to confluence into 150 mm dishes, differentiated using MDI for 10 days, and browning induced for 7 days with forskolin.

RT-PCR. Adipocyte markers were measured by RT-PCR in RNA extracted from one well of a confluent 6 well multi-well dish of cells. Adipocyte markers were measured in RNA extracted from 3 explants per condition, or from one well of a confluent 6 well multiwell dish of cells. Probe sets used are shown in Table 3.

Affymetrix arrays. Total RNA was isolated using TRIzol. Affymetrix protocols were followed for the preparation of cRNA, which was hybridized to HTA-2.0 arrays. Raw expression data collected from an Affymetrix HP GeneArrayScanner was normalized across all data sets using the RMA algorithm as implemented by the Affymetrix Expression Console. Expression analysis was performed using the Affymetrix Transcriptome Analysis Console v.3.0. The data discussed in this publication have been deposited in NCBI's Gene Expression Omnibus and are accessible through GEO Series accession number GSE73385.

Statistical analyses. RT-PCR results are presented as means of technical replicates with error range indicated. Experiments shown are representative, and have been repeated a minimal of 3 times per depot with cells derived from different individuals, with no a priori selection. Software employed was GraphPad Prism v.6. To compare groups with normally distributed values, 2-tailed unpaired Student t-tests were used. When normality could not be determined, the Mann-Whitney test was used. Data are presented as mean values ± s.e.m. or range between technical replicates when experiments were representative, as indicated in each figure legend. P-values are indicated in each case.

Table 4. Patient Characteristics (Carotid endarterectomy)

Collected Fat Tissues	Surgery Procedure	Gender	Age	BMI	T2DM	HTN
Carotid	Carotid endarterectomy	Female	74	31	No	Yes
Carotid Neck SQ	Carotid endarterectomy	Female	77	30	Yes	Yes
Carotid Neck SQ	Carotid endarterectomy	Female	82	24	No	Yes
Carotid Neck SQ	Carotid endarterectomy	Female	65	26	No	Yes

SQ: subcutaneous; BMI: Body Mass Index; T2DM: Type 2 Diabetes Mellitus; HTN: Hypertension.

Results

Embedded adipose tissue explants from both carotid peri-vascular (PV) and neck

subcutaneous (SQ) sprouted capillary cells in EGM-2 MV, which appeared to be similar

to the observation with abdominal SQ from panniculectomies (Chapter II). Isolated

capillary cells were plated on dishes and differentiated into adipocytes in the same way as

described in Chapter II. Morphology of the adipocytes from PV and SQ looked virtually

identical except for the slightly larger adipocyte size from SQ progenitor cells (Figure

4.1). Upon 7-days of forskolin treatment on differentiated capillary cells from each depot,

both PV and SQ induced UCP1 mRNA expression (Figure 4.2). There was a trend of

higher UCP1 in PV compared to SQ for both preadipocytes and adipocytes without

statistical significance. Based on the results from earlier chapters and this result, it is

likely that brite/beige adipocyte progenitors can originate from multiple depots in human,

including all three white, brite/beige, and brown adipose tissues without much difference

in their progenitor population and the potential to be induced as thermogenic fat. These

data suggest that environmental cues in the specific location of the body might be a more

important controlling factor to explain the anatomical distribution of human brown and

brite/beige depots.

Nevertheless, global gene expression profile revealed the progenitor populations

from different depots can be distinguished from each other (Figure 4.3). We compared

the transcriptome signatures of adipose progenitors derived either from human carotid

peri-vascular (Carotid), neck subcutaneous (NeckSQ), or abdominal subcutaneous

(AbdSQ). Heat map from the transcriptome array using genes that differed at an ANOVA P value of 0.001 clearly clustered the biological triplicates of each depot together, suggesting tissues from different anatomical sites have specific transcriptome patterns. Assuring our data represent biologically relevant results, patterning gene SHOX2 was expressed abundantly in the AbdSQ samples, which confirms the previous findings that subcutaneous fat shows higher SHOX2[153] although HOX10, which is known to have a higher expression level in subcutaneous adipose tissue[153], was not abundant in the AbdSQ samples. HOX6, another HOX gene found to be highly expressed in cervical, thoracic and upper rib regions[146], was abundantly expressed in our Carotid samples in accordance with previous studies.

To determine whether any of the differentially expressed genes might contribute to depot-specific functional differences, we performed cluster analysis on a set comprised of differentiated cells from each depot, with and without forskolin stimulation (Figure 4.4). Comparison of adipocytes and forskolin-induced adipocytes generated from three depots revealed that forskolin-treated Carotid and NeckSQ clustered together, being the farthest and the most different from AbdSQ as expected. Next, control Carotid and control NeckSQ clustered together while AbdSQ and AbdSQ+Fsk clustered together, implying abdominal adipocytes are significantly dissimilar from neck fat-derived adipocytes, regardless of forskolin-treatment. Most importantly, in all groups three biological replicates from individual patients were clustered together, indicating biological differences in progenitors from each depot and their response to forskolin prevail over individual variances.

One of the most distinctive clusters comprised the genes LINC00473, AREG, NR4A2, RELL1, SLC6A15 and WNT5A (Figure 4.4). Among these genes, LINC00473 drew our attention due to the recent study demonstrating the role of LINC00473 in one of the pathways that is involved in adrenergic stimulation. Chen *et al*. found that LINC00473 facilitates CRTC/cyclic AMP-responsive element-binding protein (CREB)-mediated transcription in non-small cell lung cancers[162]. In brown adipocytes, cold and sympathetic stimulation works through β3-adrenergic receptor-cAMP-CREB/ATF2 pathway to induce BAT-enriched genes, including UCP1[57]. The mRNA expression level of LINC00473 was confirmed by RT-PCR, which strongly correlated with UCP1 expression in adipocytes and even in preadipocytes (Figure 4.5), generated from PV, NeckSQ and AbdSQ. In human adipose tissues, abundance of brite/beige adipocytes in different depots may result from expression of factors such as LINC00473 that could modulate sensitivity to catecholamines.
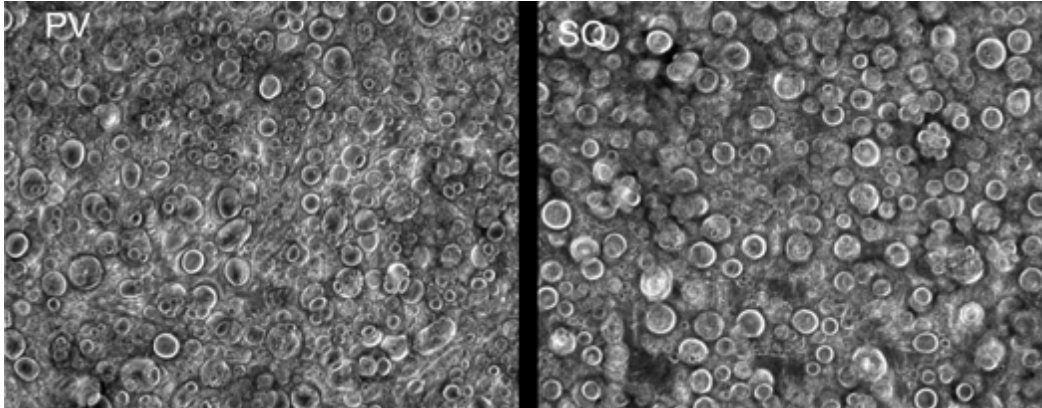
Figure 4.1. Morphology of differentiated capillary cells derived from human carotid peri-vascular (PV) and neck subcutaneous (SQ).

Figure 4.2. UCP1 expression in preadipocytes and adipocytes derived from neck fat depots with or without forskolin. Values represent fold difference over the lowest detectable value in the series for the respective probe set. Plotted are means of UCP1 expression relative to PLIN1, normalizing UCP1 expression by number of adipocytes to compensate the variance in differentiation, and s.e.m. from 2 technical replicates of samples from 3 PV and 3 SQ individuals.
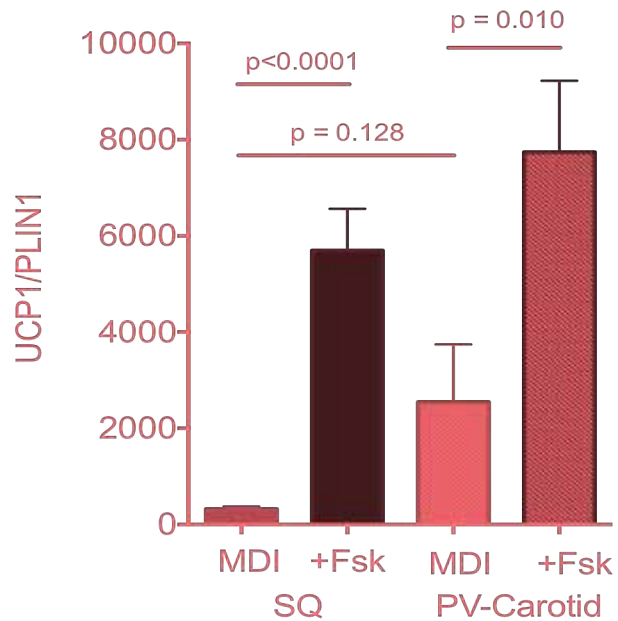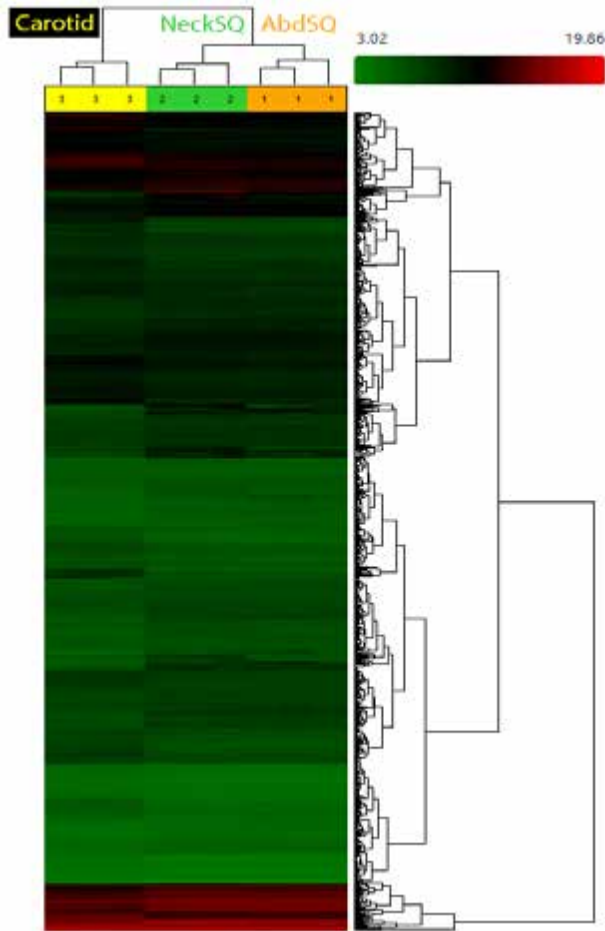
Figure 4.3. Heat map comparing the progenitors derived from Carotid, NeckSQ and AbdSQ.
Top: Heat map from Affymatrix HTA 2.0 array comparing the transcriptome signature of adipose progenitors derived from human carotid peri-vascular (Carotid), neck subcutaneous (NeckSQ), and abdominal subcutaneous (AbdSQ). The biological triplicates of each depot were clustered together.
Bottom: Enlarged heat map for patterning HOX genes.
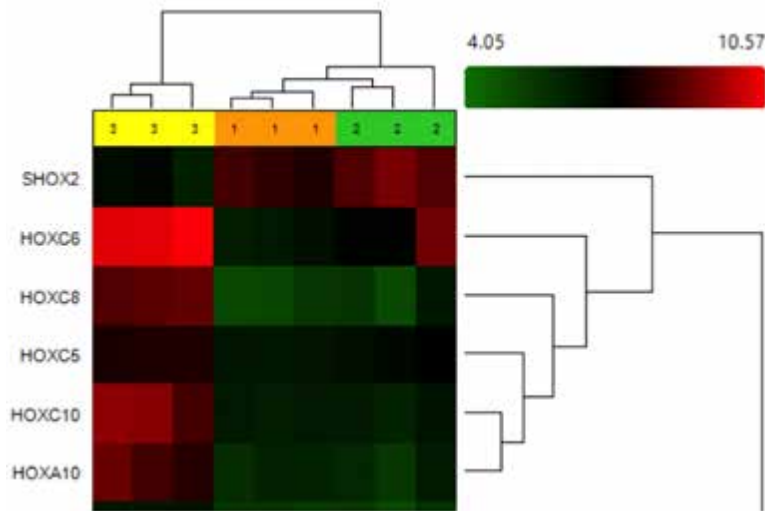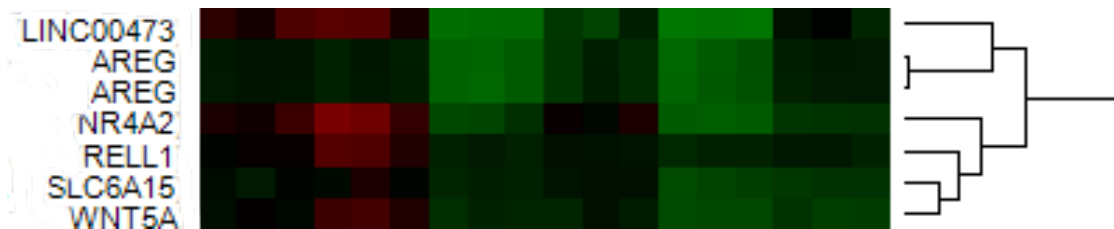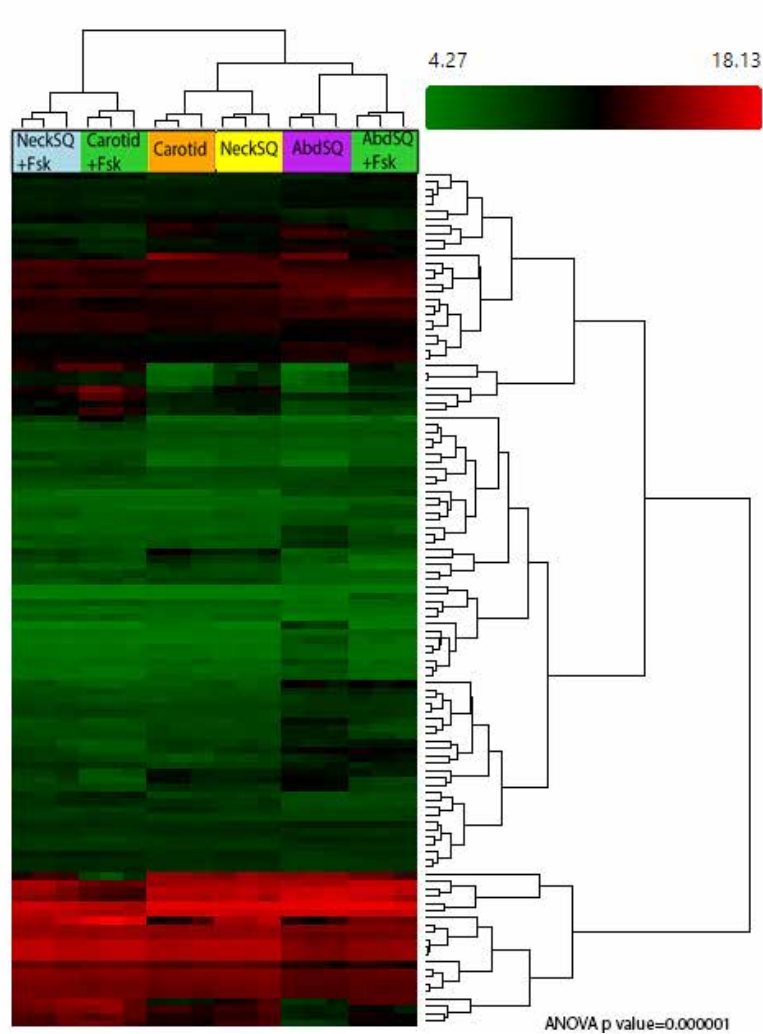
Figure 4.4. Heat map comparing the adipocytes derived from Carotid, NeckSQ and AbdSQ with or without forskolin-treatment.

Top: Heat map comparing differentiated adipocytes and forskolin-induced (+Fsk) adipoctyes derived from human carotid peri-vascular (Carotid), neck subcutaneous (NeckSQ), and abdominal subcutaneous (AbdSQ).

Bottom: Enlarged area in the heat map, displaying upregulared genes in the most thermogenic conditions such carotid+Fsk and neck SQ+Fsk.
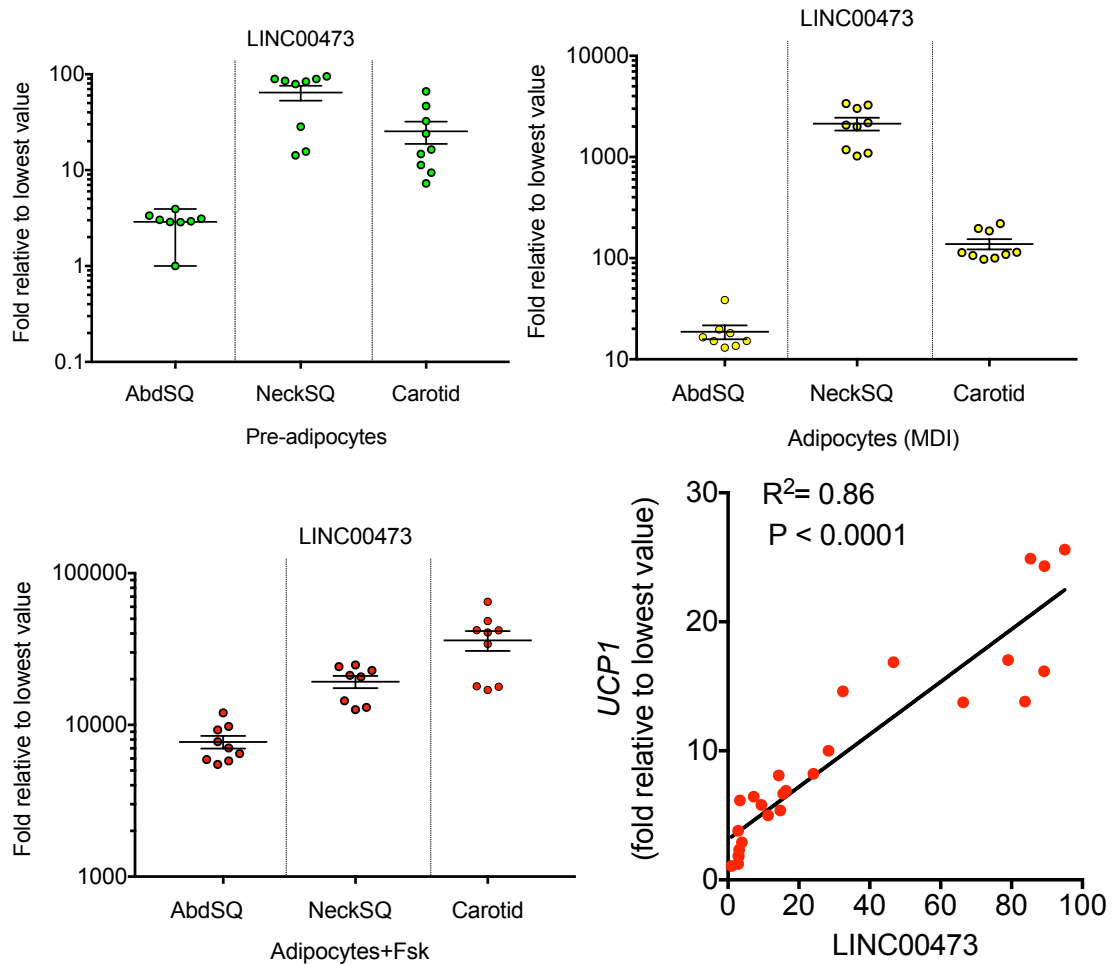
Figure 4.5. LINC00473 expression correlated with the level of UCP1

Top and bottom right: RT-PCR for LINC00473 on pre-adipocytes, adipocytes and forskolin-treated adipocytes (Adipocytes+Fsk), derived from human carotid peri-vascular (Carotid), neck subcutaneous (NeckSQ) and abdominal subcutaneous (AbdSQ). Technical triplicates. N=3.

Bottom left: The strong positive correlation between UCP1 and LINC00473 mRNA expression. Values represent pre-adipocytes, adipocytes and adipocytes+Fsk from Carotid, NeckSQ and AbdSQ.

Discussion

In this chapter, we analyzed the global gene expression profile of progenitors and adipocytes from three human adipose depots that are considered to be representative of brown, beige and white fat: peri-carotid (brown), neck subcutaneous (beige) and abdominal subcutaneous (white). The results from chapter II, III and IV clearly demonstrate that all three depots contain adipose progenitor population that can give rise to thermogenic fat cells. However, the gene array data revealed their differences in global gene expression level, suggesting the progenitor population from each depot is distinct. The data also discovered several potential thermogenic regulators (e.g. LINC00473), which could explain the variations in thermogenic capacities of different adipose depots relating to their physiological locations.

Non-coding RNAs fundamentally contribute to the regulation of gene expression in brown and beige adipocytes. MicroRNAs (miR) such as miR-133, miR-193b, and miR-365 target PRDM16 and decrease brown and beige adipocyte development in mice[163, 164]. miR-196a represses HoxC8, a negative regulator of C/EBPβ, resulting in induction of beige adipocyte differentiation[165] Similarly, long non-coding RNAs also provide another layer of regulation; for example, Inc-BATE1 and Blinc1 are required for brown and beige adipocyte differentiation through formation of a nuclear ribonucleoprotein complex that controls the thermogenic gene expression[166, 167] (Alvarez-Dominguez et al., 2015; Zhao et al., 2014). A long non-conding RNA 00473, on which I discussed in this chapter, was recently reported by Chen *et al*. LINC00473 was

induced by LKB1 inactivation in a lung cancer cells, leading to the subsequent

CREB/CREB-regulated transcription co-activator (CRTC) activation. The authors

showed that LINC00473 is a nuclear lncRNA that interacts with NONO, a component of

the cAMP signaling pathway, thereby facilitating CRTC/CREB-mediated transcription

(Figure 4. 9)[162]. Further studies including genetic manipulation of LINC00473 in

human preadipocytes and adipocytes will be useful to understand the biology of

LINC00473 in human adipocytes.

Chapter V: Concluding remarks and future directions

Concluding remarks: capillary networks as a niche of human white, brown and brite/beige adipocyte progenitors

In the efforts to answer the questions that I addressed earlier in the Project Goals, this thesis led to these findings: 1) *in vitro* adipose tissue angiogenesis system generates human adipocyte progenitors, which can be readily isolated and further expanded. These adipose progenitor cells have the potential to differentiate into adipocytes, which makes this advancement valuable to researchers and clinicians in the field. 2) The isolated adipose progenitors with or without *in vitro* differentiation are able to form a fat pad *in vivo*, which can be successfully vascularized and integrated into mouse circulatory system. 3) The capillary-associated origin of human brite/beige adipocyte is discovered. Functional brite/beige adipocytes can be generated from capillary-derived adipocyte progenitors of human subcutaneous white adipose tissue. 4) When transplanted into humanized mice, human brite/beige adipocytes show strong effects on whole body metabolism. 5) Human brite/beige adipocytes produce neurocrine and secretory proteins (e.g. IL-33, PCSK1, PENK) that may mediate effects on systemic metabolism. 6) The global transcriptome analysis reveals the distinct signatures of the progenitors and adipocytes of human brown (carotid perivascular), brite/beige (neck subcutaneous) and white (abdominal subcutaneous) adipose tissue. 7) The gene array analysis identifies LINC00473 as a potential thermogenic regulator. Major findings are summarized in the Figure 5.1.

The identification and development of a robust adipose stem cell population is attracting great attention due to the strong need for tissue replacement and regeneration in human patients. "Adipose-derived stem cells"-enriched lipo-transfer has markedly improved the survival of transplanted fat as well as decreased adverse effects in human patients. However, the limited expandability and the differentiation potential of adipose-derived stem cells still require the development of advanced adipogenic adipose stem cells. In this thesis, the results in chapter II show that better enriched human adipocyte progenitors can be generated by expanding adipose tissue capillary networks under pro-angiogenic stimuli. Furthermore, capillary-derived adipocytes recapitulate the characteristics of human primary adipocytes and form a vascularized fat pad when put into Nude mice. Comparison between adipose subcutaneous capillary cells and conventional adipose-derived stem cells suggests that capillary-derived adipocyte progenitors retain higher viability and superior differentiation potential. The development of improved harvesting and expanding methods for adult adipose stem cells in this thesis may advance the use of these adipose stem cells in clinical applications (e.g. fat transplantation, reconstruction, wound repair). Also, further investigation of the mechanism by which capillary-derived adipose stem cells expand will be immensely useful in optimizing the production process of the adipose stem cells.

The results described in chapter III and IV indicate that brite/beige cells can be generated from multiple fat tissues *in vitro*, differentiated into beige adipocytes, and implanted back into the humans for a therapeutic use. Up to date, main challenges in leveraging browning to enhance insulin insensitivity include that thermogenic fat is

scarce in obese or diabetic patients, and that the thermogenic depots need to be activated. One approach can be to increase the amount of functional thermogenic fats by recruiting more beige cells that are metabolically active using environmental or pharmacological agents. So far, numbers of pharmacologic activators of the β-adrenergic pathway have been tested but failed due to the lack of efficacy in obese populations or adverse effects (e.g. elevated blood pressure and heart rate)[168]. Another approach can be activating endogenous thermogenic fat in human. One recent example of this attempt is demonstrated by Cypess *et al*.[107] where β-adrenergic receptor agonist Mirabegron shows acutely enhanced glucose uptake of brown fat in human subjects. The findings in this thesis that multiple human adipose depots contain the progenitors of recruitable and inducible thermogenic adipocytes validate the idea of boosting browning as a therapeutic use. The new method to generate human brite/beige adipocyte progenitors developed in this thesis not only provides the necessary material to study but also suggests a possible way of producing metabolically beneficial fat cells for clinical applications. Fundamentally, the knowledge from this thesis and further investigation on expansion, characteristics and function of human brite/beige fat cells will enable us to eventually discover specific and safe new targets for browning to achieve metabolic health in humans.
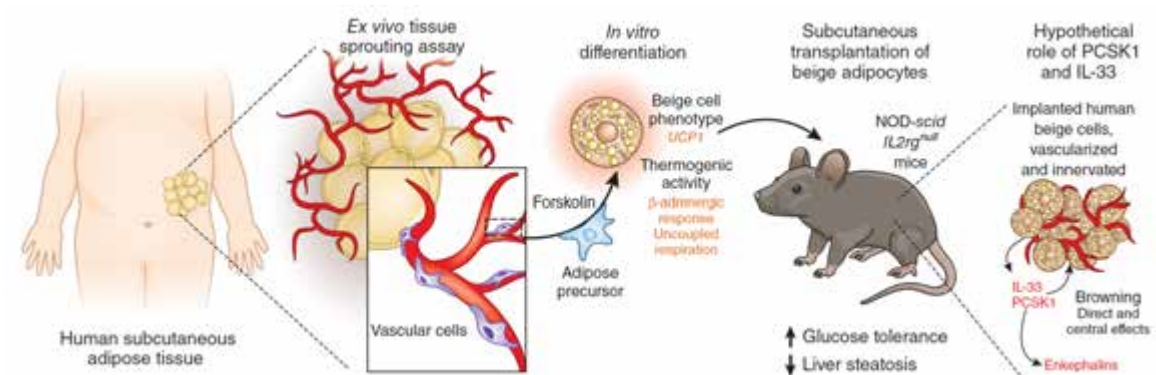
Figure 5.1. Summary of the findings. Beige adipocytes subcutaneously transplanted into mice improved glucose homoeostasis. Once cultured on Matrigel with angiogenic growth factors, the WAT explant undergoes vascular sprouting with new capillaries made up of endothelial cells and perivascular cells expressing stem cells and/or pericyte markers. The differentiation *in vitro* of these capillary-derived cells in the presence of adipogenic factors and, subsequently, the pharmacological browning compound forskolin gives rise to functional beige adipocytes. Once transplanted into high fat diet-fed obese mice (immune-deficient NOD-*scid IL2rg_{null}* mice) for 2 weeks, systemic glucose tolerance is improved. The authors also find PCSK1 and IL-33 to be potential molecular regulators of beige adipocyte functionality and the maintenance of the beige/brite phenotype. *Pellegrinelli, V. and A. Vidal-Puig, Deriving functional beige fat from capillaries. Nat Med, 2016. 22(3): p. 234-236.*

Future directions I: clonal-level transcriptome analysis on adipogenic progenitors

The finding in this thesis that human pre-adipocytes can be isolated and expanded from *in vitro* formed capillary networks, without the need of transformation, enables the in depth analysis of unaltered primary human adipose progenitors. The profound advancement of deep sequencing and bioinformatics platforms also facilitates the classification of progenitor cells using very low RNA input. As a future study, we aim to address the question of whether white and beige adipocytes emerge from the same or distinct adipocyte progenitors, and if so identify specific markers that characterize each progenitor type. The outcome will allow us to identify beige-specific signaling pathways or transcriptional patterns that may be targetable for therapeutic intervention. This information will also provide the basis for clinical studies to determine whether metabolic disease is associated with defects in specific mechanisms that induce browning. Single-cell cloning and low input RNA-seq approaches will allow us to address these questions.

Methods and results of preliminary studies:

To determine whether single adipocyte progenitors are capable of autonomous growth and differentiation, live single cells were individually sorted into wells of 384-well plates. In brief, to obtain clonal populations, single cells suspensions were obtained from capillary network cell cultures using trypsin, stained with 7-amino-actinomycin D (7-AAD) for live/dead cell identification, and sorted into individual wells of 384 well multi-well plates using a BSL3 BD FACSAria Cell Sorter (BD Biosciences). Clones were grown and expanded using EGM-2 MV. Viable clones were passaged onto 96 well multi-well plates and differentiated as described in Chapter II and III.

As expected from cells of non-hematopoietic lineage, these cells were CD45 − (Figure 5.2). Surviving colonies (approximately 10% of seeded wells) could be further passaged into 96 well multi-wells; of these, approximately 75% underwent adipogenic differentiation, as determined morphologically by lipid droplet accumulation (Figure 5.3), and functionally by secretion of adiponectin into the culture medium (Figure 5.4). Thus, human adipocyte progenitors isolated from capillary networks can be clonally expanded, and can undergo differentiation in an autonomous manner. Notably, there was a subset of the population that can become adipocytes, which define them as adipocyte progenitor cells, among these capillary cells. Thus, further investigation into the each clone was followed as below to identify the adipose progenitor population(s).
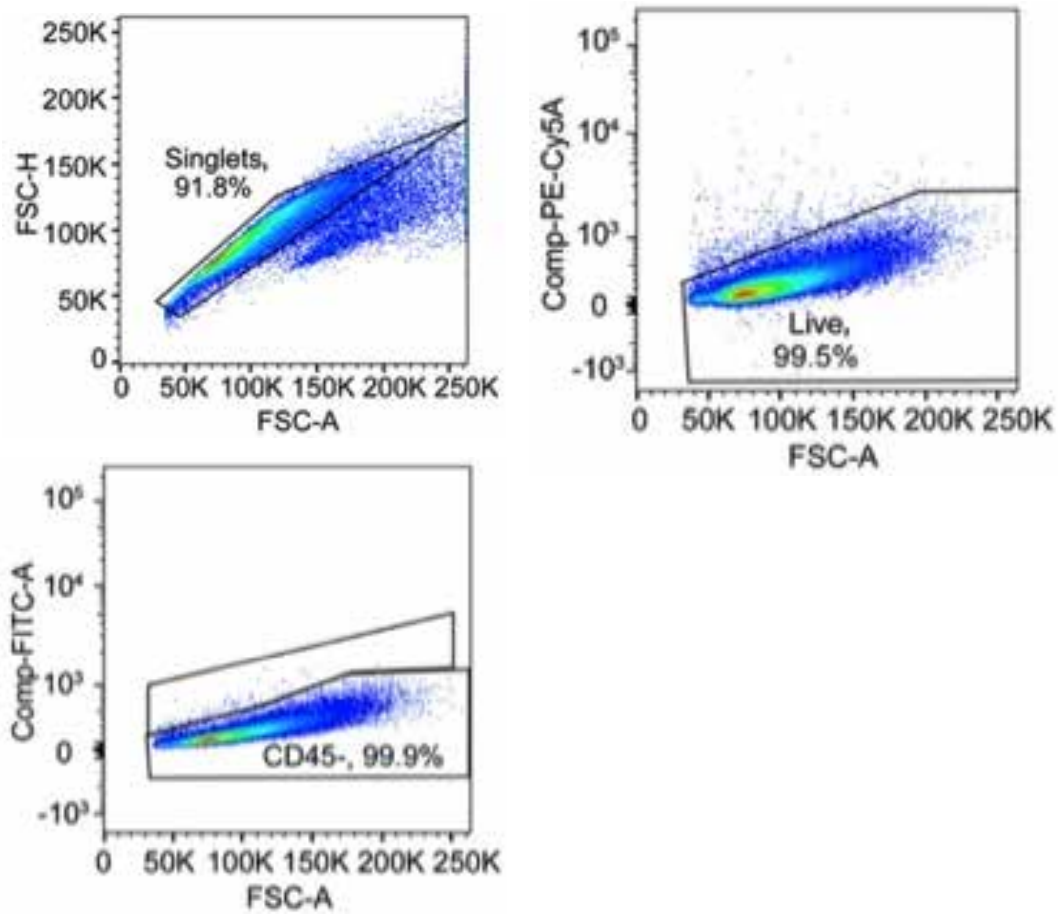
Figure 5.2. Single-cell sorting of capillary cells. FACS sorting of live (7-AAD negative) singlet cells from capillary networks. CD45-FITC positive population was less than 0.1 % of total live cells. Single cell (CD45-negative) per well was sorted on 384 multi-well plates.
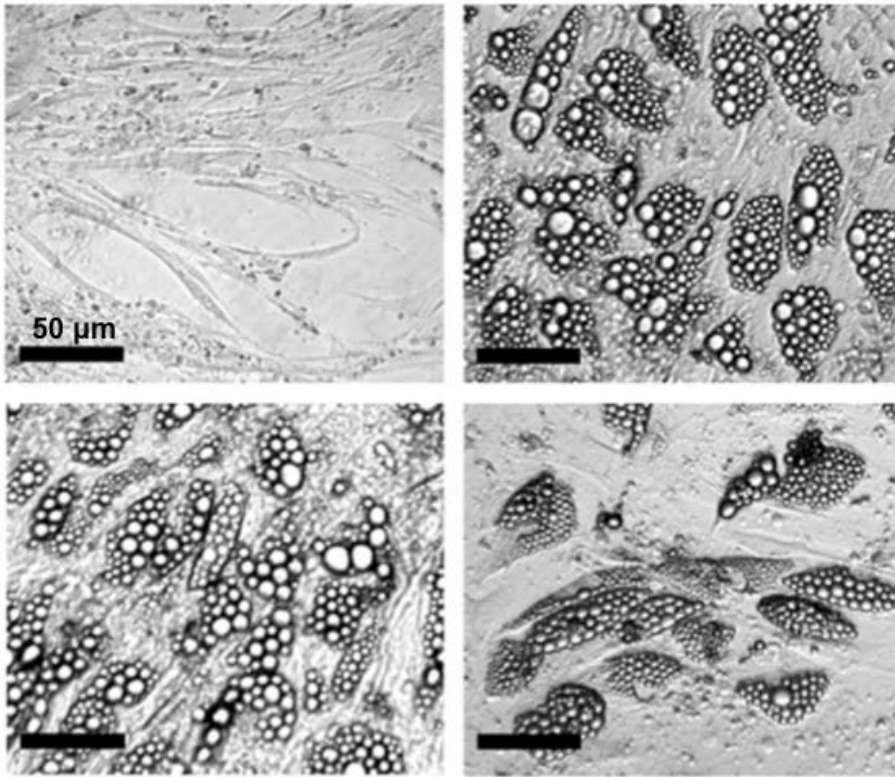
Figure 5.3. Morphology of differentiated clones. Examples of one non-adipogenic and three adipogenic clones, identified by lipid droplet contents. Scale bars are 50 μm.
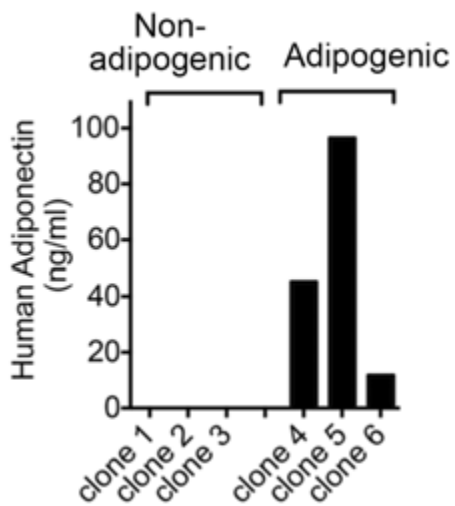
Figure 5.4. Adiponectin production from clones. Human adiponectin concentration (ng/ml) detected in culture medium from 3 non-adipogenic and 3 adipogenic clones by human-specific ELISA.

Strategy for obtaining total RNA from adipocyte progenitors:

Based on the preliminary results, the planned experimental scheme is suggested below (Figure 5.5). I expanded and differentiated the single cells clones of capillary cells and treated forskolin for 7 days, following the scheme. Out of total 3840 wells sorted, approximately 3% (118 clones) survived and successfully proliferated. Among these expandable clones, 86% (102 clones) reached confluence and were subjected to adipogenic differentiation protocol. It is noteworthy that the percentage of adipocytes in each well varied significantly despite the fact that all wells started with a single cell and expanded in the same way and we also observed several different shapes of adipocytes (Figure 5.6). Remarkably, the morphology of adipocytes with or without forskolin (Figure 5.6) suggested that not all clonal adipocytes respond to forskolin, discerned by their size of lipid droplets though the interpretation cannot be conclusive until we analyze the gene expression profile. However, it appears that there is a possibility of having distinct subtypes of human adipocytes among the clones.

Total RNA has been isolated using NucleoSpin RNA XS (Macherey-Nagel, 740902) from clonally expanded replica cells at the pre-adipocyte stage, at differentiation, and at stimulated stage with forskolin. The quality of RNA was analyzed on Fragment Analyzer (Advanced Analytical) using High Sensitivity RNA Analysis Kit (Advanced Analytical, DNF-472). Excluding the wells with dying cells at the time of collection, the isolated RNAs were intact and pure (RQN above 9 in most clones) with a good amount (at least 150~250 ng available per sample) to proceed to the next step.

As a next step, I will prepare RNA-seq library using SMART-Seq v4 3' DE Kit (Clontech, 635040) for the selected clones (healthy, adipogenic, good RNA quality) at the pre-adipocyte and adipocyte stages. Low-input RNA-seq will determine whether the UCP1-inducing beige clones are genetically distinct from the clones devoid of UCP1 induction.
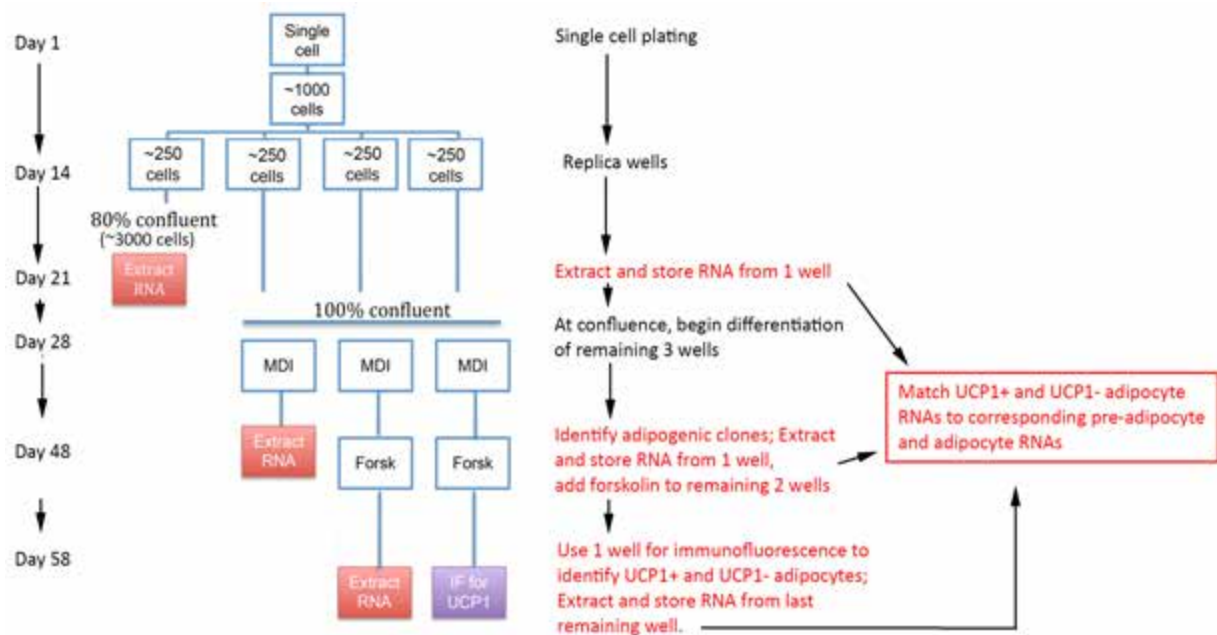
Figure 5.5. Experimental scheme of clonal RNA-seq. On day 1, single cells collected from capillary sprouts are sorted into individual wells of a 384 well multi well plate. After approximately 14 days, viable clones that have reached near confluence are split into 4 wells. After approximately 7 days, one well is harvested to extract RNA. The remaining three wells are monitored until they reach post-confluence, and adipogenic differentiation is then induced using MDI. After 10 days, adipogenic clones are identified and RNA extracted from one of the three wells. The remaining two wells are subjected to chronic stimulation by forskolin. After 10 days, RNA is extracted from one of the two wells. The remaining well is fixed and stained for the presence of UCP1. The signal is used to identify which of the clones from which RNA was previously collected corresponded to white or beige pre-adipocytes and differentiated adipocytes. In this way, previously harvested clones can be identified as progenitors for either "white" or "beige" adipocytes. After collection of RNA from 100 white pre-adipocyte clones and 100 beige pre-adipocyte clones, and from their corresponding white and beige adipocytes, RNA-seq and bioinformatics analysis will be performed. *Adapted from a NIH grant proposal of Corvera laboratory.*
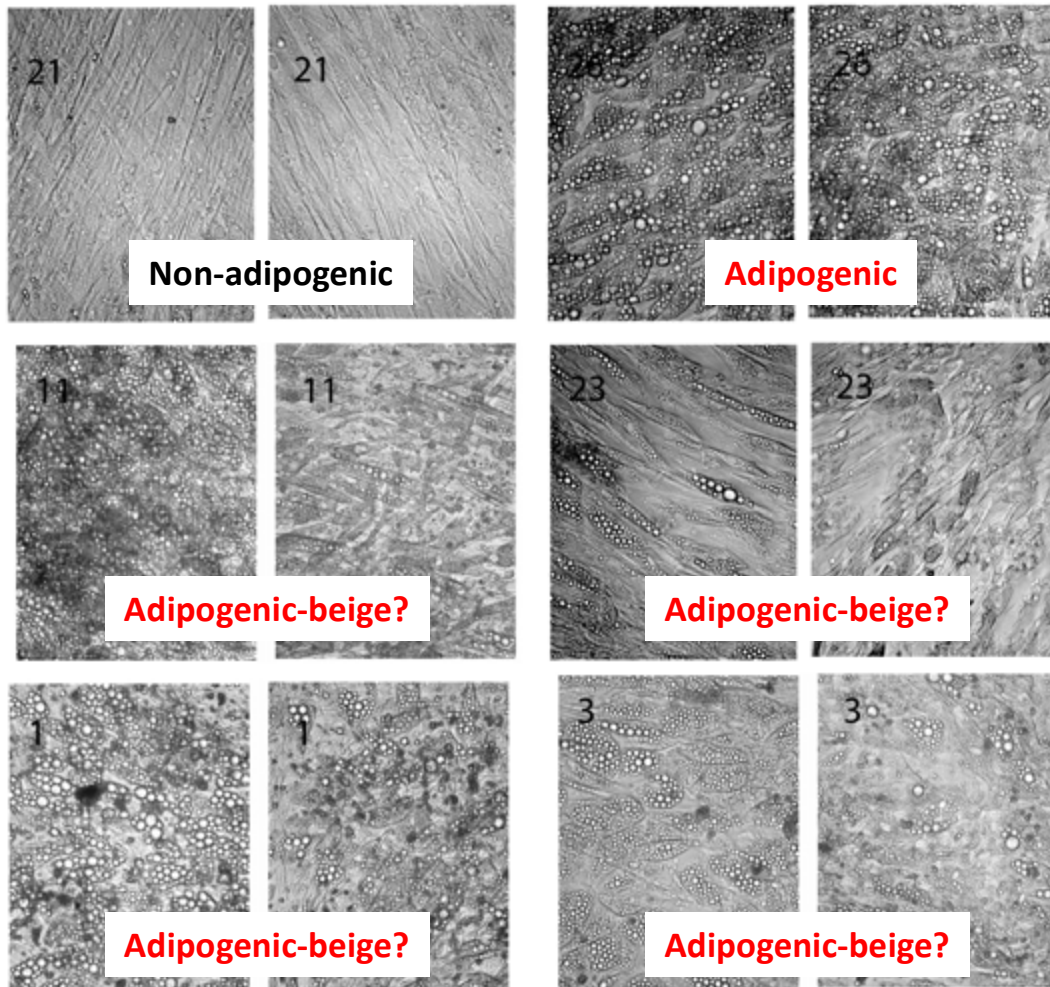
Figure 5.6. Morphology of differentiated clones with or without forskolin-treatment.
Each number on the picture represents the identifier for each clone. In each clone, left panel shows without forskolin and right panel shows with forskolin-treatment.

Sequencing and bioinformatics approach to determine whether "white" and "beige" adipocytes originate from distinct pre-adipocytes:

(*Adapted with some modifications from a NIH grant proposal of Corvera laboratory*)

The current pipeline consists of the following steps: (i) Sequence reads are evaluated for overall quality using the FastQC suite (http://www.bioinformatics.-babraham.ac.uk/projects/fastqc/), and trimmed whenever average base quality scores at either end are below 20. (ii) Trimmed, high quality reads are mapped to the rat ribosomal RNA using bowtie2 [169] to estimate ribosomal contamination and to eliminate reads mapping to the ribosome from further processing. (iii) non-ribosomal reads are used to estimate gene expression using the RSEM program [170], which implements a probabilistic approach of read to isoform assignment to compute isoform level counts. (iv) For small input libraries we concentrate on gene level counts estimated by RSEM as an input for differential expression analysis using DESeq [133] Markers enriched in PCA-defined clusters will be used to further enrich for specific cell populations, followed by subsequent rounds of RNA-seq and refinement of genetic identity of progenitor cells.

Based on the lineage tracing studies in mouse, adipocyte progenitors that give rise to white, beige and brown adipocytes are distinct[86, 171-175]. Hence, we expect, also in human adipose tissues, to distinguish differential genetic signatures in progenitors of each adipocyte type. However, it is possible that a discrete segregation into clusters will not be seen if our sequencing depth does not allow detecting lowly expressed transcripts. If so, we will maximize sequencing reads to pick up the even subtle differences in gene

expression. If no clustering is seen even with this strategy, this might represent a stochastic process.

Future Directions II: the possible metabolic functions of secretory factors produced by brite/beige adipocytes

(Some contents are adapted with modifications from a NIH grant proposal of Corvera laboratory)

As we better understand the physiological roles of brown and beige adipocytes, it is becoming clear that these thermogenic adipose tissues are not mere heat-generating organs. Significant improvements in glucose and lipid homeostasis by the activated thermogenic adipocytes may not be entirely mediated by UCP1.

To investigate the possible mechanisms by which human capillary-derived beige adipocytes affect systemic metabolism, in Chapter III of this thesis, we conducted global gene expression analysis of the adipocytes before and after forskolin-treatment. Notably, among the 20 most highly induced genes in response to forskolin were the proprotein-convertase subtilisin/kexin type-1 (PCSK1) and its substrate proenkephalin (PENK) (Figure 5.6, Graph). Mutations in PCSK1 are strongly associated with human obesity[131, 176-184] and it cleaves pro-hormones including pro-insulin, POMC and PENK, producing numerous bioactive peptides and enkephalins in various tissues [132, 185, 186]. These findings collectively raise the possibility that PCSK1 may underlie the relationship between the presence of thermogenic adipose tissue in lean and healthy humans. Enkephalins whose precursor is PENK are potent activators in the central

nervous system and peripheral tissues, and recent findings suggest that enkephalins affect energy metabolism[134]. In addition to PCSK1 and PENK, the human beige adipocytes express mRNAs for other secreted proteins (Figure 5.6, Table). A remarkable example is IL-33, which has been demonstrated to decrease adiposity, mitigate atherosclerosis and be necessary for normal glucose homeostasis in rodents[133, 134].

As future directions, we propose to further test whether the human beige cells do secrete these peptides and interleukins, resulting in a physiologically bioactive level *in vivo*. In brief, we will perform ELISA and proteomic analysis using LTQ Orbitrap Mass Spectrometry to investigate the secreted proteins of interest (e.g. enkephanlins, IL-33) and global secretome of these cells, which may allow us to identify the potential pro-hormones that are substrates to PCSK1. In the preliminary experiments, the collected *in vitro* culture media from human beige cells were frozen, lyophilized to a volume of 2 ml and applied to a pre-equilibrated C18 reversed-phase liquid chromatography column to enrich small hydrophobic peptides. Adsorbed peptides were eluted with 80% acetonitrile, and run through a LTQ Orbitrap Mass Spectometer. MS/MS analysis verified the presence of secreted PCSK1 (D6RJA3) exclusively in the forskolin-treated samples and two additional secreted proteins of unclear function, TICN1/SPOCK1 and TMEM263 were identified. Because this convertase is packaged into secretory vesicles and proteolytically processed into an active form, the finding of PCSK1 peptides in the culture medium is also strongly suggestive of functional PCSK1 activity in human beige adipocytes. The knowledge to be achieved by these suggested works will bolster the basic

understanding of the mechanism through which human beige adipocytes and their secreted factors enhance whole body homeostasis.
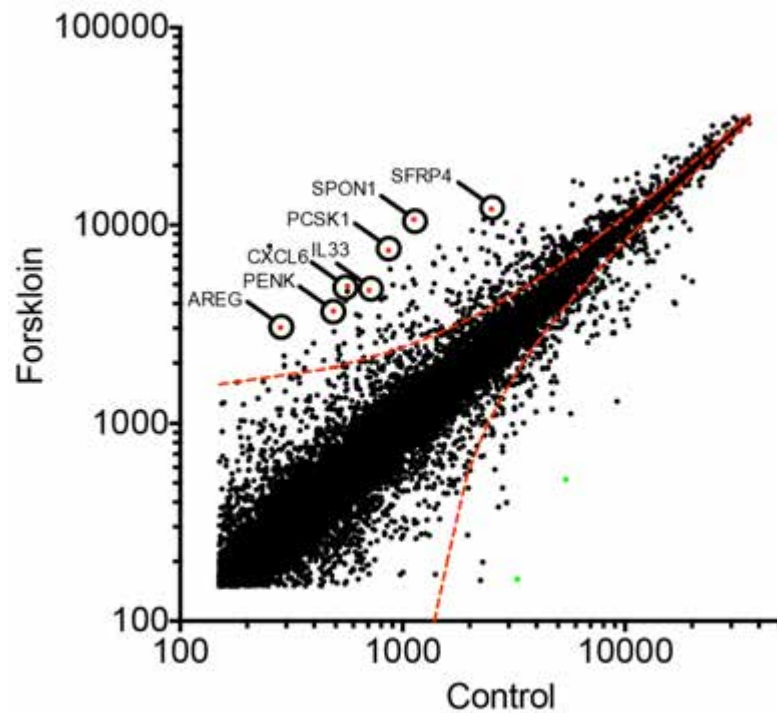
Name	Symbol	Fold difference (	p value
vasohibin 2	VASH2	17.39641927	0.0116559
spondin 1	SPON1	12.89354591	0.00918132
tachykinin, precursor 1	TAC1	10.9756317	0.0153774
amphiregulin	AREG	10.7177511	0.0198066
chemokine (C-X-C motif) ligand 6	CXCL6	8.676803504	0.00067798
proprotein convertase subtilisin/kexin type 1	PCSK1	8.592670054	0.00189798
platelet factor 4 variant 1	PF4V1	8.202188132	0.0139934
proenkephalin	PENK	7.505035253	0.0184174
secreted frizzled-related protein 4	SFRP4	6.794224687	0.0293923
interleukin 33	IL33	6.615438344	0.0229864

Figure 5.7. List of the genes encoding potential secretory proteins from human beige adipocytes
Top: Scatter plot of gene expression levels in differentiated cells without (control) or with forskolin-treatment for 7 days, indicating genes of interest outside the linear regression 95% prediction band.
Bottom: A summary of most highly up-regulated secretory factors by forskolin-treatment.

Bibliography

1.   Lidell, M.E., M.J. Betz, and S. Enerback, *Two types of brown adipose tissue in humans.* Adipocyte, 2014. **3**(1): p. 63-6.
2.   Crandall, D.L., G.J. Hausman, and J.G. Kral, *A review of the microcirculation of adipose tissue: anatomic, metabolic, and angiogenic perspectives.* Microcirculation, 1997. **4**(2): p. 211-232.
3.   Han, J., et al., *The spatiotemporal development of adipose tissue.* Development, 2011. **138**(22): p. 5027-5037.
4.   Bouloumié, A., et al. *Angiogenesis in adipose tissue.* in *Annales d'endocrinologie.* 2002.
5.   Tang, W., et al., *White Fat Progenitor Cells Reside in the Adipose Vasculature.* Science, 2008. **322**(5901): p. 583-586.
6.   Gupta, R.K., et al., *Zfp423 expression identifies committed preadipocytes and localizes to adipose endothelial and perivascular cells.* Cell metabolism, 2012. **15**(2): p. 230-239.
7.   Harms, M. and P. Seale, *Brown and beige fat: development, function and therapeutic potential.* Nature medicine, 2013. **19**(10): p. 1252-1263.
8.   Frontini, A., et al., *White-to-brown transdifferentiation of omental adipocytes in patients affected by pheochromocytoma.* Biochimica et Biophysica Acta (BBA)-Molecular and Cell Biology of Lipids, 2013. **1831**(5): p. 950-959.
9.   Sidossis, L.S., et al., *Browning of subcutaneous white adipose tissue in humans after severe adrenergic stress.* Cell metabolism, 2015. **22**(2): p. 219-227.
10.   Cypess, A.M., et al., *Identification and importance of brown adipose tissue in adult humans.* New England Journal of Medicine, 2009. **360**(15): p. 1509-1517.
11.   van Marken Lichtenbelt, W.D., et al., *Cold-activated brown adipose tissue in healthy men.* New England Journal of Medicine, 2009. **360**(15): p. 1500-1508.
12.   Herman, M.A. and B.B. Kahn, *Glucose transport and sensing in the maintenance of glucose homeostasis and metabolic harmony.* The Journal of clinical investigation, 2006. **116**(7): p. 1767-1775.
13.   Jiang, G. and B.B. Zhang, *Glucagon and regulation of glucose metabolism.* Am J Physiol Endocrinol Metab, 2003. **284**(4): p. E671-8.
14.   Rosen, E.D. and B.M. Spiegelman, *Adipocytes as regulators of energy balance and glucose homeostasis.* Nature, 2006. **444**(7121): p. 847-853.
15.   Grundy, S.M., *Obesity, Metabolic Syndrome, and Cardiovascular Disease.* The Journal of Clinical Endocrinology & Metabolism, 2004. **89**(6): p. 2595-2600.
16.   Kim, J.K., et al., *Mechanism of Insulin Resistance in A-ZIP/F-1 Fatless Mice.* Journal of Biological Chemistry, 2000. **275**(12): p. 8456-8460.
17.   Perugini, R.A., et al., *Metabolic Characterization of Nondiabetic Severely Obese Patients Undergoing Roux-en-Y Gastric Bypass: Preoperative Classification Predicts the Effects of Gastric Bypass on Insulin–Glucose Homeostasis.* Journal of Gastrointestinal Surgery, 2007. **11**(9): p. 1083-1090.

18. Tran, T.T., et al., *Beneficial Effects of Subcutaneous Fat Transplantation on Metabolism.* Cell Metabolism, 2008. **7**(5): p. 410-420.

19. Gesta, S., Y.-H. Tseng, and C.R. Kahn, *Developmental Origin of Fat: Tracking Obesity to Its Source.* Cell, 2007. **131**(2): p. 242-256.

20. Smith, J.D., et al., *Visceral Adipose Tissue Indicates the Severity of Cardiometabolic Risk in Patients with and without Type 2 Diabetes: Results from the INSPIRE ME IAA Study.* The Journal of Clinical Endocrinology & Metabolism, 2012. **97**(5): p. 1517-1525.

21. Wang, Y., et al., *Comparison of abdominal adiposity and overall obesity in predicting risk of type 2 diabetes among men.* The American Journal of Clinical Nutrition, 2005. **81**(3): p. 555-563.

22. Kusminski, C.M., et al., *Diabetes and apoptosis: lipotoxicity.* Apoptosis, 2009. **14**(12): p. 1484-1495.

23. Unger, R.H., *Lipotoxic Diseases.* Annual Review of Medicine, 2002. **53**(1): p. 319-336.

24. Marchetti, P., et al., *An overview of pancreatic beta-cell defects in human type 2 diabetes: Implications for treatment.* Regulatory Peptides, 2008. **146**(1–3): p. 4-11.

25. Jo, J., et al., *Hypertrophy and/or Hyperplasia: Dynamics of Adipose Tissue Growth.* PLoS Comput Biol, 2009. **5**(3): p. e1000324.

26. Jules Hirsch, B.B., *Adipose tissue cellularity in human obesity.* Clinics in Endocrinology and Metabolism, 1976. **5**(2): p. 299-311.

27. Arner, E., et al., *Adipocyte Turnover: Relevance to Human Adipose Tissue Morphology.* Diabetes, 2010. **59**(1): p. 105-109.

28. Risau, W., *Mechanisms of angiogenesis.* Nature, 1997. **386**(17): p. 671-674.

29. Prins, J.B. and S. O'rahilly, *Regulation of Adipose Cell Number in Man.* Clinical Science, 1997. **92**(1): p. 3-11.

30. Björntorp P, B.C., Blohmé G, Jonsson A, Sjöström L, Tibblin E, Tibblin G, Wilhelmsen L, *Adipose tissue fat cell size and number in relation to metabolism in randomly selected middle-aged men and women.* Metabolism, 1971. **20**(10): p. 927-935.

31. Per Björntorp, A.G., Bengt Persson, *ADIPOSE TISSUE FAT CELL SIZE AND NUMBER IN RELATION TO METABOLISM IN ENDOGENOUS HYPERTRIGLYCERIDEMIA.* Journal of Internal Medicine, 1971. **190**(1-6): p. 363–367.

32. van Harmelen, V., K. Röhrig, and H. Hauner, *Comparison of proliferation and differentiation capacity of human adipocyte precursor cells from the omental and subcutaneous adipose tissue depot of obese subjects.* Metabolism, 2004. **53**(5): p. 632-637.

33. Joe, A.W.B., et al., *Depot-Specific Differences in Adipogenic Progenitor Abundance and Proliferative Response to High-Fat Diet.* STEM CELLS, 2009. **27**(10): p. 2563-2570.

34. Hoffstedt, J., et al., *Regional impact of adipose tissue morphology on the metabolic profile in morbid obesity.* Diabetologia, 2010. **53**(12): p. 2496-2503.

35. Veilleux, A., et al., *Visceral Adipocyte Hypertrophy is Associated With Dyslipidemia Independent of Body Composition and Fat Distribution in Women.* Diabetes, 2011. **60**(5): p. 1504-1511.

36. Harms, M. and P. Seale, *Brown and beige fat: development, function and therapeutic potential.* Nat Med, 2013. **19**(10): p. 1252-63.

37. van Dijk, C.G.M., et al., *The complex mural cell: Pericyte function in health and disease.* International Journal of Cardiology, 2015. **190**: p. 75-89.

38. Carmeliet, P., *Mechanisms of angiogenesis and arteriogenesis.* Nature medicine, 2000. **6**(4): p. 389-396.

39. Otrock, Z.K., et al., *Understanding the biology of angiogenesis: Review of the most important molecular mechanisms.* Blood Cells, Molecules, and Diseases, 2007. **39**(2): p. 212-220.

40. Ferrara, N. and R.S. Kerbel, *Angiogenesis as a therapeutic target.* Nature, 2005. **438**(7070): p. 967-74.

41. Crandall, D.L., Hausman, G. J. and Kral, J. G., *A Review of the Microcirculation of Adipose Tissue: Anatomic, Metabolic, and Angiogenic Perspectives.* Microcirculation, 1997. **4**: p. 211–232.

42. Rosen, E.D. and B.M. Spiegelman, *Molecular Regulation of Adipogenesis.* Annual Review of Cell and Developmental Biology, 2000. **16**(1): p. 145-171.

43. Gabor Voros, E.M., Diego Demeulemeester, Natalie Clerx, Désiré Collen, and H. Roger Lijnen, *Modulation of Angiogenesis during Adipose Tissue Development in Murine Models of Obesity.* Endocrinology, 2005. **146**(10): p. 4545–4554.

44. Rupnick, M.A., Panigrahy, D., Zhang, C. Y., Dallabrida, S. M., Lowell, B. B., Langer, R., and and M.J. Folkman, *Adipose tissue mass can be regulated through the vasculature.* Proc Natl Acad Sci U S A, 2002. **99**(16): p. 10730–10735.

45. Gupta, Rana K., et al., *Zfp423 Expression Identifies Committed Preadipocytes and Localizes to Adipose Endothelial and Perivascular Cells.* Cell Metabolism, 2012. **15**(2): p. 230-239.

46. Crisan, M., et al., *A Perivascular Origin for Mesenchymal Stem Cells in Multiple Human Organs.* Cell Stem Cell, 2008. **3**(3): p. 301-313.

47. Barnhart, K.F., et al., *A Peptidomimetic Targeting White Fat Causes Weight Loss and Improved Insulin Resistance in Obese Monkeys.* Science Translational Medicine, 2011. **3**(108): p. 108ra112-108ra112.

48. Kolonin, M.G., et al., *Reversal of obesity by targeted ablation of adipose tissue.* Nat Med, 2004. **10**(6): p. 625-632.

49. Tran, K.-V., et al., *The Vascular Endothelium of the Adipose Tissue Gives Rise to Both White and Brown Fat Cells.* Cell Metabolism, 2012. **15**(2): p. 222-229.

50. Napolitano, L., *THE DIFFERENTIATION OF WHITE ADIPOSE CELLS.* An Electron Microscope Study, 1963. **18**(3): p. 663-679.

51. Rodeheffer, M.S., K. Birsoy, and J.M. Friedman, *Identification of White Adipocyte Progenitor Cells In Vivo.* Cell, 2008. **135**(2): p. 240-249.

52. Bo Zheng, B.C., Guangheng Li, and Johnny Huard, *Mouse Adipose-Derived Stem Cells Undergo Multilineage Differentiation in Vitro but Primarily Osteogenic and Chondrogenic Differentiation in Vivo.* Tissue Engineering, 2006. **12**(7): p. 1891-1901.

53. Patricia A. Zuk, M.Z., Hiroshi Mizuno, Jerry Huang, J. William Futrell, Adam J. Katz, Prosper Benhaim, H. Peter Lorenz, and Marc H. Hedrick, *Multilineage Cells from Human Adipose Tissue: Implications for Cell-Based Therapies.* Tissue Engineering, 2004. **7**(2): p. 211-228.

54. Hemmrich, K., et al., *Implantation of preadipocyte-loaded hyaluronic acid-based scaffolds into nude mice to evaluate potential for soft tissue engineering.* Biomaterials, 2005. **26**(34): p. 7025-7037.

55. Hong, L., et al., *Adipose Tissue Engineering by Human Adipose-Derived Stromal Cells.* Cells Tissues Organs, 2006. **183**(3): p. 133-140.

56. Sengenès, C., et al., *Preadipocytes in the human subcutaneous adipose tissue display distinct features from the adult mesenchymal and hematopoietic stem cells.* Journal of Cellular Physiology, 2005. **205**(1): p. 114-122.

57. CANNON, B. and J. NEDERGAARD, *Brown Adipose Tissue: Function and Physiological Significance.* Physiological Reviews, 2004. **84**(1): p. 277-359.

58. Lowell, B.B. and B.M. Spiegelman, *Towards a molecular understanding of adaptive thermogenesis.* Nature, 2000. **404**(6778): p. 652-660.

59. Lee, Y.-H., et al., *In Vivo Identification of Bipotential Adipocyte Progenitors Recruited by β3-Adrenoceptor Activation and High-Fat Feeding.* Cell Metabolism, 2012. **15**(4): p. 480-491.

60. Bronnikov, G., J. Houstěk, and J. Nedergaard, *Beta-adrenergic, cAMP-mediated stimulation of proliferation of brown fat cells in primary culture. Mediation via beta 1 but not via beta 3 adrenoceptors.* Journal of Biological Chemistry, 1992. **267**(3): p. 2006-13.

61. Bordicchia, M., et al., *Cardiac natriuretic peptides act via p38 MAPK to induce the brown fat thermogenic program in mouse and human adipocytes.* The Journal of Clinical Investigation, 2012. **122**(3): p. 1022-1036.

62. Guerra, C., et al., *Emergence of brown adipocytes in white fat in mice is under genetic control. Effects on body weight and adiposity.* The Journal of Clinical Investigation, 1998. **102**(2): p. 412-420.

63. Vitali, A., et al., *The adipose organ of obesity-prone C57BL/6J mice is composed of mixed white and brown adipocytes.* Journal of Lipid Research, 2012. **53**(4): p. 619-629.

64. Petrovic, N., et al., *Chronic Peroxisome Proliferator-activated Receptor γ (PPARγ) Activation of Epididymally Derived White Adipocyte Cultures Reveals a Population of Thermogenically Competent, UCP1-containing Adipocytes Molecularly Distinct from Classic Brown Adipocytes.* The Journal of Biological Chemistry, 2010. **285**(10): p. 7153-7164.

65. Ishibashi, J. and P. Seale, *Beige can be slimming.* Science (New York, N.Y.), 2010. **328**(5982): p. 1113-1114.

66. Long, Jonathan Z., et al., *A Smooth Muscle-Like Origin for Beige Adipocytes.* Cell Metabolism, 2014. **19**(5): p. 810-820.

67. Wu, J., et al., *Beige Adipocytes Are a Distinct Type of Thermogenic Fat Cell in Mouse and Human.* Cell, 2012. **150**(2): p. 366-376.

68. Sharp, L.Z., et al., *Human BAT Possesses Molecular Signatures That Resemble Beige/Brite Cells.* PLoS ONE, 2012. **7**(11): p. e49452.

69. Feldmann, H.M., et al., *UCP1 Ablation Induces Obesity and Abolishes Diet-Induced Thermogenesis in Mice Exempt from Thermal Stress by Living at Thermoneutrality.* Cell Metabolism, 2009. **9**(2): p. 203-209.

70. Stanford, K.I., et al., *Brown adipose tissue regulates glucose homeostasis and insulin sensitivity.* The Journal of Clinical Investigation. **123**(1): p. 215-223.

71. Bartelt, A., et al., *Brown adipose tissue activity controls triglyceride clearance.* Nat Med, 2011. **17**(2): p. 200-205.

72. Lee, P., et al., *A critical appraisal of the prevalence and metabolic significance of brown adipose tissue in adult humans.* American Journal of Physiology - Endocrinology And Metabolism, 2010. **299**(4): p. E601-E606.

73. Jacene, H.A., et al., *The Relationship between Patients' Serum Glucose Levels and Metabolically Active Brown Adipose Tissue Detected by PET/CT.* Molecular Imaging and Biology, 2011. **13**(6): p. 1278-1283.

74. Ouellet, V., et al., *Outdoor Temperature, Age, Sex, Body Mass Index, and Diabetic Status Determine the Prevalence, Mass, and Glucose-Uptake Activity of 18F-FDG-Detected BAT in Humans.* The Journal of Clinical Endocrinology & Metabolism, 2011. **96**(1): p. 192-199.

75. Chondronikola, M., et al., *Brown Adipose Tissue Improves Whole-Body Glucose Homeostasis and Insulin Sensitivity in Humans.* Diabetes, 2014. **63**(12): p. 4089-4099.

76. Yoneshiro, T., et al., *Recruited brown adipose tissue as an antiobesity agent in humans.* The Journal of Clinical Investigation. **123**(8): p. 3404-3408.

77. van Marken Lichtenbelt , W.D., et al., *Cold-Activated Brown Adipose Tissue in Healthy Men.* New England Journal of Medicine, 2009. **360**(15): p. 1500-1508.

78. Yoneshiro, T., et al., *Brown Adipose Tissue, Whole-Body Energy Expenditure, and Thermogenesis in Healthy Adult Men.* Obesity, 2011. **19**(1): p. 13-16.

79. Matsushita, M., et al., *Impact of brown adipose tissue on body fatness and glucose metabolism in healthy humans.* Int J Obes, 2014. **38**(6): p. 812-817.

80. Orava, J., et al., *Blunted metabolic responses to cold and insulin stimulation in brown adipose tissue of obese humans.* Obesity, 2013. **21**(11): p. 2279-2287.

81. Ouellet, V., et al., *Brown adipose tissue oxidative metabolism contributes to energy expenditure during acute cold exposure in humans.* The Journal of Clinical Investigation. **122**(2): p. 545-552.

82. Crandall, D.L., G.J. Hausman, and J.G. Kral, *A review of the microcirculation of adipose tissue: anatomic, metabolic, and angiogenic perspectives.* Microcirculation, 1997. **4**(2): p. 211-32.

83. Han, J., et al., *The spatiotemporal development of adipose tissue.* Development, 2011. **138**(22): p. 5027-37.

84. Bouloumie, A., et al., *Angiogenesis in adipose tissue.* Ann Endocrinol (Paris), 2002. **63**(2 Pt 1): p. 91-5.

85. Tang, W., et al., *White fat progenitor cells reside in the adipose vasculature.* Science, 2008. **322**(5901): p. 583-6.

86. Gupta, R.K., et al., *Zfp423 expression identifies committed preadipocytes and localizes to adipose endothelial and perivascular cells.* Cell metabolism, 2012. **15**(2): p. 230-9.

87. Gealekman, O., et al., *Enhanced angiogenesis in obesity and in response to PPARγ activators through adipocyte VEGF and ANGPTL4 production.* American Journal of Physiology - Endocrinology and Metabolism, 2008. **295**(5): p. E1056-E1064.

88. Rojas-Rodriguez, R., et al., *Human adipose tissue expansion in pregnancy is impaired in gestational diabetes mellitus.* Diabetologia, 2015. **58**(9): p. 2106-2114.

89. Gealekman, O., et al., *Depot-Specific Differences and Insufficient Subcutaneous Adipose Tissue Angiogenesis in Human Obesity.* Circulation, 2011. **123**(2): p. 186-194.

90. Cherubino, M. and K.G. Marra, *Adipose-derived stem cells for soft tissue reconstruction.* Regenerative Medicine, 2008. **4**(1): p. 109-117.

91. Hyakusoku, H., et al., *Complications after Autologous Fat Injection to the Breast.* Plastic and Reconstructive Surgery, 2009. **123**(1): p. 360-370.

92. Yoshimura, K., et al., *Cell-Assisted Lipotransfer for Cosmetic Breast Augmentation: Supportive Use of Adipose-Derived Stem/Stromal Cells.* Aesthetic Plastic Surgery, 2008. **32**(1): p. 48-55.

93. Kølle, S.-F.T., et al., *Enrichment of autologous fat grafts with ex-vivo expanded adipose tissue-derived stem cells for graft survival: a randomised placebo-controlled trial.* The Lancet. **382**(9898): p. 1113-1120.

94. Hassan, W.U., U. Greiser, and W. Wang, *Role of adipose-derived stem cells in wound healing.* Wound Repair and Regeneration, 2014. **22**(3): p. 313-325.

95. Geiger, P.C.B.a.H., *Adipose-Derived Mesenchymal Stromal/Stem Cells: Tissue Localization, Characterization, and Heterogeneity.* Stem Cells International, 2012. **2012**: p. 11.

96. Rojas-Rodriguez, R., et al., *Adipose tissue angiogenesis assay.* Methods in enzymology, 2014. **537**: p. 75-91.

97. Fitzgibbons, T.P., et al., *Similarity of mouse perivascular and brown adipose tissues and their resistance to diet-induced inflammation.* American Journal of Physiology - Heart and Circulatory Physiology, 2011. **301**(4): p. H1425-H1437.

98.   Gealekman, O., et al., *Depot-specific differences and insufficient subcutaneous adipose tissue angiogenesis in human obesity.* Circulation, 2011. **123**(2): p. 186-94.

99.   Tran, K.V., et al., *The vascular endothelium of the adipose tissue gives rise to both white and brown fat cells.* Cell Metab, 2012. **15**(2): p. 222-9.

100.   van de Vyver, M., et al., *Thiazolidinedione-induced lipid droplet formation during osteogenic differentiation.* J Endocrinol, 2014. **223**(2): p. 119-32.

101.   Schäffler, A. and C. Büchler, *Concise review: adipose tissue‐derived stromal cells−basic and clinical implications for novel cell‐based therapies.* Stem cells, 2007. **25**(4): p. 818-827.

102.   Shinoda, K., et al., *Genetic and functional characterization of clonally derived adult human brown adipocytes.* Nature medicine, 2015. **21**(4): p. 389-94.

103.   Xue, R., et al., *Clonal analyses and gene profiling identify genetic biomarkers of the thermogenic potential of human brown and white preadipocytes.* Nature medicine, 2015. **21**(7): p. 760-8.

104.   Nishio, M., et al., *Production of functional classical brown adipocytes from human pluripotent stem cells using specific hemopoietin cocktail without gene transfer.* Cell metabolism, 2012. **16**(3): p. 394-406.

105.   Cypess , A.M., et al., *Identification and Importance of Brown Adipose Tissue in Adult Humans.* New England Journal of Medicine, 2009. **360**(15): p. 1509-1517.

106.   Cypess, Aaron M., et al., *Brown Fat in Humans: Consensus Points and Experimental Guidelines.* Cell Metabolism, 2014. **20**(3): p. 408-415.

107.   Cypess, Aaron M., et al., *Activation of Human Brown Adipose Tissue by a β3-Adrenergic Receptor Agonist.* Cell Metabolism, 2015. **21**(1): p. 33-38.

108.   Nedergaard, J., T. Bengtsson, and B. Cannon, *Unexpected evidence for active brown adipose tissue in adult humans.* American Journal of Physiology - Endocrinology And Metabolism, 2007. **293**(2): p. E444-E452.

109.   Saito, M., et al., *High Incidence of Metabolically Active Brown Adipose Tissue in Healthy Adult Humans.* Effects of Cold Exposure and Adiposity, 2009. **58**(7): p. 1526-1531.

110.   Cypess, A.M., et al., *Anatomical localization, gene expression profiling and functional characterization of adult human neck brown fat.* Nature medicine, 2013. **19**(5): p. 635-639.

111.   Jespersen, Naja Z., et al., *A Classical Brown Adipose Tissue mRNA Signature Partly Overlaps with Brite in the Supraclavicular Region of Adult Humans.* Cell Metabolism, 2013. **17**(5): p. 798-805.

112.   Lidell, M.E., M.J. Betz, and S. Enerbäck, *Two types of brown adipose tissue in humans.* Adipocyte, 2014. **3**(1): p. 63-66.

113.   Xue, R., et al., *Clonal analyses and gene profiling identify genetic biomarkers of the thermogenic potential of human brown and white preadipocytes.* Nat Med, 2015. **21**(7): p. 760-768.

114. Shinoda, K., et al., *Genetic and functional characterization of clonally derived adult human brown adipocytes.* Nat Med, 2015. **21**(4): p. 389-394.
115. van der Lans, A.A.J.J., et al., *Cold acclimation recruits human brown fat and increases nonshivering thermogenesis.* The Journal of Clinical Investigation. **123**(8): p. 3395-3403.
116. Lee, P., et al., *Temperature-Acclimated Brown Adipose Tissue Modulates Insulin Sensitivity in Humans.* Diabetes, 2014. **63**(11): p. 3686-3698.
117. Kajimura, S., Bruce M. Spiegelman, and P. Seale, *Brown and Beige Fat: Physiological Roles beyond Heat Generation.* Cell Metabolism, 2015. **22**(4): p. 546-559.
118. Brehm, M.A., et al., *Engraftment of human HSCs in nonirradiated newborn NOD-scid IL2rgamma null mice is enhanced by transgenic expression of membrane-bound human SCF.* Blood, 2012. **119**(12): p. 2778-88.
119. Shabalina, I.G., et al., *Carboxyatractyloside effects on brown-fat mitochondria imply that the adenine nucleotide translocator isoforms ANT1 and ANT2 may be responsible for basal and fatty-acid-induced uncoupling respectively.* Biochem J, 2006. **399**(3): p. 405-14.
120. Wu, J., et al., *Beige adipocytes are a distinct type of thermogenic fat cell in mouse and human.* Cell, 2012. **150**(2): p. 366-76.
121. Cypess, A.M., et al., *Activation of human brown adipose tissue by a beta3-adrenergic receptor agonist.* Cell Metab, 2015. **21**(1): p. 33-8.
122. Cousin, B., et al., *Occurrence of brown adipocytes in rat white adipose tissue: molecular and morphological characterization.* Journal of cell science, 1992. **103 (Pt 4)**: p. 931-42.
123. Orlicky, D.J., et al., *Dynamics and molecular determinants of cytoplasmic lipid droplet clustering and dispersion.* PLoS One, 2013. **8**(6): p. e66837.
124. Marcinkiewicz, A., et al., *The phosphorylation of serine 492 of perilipin a directs lipid droplet fragmentation and dispersion.* J Biol Chem, 2006. **281**(17): p. 11901-9.
125. Zhang, Y., et al., *Regulation of adiponectin and leptin gene expression in white and brown adipose tissues: influence of beta3-adrenergic agonists, retinoic acid, leptin and fasting.* Biochim Biophys Acta, 2002. **1584**(2-3): p. 115-22.
126. Behan, J.W., et al., *Activation of adipose tissue macrophages in obese mice does not require lymphocytes.* Obesity (Silver Spring), 2013. **21**(7): p. 1380-8.
127. Xiao, C., et al., *Anti-obesity and metabolic efficacy of the beta3-adrenergic agonist, CL316243, in mice at thermoneutrality compared to 22 degrees C.* Obesity (Silver Spring), 2015. **23**(7): p. 1450-9.
128. Hocking, S.L., et al., *Subcutaneous fat transplantation alleviates diet-induced glucose intolerance and inflammation in mice.* Diabetologia, 2015. **58**(7): p. 1587-600.
129. Wang, G.X., et al., *The brown fat-enriched secreted factor Nrg4 preserves metabolic homeostasis through attenuation of hepatic lipogenesis.* Nat Med, 2014. **20**(12): p. 1436-43.

130. Jackson, R.S., et al., *Obesity and impaired prohormone processing associated with mutations in the human prohormone convertase 1 gene.* Nature genetics, 1997. **16**(3): p. 303-6.

131. Benzinou, M., et al., *Common nonsynonymous variants in PCSK1 confer risk of obesity.* Nat Genet, 2008. **40**(8): p. 943-5.

132. Denning, G.M., et al., *Proenkephalin expression and enkephalin release are widely observed in non-neuronal tissues.* Peptides, 2008. **29**(1): p. 83-92.

133. Miller, A.M., et al., *Interleukin-33 induces protective effects in adipose tissue inflammation during obesity in mice.* Circulation research, 2010. **107**(5): p. 650-8.

134. Brestoff, J.R., et al., *Group 2 innate lymphoid cells promote beiging of white adipose tissue and limit obesity.* Nature, 2015. **519**(7542): p. 242-6.

135. Elias, I., et al., *Adipose tissue overexpression of vascular endothelial growth factor protects against diet-induced obesity and insulin resistance.* Diabetes, 2012. **61**(7): p. 1801-13.

136. Sun, K., et al., *Dichotomous effects of VEGF-A on adipose tissue dysfunction.* Proc Natl Acad Sci U S A, 2012. **109**(15): p. 5874-9.

137. Chang, L., et al., *Loss of perivascular adipose tissue on peroxisome proliferator-activated receptor-gamma deletion in smooth muscle cells impairs intravascular thermoregulation and enhances atherosclerosis.* Circulation, 2012. **126**(9): p. 1067-78.

138. Fitzgibbons, T.P., et al., *Similarity of mouse perivascular and brown adipose tissues and their resistance to diet-induced inflammation.* American journal of physiology. Heart and circulatory physiology, 2011. **301**(4): p. H1425-37.

139. Szasz, T. and R.C. Webb, *Perivascular adipose tissue: more than just structural support.* Clinical Science, 2012. **122**(1): p. 1-12.

140. D. Margriet Ouwens, H.S., Sabrina Greulich, Juergen Eckel, *The role of epicardial and perivascular adipose tissue in the pathophysiology of cardiovascular disease.* J. Cell. Mol. Med., 2010. **14**(9): p. 2223-2234.

141. Chatterjee, T.K., et al., *Proinflammatory Phenotype of Perivascular Adipocytes.* Influence of High-Fat Feeding, 2009. **104**(4): p. 541-549.

142. Police, S.B., et al., *Obesity Promotes Inflammation in Periaortic Adipose Tissue and Angiotensin II-Induced Abdominal Aortic Aneurysm Formation.* Arteriosclerosis, Thrombosis, and Vascular Biology, 2009. **29**(10): p. 1458-1464.

143. Gálvez-Prieto, B., et al., *Comparative expression analysis of the renin–angiotensin system components between white and brown perivascular adipose tissue.* Journal of Endocrinology, 2008. **197**(1): p. 55-64.

144. Chang, L., et al., *Loss of Perivascular Adipose Tissue on Peroxisome Proliferator–Activated Receptor-Deletion in Smooth Muscle Cells Impairs Intravascular Thermoregulation and Enhances Atherosclerosis.* Circulation, 2012. **126**(9): p. 1067-1078.

145. Bartelt, A. and J. Heeren, *Adipose tissue browning and metabolic health.* Nat Rev Endocrinol, 2014. **10**(1): p. 24-36.
146. Wellik, D.M., *Hox patterning of the vertebrate axial skeleton.* Developmental Dynamics, 2007. **236**(9): p. 2454-2463.
147. Nowicki, J.L. and A.C. Burke, *Hox genes and morphological identity: axial versus lateral patterning in the vertebrate mesoderm.* Development, 2000. **127**(19): p. 4265-4275.
148. Burke, A.C., et al., *Hox genes and the evolution of vertebrate axial morphology.* Development, 1995. **121**(2): p. 333-346.
149. Daftary, G.S. and H.S. Taylor, *Endocrine Regulation of HOX Genes.* Endocrine Reviews, 2006. **27**(4): p. 331-355.
150. Cantile, M., et al., *HOX gene network is involved in the transcriptional regulation of in vivo human adipogenesis.* Journal of Cellular Physiology, 2003. **194**(2): p. 225-236.
151. Procino, A.a.C., Clemente, *The HOX genes network in metabolic diseases.* Cell Biology International, 2013. **37**(11): p. 1145-1148.
152. Karastergiou, K., et al., *Distinct Developmental Signatures of Human Abdominal and Gluteal Subcutaneous Adipose Tissue Depots.* The Journal of Clinical Endocrinology & Metabolism, 2013. **98**(1): p. 362-371.
153. Gesta, S., et al., *Evidence for a role of developmental genes in the origin of obesity and body fat distribution.* Proceedings of the National Academy of Sciences, 2006. **103**(17): p. 6676-6681.
154. Nakagami, H., *The Mechanism of White and Brown Adipocyte Differentiation.* Diabetes Metab J, 2013. **37**(2): p. 85-90.
155. Ng, M.C.Y., et al., *Association of the POU class 2 homeobox 1 gene (POU2F1) with susceptibility to Type 2 diabetes in Chinese populations.* Diabetic Medicine, 2010. **27**(12): p. 1443-1449.
156. Foucher, I., et al., *Hoxa5 overexpression correlates with IGFBP1 upregulation and postnatal dwarfism: evidence for an interaction between Hoxa5 and Forkhead box transcription factors.* Development, 2002. **129**(17): p. 4065-4074.
157. Gupta, R.A., et al., *Long non-coding RNA HOTAIR reprograms chromatin state to promote cancer metastasis.* Nature, 2010. **464**(7291): p. 1071-1076.
158. Wapinski, O. and H.Y. Chang, *Long noncoding RNAs and human disease.* Trends in Cell Biology. **21**(6): p. 354-361.
159. Scott, L.J., et al., *A Genome-Wide Association Study of Type 2 Diabetes in Finns Detects Multiple Susceptibility Variants.* Science, 2007. **316**(5829): p. 1341-1345.
160. Millar, J.K., et al., *Disruption of two novel genes by a translocation co-segregating with schizophrenia.* Human Molecular Genetics, 2000. **9**(9): p. 1415-1423.
161. Kung, J.T.Y., D. Colognori, and J.T. Lee, *Long Noncoding RNAs: Past, Present, and Future.* Genetics, 2013. **193**(3): p. 651-669.

162. Chen, Z., et al., *cAMP/CREB-regulated LINC00473 marks LKB1-inactivated lung cancer and mediates tumor growth.* The Journal of Clinical Investigation, 2016. **126**(6): p. 2267-2279.
163. Liu, W., et al., *miR-133a Regulates Adipocyte Browning In Vivo.* PLoS Genet, 2013. **9**(7): p. e1003626.
164. Sun, L., et al., *Mir193b-365 is essential for brown fat differentiation.* Nat Cell Biol, 2011. **13**(8): p. 958-965.
165. Mori, M., et al., *Essential Role for miR-196a in Brown Adipogenesis of White Fat Progenitor Cells.* PLoS Biol, 2012. **10**(4): p. e1001314.
166. Alvarez-Dominguez, Juan R., et al., *De Novo Reconstruction of Adipose Tissue Transcriptomes Reveals Long Non-coding RNA Regulators of Brown Adipocyte Development.* Cell Metabolism, 2015. **21**(5): p. 764-776.
167. Zhao, X.-Y., et al., *A Long Noncoding RNA Transcriptional Regulatory Circuit Drives Thermogenic Adipocyte Differentiation.* Molecular Cell, 2014. **55**(3): p. 372-382.
168. Carey, A.L., et al., *Ephedrine activates brown adipose tissue in lean but not obese humans.* Diabetologia, 2013. **56**(1): p. 147-155.
169. Langmead, B. and S.L. Salzberg, *Fast gapped-read alignment with Bowtie 2.* Nature methods, 2012. **9**(4): p. 357-9.
170. Li, B. and C.N. Dewey, *RSEM: accurate transcript quantification from RNA-Seq data with or without a reference genome.* BMC bioinformatics, 2011. **12**: p. 323.
171. Berry, R. and M.S. Rodeheffer, *Characterization of the adipocyte cellular lineage in vivo.* Nature cell biology, 2013. **15**(3): p. 302-8.
172. Liu, W., et al., *A heterogeneous lineage origin underlies the phenotypic and molecular differences of white and beige adipocytes.* Journal of cell science, 2013. **126**(Pt 16): p. 3527-32.
173. Sanchez-Gurmaches, J. and D.A. Guertin, *Adipocyte lineages: Tracing back the origins of fat.* Biochimica et biophysica acta, 2014. **1842**(3): p. 340-51.
174. Long, J.Z., et al., *A smooth muscle-like origin for beige adipocytes.* Cell metabolism, 2014. **19**(5): p. 810-20.
175. Seale, P., et al., *Prdm16 determines the thermogenic program of subcutaneous white adipose tissue in mice.* The Journal of clinical investigation, 2011. **121**(1): p. 96-105.
176. Kilpelainen, T.O., et al., *Association of variants in the PCSK1 gene with obesity in the EPIC-Norfolk study.* Hum Mol Genet, 2009. **18**(18): p. 3496-501.
177. Chang, Y.C., et al., *Common PCSK1 haplotypes are associated with obesity in the Chinese population.* Obesity (Silver Spring), 2010. **18**(7): p. 1404-9.
178. Heni, M., et al., *Association of obesity risk SNPs in PCSK1 with insulin sensitivity and proinsulin conversion.* BMC medical genetics, 2010. **11**: p. 86.
179. Choquet, H., P. Stijnen, and J.W. Creemers, *Genetic and functional characterization of PCSK1.* Methods Mol Biol, 2011. **768**: p. 247-53.

180. Gjesing, A.P., et al., *The effect of PCSK1 variants on waist, waist-hip ratio and glucose metabolism is modified by sex and glucose tolerance status.* PLoS One, 2011. **6**(9): p. e23907.
181. Creemers, J.W., et al., *Heterozygous mutations causing partial prohormone convertase 1 deficiency contribute to human obesity.* Diabetes, 2012. **61**(2): p. 383-90.
182. Li, X.M., et al., *The obesity-related polymorphism PCSK1 rs6235 is associated with essential hypertension in the Han Chinese population.* Hypertension research : official journal of the Japanese Society of Hypertension, 2012. **35**(10): p. 994-9.
183. Rouskas, K., et al., *Common variants in FTO, MC4R, TMEM18, PRL, AIF1, and PCSK1 show evidence of association with adult obesity in the Greek population.* Obesity, 2012. **20**(2): p. 389-95.
184. Wen, W., et al., *Meta-analysis identifies common variants associated with body mass index in east Asians.* Nature genetics, 2012. **44**(3): p. 307-11.
185. Breslin, M.B., et al., *Differential processing of proenkephalin by prohormone convertases 1(3) and 2 and furin.* The Journal of biological chemistry, 1993. **268**(36): p. 27084-93.
186. Lembo, P.M., et al., *Proenkephalin A gene products activate a new family of sensory neuron--specific GPCRs.* Nature neuroscience, 2002. **5**(3): p. 201-9.